REPUBLIC OF TURKEY

YILDIZ TECHNICAL UNIVERSITY

GRADUATE SCHOOL OF SCIENCE AND ENGINEERING

ENERGY PRODUCTION FROM VARIOUS BIOMASS WASTES VIA CO-FIRING AND PHOTOVOLTAIC-BIOGAS HYBRID SYSTEMS

Yavuz KIRIM

DOCTOR OF PHILOSOPHY THESIS

Department of Chemical Engineering

Chemical Engineering Program

Supervisor

Prof. Dr. Hasan SADIKOGLU

Co-Supervisor

Prof. Dr. Mehmet MELIKOGLU

January, 2022

REPUBLIC OF TURKEY

YILDIZ TECHNICAL UNIVERSITY

GRADUATE SCHOOL OF SCIENCE AND ENGINEERING

ENERGY PRODUCTION FROM VARIOUS BIOMASS WASTES VIA CO-FIRING AND PHOTOVOLTAIC-BIOGAS HYBRID SYSTEMS

A thesis submitted by Yavuz KIRIM in partial fulfillment of the requirements for the degree of DOCTOR OF PHILOSOPHY is approved by the committee on 05.01.2022 in Department of Chemical Engineering, Chemical Engineering Program.

Prof. Dr. Hasan SADIKOĞLU
Yıldız Technical University
Supervisor

Prof. Dr. Mehmet MELİKOĞLU
Gebze Technical University
Co- supervisor

Approved By the Examining Committee

Prof. Dr. Hasan SADIKOĞLU, Supervisor
Yildiz Technical University _____

Prof. Dr. Fatma Jale GÜLEN, Member
Yildiz Technical University _____

Assist. Prof. Dr. Özgün YÜCEL, Member
Gebze Technical University _____

Assoc. Prof. Dr. Nil ACARALI, Member
Yildiz Technical University _____

Prof. Dr. Mustafa ÖZİLGEN, Member
Yeditepe University _____

I hereby declare that I have obtained the required legal permissions during data collection and exploitation procedures, that I have made the in-text citations and cited the references properly, that I haven't falsified and/or fabricated research data and results of the study and that I have abided by the principles of the scientific research and ethics during my Thesis Study under the title of energy production from various biomass wastes via co-firing and photovoltaic-biogas hybrid systems supervised by my supervisor, Prof. Dr. Hasan SADIKOĞLU. In the case of a discovery of false statement, I am to acknowledge any legal consequence.

Yavuz KIRIM

Dedicated to my lovely

daughter Zeynep Doğa

ACKNOWLEDGEMENTS

I would like to thank to,

my valuable advisor, Prof. Dr. Hasan SADIKOĞLU to provide endless support in my doctorate study,

my esteemed co-advisor Prof. Dr. Mehmet MELİKOĞLU, who stood by me with his knowledge, guidance and ideas,

Research Assist. Günay BAYDAR ATAK, who did not spare her help throughout my doctorate.

Asst. Prof. Dr. Sungur GÜREL, and Research Assist. Dr. Serdar ABUT, who helped with their knowledge and experience in all matters.

Yavuz KIRIM

TABLE OF CONTENTS

LIST OF SYMBOLS viii

LIST OF ABBREVIATIONS ix

LIST OF FIGURES xi

LIST OF TABLES xii

ABSTRACT xiii

ÖZET xv

1 INTRODUCTION 1

1.1 Literature Review 1

1.2 Objective of the Thesis 4

1.3 Original Contribution 5

2 ELECTRICITY GENERATION FROM BIOMASS RESOURCES 6

2.1 Biogas Production from Biomass and Its Use in Electricity Generation .. 6

2.2 Electricity Generation from Animal Wastes 7

2.3 Co-Firing Technology for Energy Generation 10

2.4 Solar Energy in Electricity Generation 13

2.5 Biomass and Solar Hybrid Energy System for Electricity Generation ... 14

3 DATA AND METHODOLOGY OF MODULAR HYBRID SYSTEM DESIGN 16

3.1 Economic Parameters in HOMER 16

3.1.1 Initial Capital Cost 16

3.1.2 Replacement Cost 16

3.1.3 Operation and Maintenance Cost 16

3.1.4 Salvage Value 17

3.1.5 Annualized Cost 17

3.1.6 Operating Cost 17

3.1.7 Cost of Energy 18

3.1.8 Net Present Cost 18

3.1.9 Return on Investment 19

3.2 Solar Energy 19

3.3 Biomass 21

3.4 Load Profile 22

3.5 Modeling and Sizing of HRES 25

3.5.1 Photovoltaic Panel 26
3.5.2 Biomass Generator Inputs 27
3.5.3 Converter Inputs 27
3.5.4 Grid Inputs 27
3.6 Basic Terms in Regression Models 28
3.6.1 Train and Test Data Set 28
3.6.2 Overfitting and Underfitting 28
3.6.3 Bias and Variance 29
3.6.4 Root Mean Squared Error (RMSE) 30
3.6.5 Coefficient of Determination (R^2) 31
3.6.6 Regularization 31
3.6.7 Validation 32
3.6.8 Multicollinearity 33
3.7 Definition of Regression Models 35
3.7.1 Linear Regression 35
3.7.2 Ridge Regression 36
3.7.3 Lasso Regression 37
3.7.4 Elastic Net Regression 37
3.7.5 Econometric Prediction Methods 38
4 METHODOLOGY OF HYBRID SYSTEM DESIGN WITH CO-FIRING 42
4.1 HRES Design Scenarios in HCP 42
4.1.1 Selected Region of HRES 42
4.1.2 Hazelnut Shell for Electricity Generation via Co-firing 43
4.1.3 Solar Energy Potential of Selected Region 47
4.1.4 Load Profile of HCP 48
4.2 Hybrid Energy System Components 51
4.2.1 Photovoltaic Panel 51
4.2.2 Biomass Generator 52
4.2.3 Converter 52
4.2.4 Grid 52
4.3 Economic Parameters and Formulation in HOMER 53
5 RESULTS AND DISCUSSION 54
5.1 Cost Analysis Results for Modular HRES Design 54
5.1.1 Hybrid System with 50, 100, 500, 1000 and 5000 Cattle 61
5.1.2 Linear Regression Results 74

5.1.3 Ridge Lasso and Elastic Net Regression Results 79
5.2 Results and Discussion of HRES Design with Co-firing 85
5.2.1 Comparison of Option A and B Based on Feed in Tariff..... 85
5.2.2 Sensitivity Analysis for HRES 88
5.2.3 Sensitivity Variables Effect on TNPC and COE..... 89
5.2.4 Comparison of Four Different Scenarios Based on NPC COE and Greenhouse Gas Emission Analysis 92
5.3 Conclusions 96
REFERENCES 98
PUBLICATIONS FROM THE THESIS 108

LIST OF SYMBOLS

$	American Dollar
m^3	Cubic Meter
°	Degree
E	East
EJ	Egzajoule
GWh	Gigawatt-hour
hr	Hour
L	Liter
kg	Kilogram
kW	Kilowatt
kWh	Kilowatt-hour
MWe	Megawatt Electric
MWh	Megawatt-hour
‘	Minute
M	Million
N	North
%	Percentage
PJ	Pikajoule
m^2	Square Meter
TJ	Terajoule
toe	Tons of Equivalent
W	Watt
yr	Year

LIST OF ABBREVIATIONS

AC	Alternative Current
AW	Annual Worth
CH_4	Methane
CM	Cattle Manure
CO	Carbon Monoxide
CO_2	Carbon Dioxide
COE	Cost of Energy
CRF	Capital Recovery Factor
DC	Direct Current
EMRA	Energy Market Regularity Authority
ENR	Elastic Net Regression
GDP	Gross Domestic Product
H	Hydrogen
HCP	Hazelnut Cracking Plant
HOMER	Hybrid Optimization Multiple Electric Renewables
HRES	Hybrid Renewable Energy System
IRR	Internal Rate of Return
LCOE	Levelized Cost of Energy
LHV	Lower Heating Value
LR	Lasso Regression
MENR	Ministry of Energy and Natural Sources
N	Nitrogen
NA	Not Available
NASA	National Aeronautics and Space Administration
NG	Natural Gas
NO_x	Nitrogen Oxides
NPC	Net Present Cost
NREL	National Renewable Energy Laboratories
O&M	Operation and Maintenance
OLS	Ordinary Least Squares
PV	Photovoltaic

r	Correlation Coefficient
R^2	Coefficient of Determination
RC	Regression Coefficient
RF	Renewable Fraction
ROI	Return on Investment
RR	Ridge Regression
SO_2	Sulfur Oxide
SO_x	Sulfur Oxides
TNPC	Total Net Present Cost
UK	United Kingdom
US	United States
VIF	Variation Inflation Factor

LIST OF FIGURES

Figure 3.1 Daily radiation and clearness index of a) Konya, b) Erzurum and c) İzmir 20

Figure 3.2 Five different size of the system configurations (a) 50 b) 100 c) 500 d) 1000 e) 5000) including biomass generator, PV, converter, two electric load and grid components 26

Figure 3.3 Representation of bias and variance tradeoff considering underfitting and overfitting using bulls-eye diagram 30

Figure 3.4 Representation 5-fold cross validation 33

Figure 3.5 Schematic diagram of possible inferences to be used with regression methods 39

Figure 4.1 HRES configuration of HCP 51

Figure 5.1 Effects of capital costs on the components for a) 50 b) 100 c) 500 d) 1000 e) 5000 dairy cattle barns 65

Figure 5.2 Change in coefficients vs a) lambda value and b) standard deviation 81

Figure 5.3 Mean squared error (MSE) vs log λ graph for the train data set of RR 82

Figure 5.4 Mean squared error (MSE) vs log λ graph for the test data set of RR 83

Figure 5.5 Importance of 13 dependent variables on the dependent variable Y 84

Figure 5.6 Monthly electric production from PV and biomass co-fired with NG of HRES 85

Figure 5.7 Distribution of costs related to the components of Option A 86

Figure 5.8 Distribution of costs related to the components of Option B 87

Figure 5.9 Monthly electricity production of Option B corresponding to the components 88

Figure 5.10 The variation of grid sale capacity between 250 and 750 kW 89

Figure 5.11 Comparison of TNPC and COE values for expected inflation rate .. 90

Figure 5.12 The impact of nominal discount rate on the TNPC and COE 90

Figure 5.13 The outcome of hazelnut shell price on TNPC and COE 91

Figure 5.14 The price change of sellback rate 91

Figure 5.15 Amount of average fuel consumption of NG-Biogas co-firing generator throughout the year 94

LIST OF TABLES

Table 3.1 Monthly solar sources of Konya, Erzurum and İzmir 20

Table 3.2 Adults live weights of dairy cattle and average daily manure generations 22

Table 3.3 A typical farmhouse daily electric load and dairy cattle barn electric load 23

Table 3.4 Mean and standard deviation of dependent and independent variables and their notations 39

Table 4.1 Symbols units and descriptions of operations of co-fired generator... 45

Table 4.2 Clearness index and daily radiation data per month 47

Table 4.3 Daily load profile of HCP 49

Table 5.1 Most important econometric values for all hybrid system configurations 55

Table 5.2 The number of 50, 100, 500, 1000 and 5000 dairy cattle farms, their AWs and their total annual returns 59

Table 5.3 Categorized results of a) 50 b) 100 c) 500 d) 1000 e) 5000 cattle barns' hybrid system configurations 61

Table 5.4 Annualized costs of the hybrid system components..... 66

Table 5.5 Grid outputs of the all hybrid system configurations 69

Table 5.6 The possible result for linear model created in R programming 74

Table 5.7 Multicollinearity problem between the independent variables determined by the correlation matrix method..... 77

Table 5.8 The intercept coefficients of RR models 79

Table 5.9 Simulation results of Option A and B 88

Table 5.10 The value of sensitivity variables..... 89

Table 5.11 Detailed analysis of four different scenarios based on the electricity production, fuel consumption and RF 93

Table 5.12 Emission values of all scenarios including carbon dioxide, carbon monoxide, unburned hydrocarbons, particulate matters, sulfur dioxides and nitrogen oxides 95

ABSTRACT

Energy Production from Various Biomass Wastes via Co-Firing and Photovoltaic-Biogas Hybrid Systems

Yavuz KIRIM

Department of Chemical Engineering

Doctor of Philosophy Thesis

Supervisor: Prof. Dr. Hasan SADIKOGLU

Co- supervisor: Prof. Dr. Mehmet MELIKOGLU

In first part of thesis, modular hybrid renewable energy systems (HRES) comprising of biogas and solar photovoltaic (PV) are designed for various dairy cattle barns located in Konya, Erzurum and İzmir provinces of Turkey. The design also included technical and economic analyses. It is found that the grid-connected system including PV and biomass are more feasible than the stand-alone biomass system in terms of net present cost (NPC), return on investment (ROI), cost of energy (COE) and annual worth (AW). Among the different regression models, ridge regression gives the highest coefficient of determination (R^2) of 0.92, and the lowest root mean squared error (RMSE) value of 0.463 (million $). Consequently, it is found that total installed cost of solar energy has the strongest effect on the share of electricity generation in terms of the effect on the GDP, which is calculated as 97%.

In second part of thesis, a HRES composed of solar photovoltaic and biogas co-firing is designed for a hazelnut cracking plant (HCP) in Ordu province of Turkey. Technical and economic analysis are carried out based on the change in

government incentives on renewable sources before (Option A) and after 2021 (Option B) based on NPC and COE. It is found that Option A has the lowest NPC and COE values, which are estimated as $3.00 M and $0.098/kW, respectively. In the sensitivity analysis of HRES configuration, total NPC and COE values between nominal discount rate and biomass price generally increase, while the values between expected inflation rate and sellback rate are on a downward trend. Consequently, Scenario-4 has the lowest NPC and COE values, and the highest renewable fraction (RF) at around 73.6%, whereas carbon dioxide (CO_2) and nitrogen oxides (NO_x)emissions are lowest in Scenario-2.

Keywords: Co-firing, hybrid renewable energy system, net present cost, regression models, techno-economic analysis

ÖZET

Çeşitli Biyokütle Atıklarından Birlikte Yakma ve Fotovoltaik-Biyogaz Hibrit Sistemleriyle Enerji Üretimi

Yavuz KIRIM

Kimya Mühendisliği Anabilim Dalı

Doktora Tezi

Danışman: Prof. Dr. Hasan SADIKOGLU

Eş-Danışman: Prof. Dr. Mehmet MELIKOGLU

Tezin ilk kısmında, Türkiye'nin Konya, Erzurum ve İzmir illerinde bulunan çeşitli süt sığırı ahırları için biyogaz ve güneş fotovoltaik (FV) içeren modüler hibrit yenilenebilir enerji sistemleri (HYES) tasarlanır. Tasarım ayrıca teknik ve ekonomik analizleri de içermektedir. FV ve biyokütle dahil olmak üzere şebekeye bağlı sistemin, net bugünkü maliyet, (NBM) yatırım getirisi (YG), enerji maliyeti (EM) ve yıllık değer (YD) açısından tekli biyokütle sisteminden daha uygulanabilir olduğu bulunur. Farklı regresyon modelleri arasında, sırt regresyonu 0,92 ile en yüksek belirleme katsayısını (R^2) ve en düşük kök ortalama kare hata (KOKH) değerini 0,463 (milyon $) verir. Sonuç olarak, güneş enerjisinin toplam kurulu maliyetinin, %97 olarak hesaplanan GSYH üzerindeki etkisi bakımından elektrik üretiminin payı üzerinde en güçlü etkiye sahip olduğu tespit edilir.

Tezin ikinci kısmında, Ordu ilinde bir fındık kırma tesisi için güneş FV ve biyogaz birlikte yakma hibrit yenilenebilir enerji sistemleri tasarlanır. Teknik ve ekonomik analiz, NBM ve EM bazında yenilenebilir kaynaklara yönelik devlet teşviklerinde

2021 (A Seçeneği) öncesi ve 2021'den sonra (B Seçeneği) meydana gelen değişime dayalı olarak gerçekleştirilir. Seçenek A'nın sırasıyla 3.00 Milyon Dolar ve 0.098 Dolar/kW olarak tahmin edilen en düşük NBM ve EM değerlerine sahip olduğu bulunur. HYES konfigürasyonunun duyarlılık analizinde, nominal iskonto oranı ile biyokütle fiyatı arasındaki toplam NBM ve EM değerleri genel olarak artarken, beklenen enflasyon oranı ile geri satış oranı arasındaki değerler aşağı yönlü bir eğilim göstermektedir. Sonuç olarak, Senaryo-4 en düşük NBM ve EM değerlerine ve %73,6 civarında en yüksek yenilenebilir fraksiyona sahipken, karbon dioksit (CO_2) ve nitrojen oksit (NO_x) emisyonları Senaryo-2'de en düşük seviyededir.

Anahtar Kelimeler: Birlikte yakma, hibrit yenilenebilir enerji sistemi, net bugünkü maliyet, regresyon modelleri, tekno-ekonomik analiz

1 INTRODUCTION

1.1 Literature Review

Energy is one of the priorities of mankind in every field of life in past and present. Energy from fossil fuels has lost its influence due to the depletion of fossil resources and environmental problems. Renewable and sustainable energy sources are increasingly replacing fossil sources. Biomass, wind, solar, geothermal marine energy etc. have an important role in the energy supply of the future [1]. Biomass is more advantageous than other renewable energy sources since it is easy to access and store from various sources all year round. According to the estimates, biomass meets 10% of the world's energy demand in 2008, while it is estimated to be between 20% and 60% by 2050 [2]–[5]. In addition, the contribution of all biomass sources (agricultural, animal, forest and organic wastes etc.) to bioenergy is calculated theoretically by 1,100 EJ and this value is approximately three times the world's current energy requirement [6].

Biomass is the biodegradable bioenergy source produced by agricultural, animal and industrial resources, wastes, industrial, municipal and forest industry wastes. Biomass sources have the potential to be transformed from renewable raw materials into useful forms of energy (thermal energy, electrical energy and biofuels) through a wide range of process options and wide range of cycle technologies. Various biomass raw materials can be used as direct electrical energy or heat energy by using different processes or converted into solid, liquid and gas fuel form. Obtaining energy from waste biomass and organic matter differs according to different biomass types and sources, cycle type, end-use areas and infrastructure needs. [7]. Most biomass energy processes are suitable for direct conversion of biomass source to energy production or for transformation to intermediates [8].

Many studies have been carried out both off-grid especially for electric demand of remote areas and grid connected hybrid systems for generally commercial

purposes around world. Koroneos and co-workers analyzed solar, biomass and wind hybrid system to fulfil energy demand of Lemnos Island in Greece. They used optimization model to obtain minimum cost and environmental effects of hybrid system [9]. Fadaeenejad and colleagues reviewed renewable hybrid energy applied to decentralized villages for worldwide and Malaysia in order to understand present and future development. They deduced that photovoltaic (PV) and wind hybrid system backed up batteries efficient solution electrification of rural villages in Malaysia [10]. Sen and Bhattacharjee compared off grid and conventional grid extension using hydro power, wind solar and diesel system in hybrid optimization multiple energy renewables (HOMER). They concluded that hybrid system can be reasonable alternative to conventional grid extension in terms of technical and environmental applicability [11]. Bhattacharjee and Dey studied grid-connected hybrid system using PV and biomass hybrid system for rice mill facilities. They concluded that energy requirement of rice mill can be accounted for hybrid system with percentage of 90% [12]. Sigarchian and other academics analyzed comparison of standalone diesel energy system with biogas, PV and wind hybrid system to understand which system is more feasible option. They found levelized cost of energy (LCOE) and net present cost (NPC) of the hybrid system was 30% and 18% lower, respectively compared to standalone system [13]. Singh and Baredar studied off-grid renewable energy configuration to provide constant energy supply and minimize energy reliance on traditional system used tracking PV, biogas generator and battery storage system [14]. Ghenai and Janajreh carried out research to meet electric load of Sharjah combining solar and biomass resources. According to simulation and optimization analysis in HOMER, almost 14% of the total yearly electric demand of the city can be met by the 74 % of PV and 26 % of the biogas generator [15]. Rajbongshi and co-workers used PV-biomass hybrid energy system backup with diesel generator to provide energy to decentralized areas. LCOE of the area was found as $0.145/kWh in the case of peak load of 19 kW and energy demand of 178 kWh/day. LCOE of grid-connected system is lower with comparison to off-grid system. Combination of four renewable resource including wind, biomass, PV and small hydro system was used for the most feasible option. Among the various

configurations, solar-biomass system has more feasible LCOE which is $0.086/kWh [16]. Zala and Jain calculated energy demand of 300 houses in rural area of India using cattle manure (CM) as biomass source, PV and wind power to estimate financial viability of the hybrid system. They found least NPC with the configuration of 10.7 kW of PV panels, 2 kW wind turbine and 19 kW biogas generator with 332 kW storage capacity of batteries [17]. Eteiba and colleagues conducted technic economic analysis on PV/biomass hybrid system with various optimization techniques including flower pollination algorithm, harmony search algorithm, artificial bee colony algorithm and firefly algorithm to find feasible solution off-grid hybrid system. Among the algorithms, the firefly algorithm showed better performance with minimum execution time [18]. Mellouk and co-workers developed new parallel hybrid genetic algorithm- particle swarm optimization algorithm to investigate energy storage mechanism in micro grid systems. The study demonstrated that emission, energy demand and cost of the micro grid system are encouraging energy cost ($0.17/kWh) which is comparable with fossil fuel energy cost [19]. Pal and Bhattacharjee studied hybrid renewable energy system (HRES) system including PV and biogas plant energy sources using particle swarm optimization in rural area of India. They considered detailed biogas resource assessment and predicted optimum total net present cost (TNPC) and cost of energy (COE) [20]. Suresh and co-workers analyzed combination of solar, biomass, wind and battery system using genetic algorithm and HOMER pro software to reduce TNPC, COE, unmet load and carbon dioxide (CO_2) emissions. They found that solar/biomass/wind/fuel cell with battery configuration gave the 0% unmet load and lowest COE value, which is $0.163 per kWh [21]. Ji and colleagues investigated heat and power consumption of HRES system using mixed-integer linear programming optimization model for rural villages in the northwest of China to find the least total annualized cost [22]. Das and co-workers analyzed HRES that includes PV, wind turbine, biogas generator and vanadium redox flow battery for providing stable energy in rural area of Bangladesh. They used multi-objective optimization techniques to find optimum COE and emission values, and applied a fuzzy decision making technique for obtaining optimal solution [23].

Literature studies for HRES is scarce in Turkey. Some studies including Demiroren and Yilmaz, Turkay and Telli, Kalıncı and co-workers, Gokcek and Kale, Mert and colleagues, and Aykut and Terzi analyzed generally region specific HRES design [24]–[28]. However, with the regulation issued by the Energy Market Regulatory Authority (EMRA) on March 8, 2020, investments in HRES can be expected to increase [29].

Co-firing of biomass instead of direct combustion has significant environmental and economic benefits for electricity generation. The following studies found from the literature focuses on solar and biomass and based HRES system design but for our knowledge few of them focusing on biomass co-firing in HRES system. Islam and co-workers analyzed HRES system consisting of PV panels, biomass generator, battery and converter using rice husk as biomass source in rural area of Bangladesh. They observed that, COE of PV panels and biomass generator configuration is much higher than regulated tariff in Bangladesh [30]. In addition, emission of CO_2 in that configuration produced 75% lower CO_2 than emission from national grid [30]. Alotaibi and co-workers studied hybrid energy system including configuration of co-firing and diesel generator, PV solar array and batteries in order to estimate optimum NPC and COE using a hospital waste in Saudi Arabia. They found that the optimum NPC and COE were $244,000 and $0.210/kWh, respectively [31]. In another study, Jahangir and Cheraghi analyzed HRES including of PV panels, wind turbine and biogas generator in Fars province, in Iran. They used HOMER pro to find optimum system design based on NPC and COE. The most optimal system in their study is a biogas generator (150 kW), PV panels (80.7 kW), batteries and converter [32]. Malik and colleagues studied techno-economic and environmental analysis of off-grid hybrid energy system. The contribution of biomass generator and PV panel 59% and 41%, respectively. They also found that saving of 27.8 million tons CO_2 per year was obtained compared to diesel only system [33].

1.2 Objective of the Thesis

In this thesis study, it is aimed to contribute to Turkey's energy deficit with the hybrid system by using the potential of biomass and solar energy. For this purpose,

technical and economic analysis of biomass and solar energy production is made by using the roofs and CM of 50 or more dairy cattle barns. NPC, COE and annual worth (AW) are based on economic metrics in the technical and economic analysis. Thirteen independent variables including AW of modular systems are also used to estimate the contribution of electricity generation to Turkey's gross domestic product (GDP) in the modular HRES. The optimal R^2 and root mean squared error (RMSE) values are found by using linear, ridge, lasso and elastic net regressions to estimate this contribution. Moreover, technical and economic analysis of electric energy production with hybrid system is combined co-firing of the hazelnut shell, together with NG and the solar energy. PV panel and co-firing of hazelnut shell and NG for electricity production are analyzed technically and economically. Here, it is aimed to meet the energy needs of an exemplary hazelnut cracking plant (HCP) with a hybrid system and to sell the excess electrical energy to the national grid.

1.3 Original Contribution

CM and the PV panel system installed on the roof is the first HRES that has been examined technically and economically in the world and in Turkey. In this study, the contribution of the energy potential of dairy cattle barns in Turkey to generate electricity is also examined econometrically. From an economic feasibility point of view, it is seen that modular dairy cattle make a profit in terms of NPC and COE. Thus, it can contribute to the conversion of other renewable energy sources from by-product to energy and increase the number of HRES in Turkey. In the same way, combination of hazelnut shell co-fired with NG and PV panel in HRES is first studied in literature and its results shows that this HRES system is feasible in terms of NPC and COE. This co-firing supported HRES both meets the electrical energy of HCP and profits from selling the excess electricity to national grid. Also, using the hazelnut shell for electricity generation instead of using it for heating purposes in rural areas or making pellets will be beneficial in meeting the energy needs of other hazelnut cracking or integrated facilities. With all these aspects, the thesis study presented is an original study.

2
ELECTRICITY GENERATION FROM BIOMASS RESOURCES

2.1 Biogas Production from Biomass and Its Use in Electricity Generation

Increasing energy demand due to the increase in world population and the emergence of environmental problems caused by fossil fuels has increased the interest in renewable energy resources. Biogas, one of the best renewable energy sources in this regard, is a suitable option in internal combustion generators, micro-turbines, fuel cells and other energy production plants to provide heating and electrical energy [34]. Different types of biomass wastes such as agricultural and animal waste, domestic and industrial food waste, etc. are broken down in an oxygen-free environment to form CO_2 and methane gas. Methane production from organic waste with anaerobic digestion has many advantages. It reduces global warming and acid rain formation, minimizing odor problems and animal-based biogas raw material can be used as fertilizer in agriculture and can contribute to social and economic development in rural areas [35]. However, it has some disadvantages such as low biogas yield, retention time, continuous raw material source problem, high investment cost and high maintenance and operating costs [36].

Biogas was first used in the Asian continent for heating purposes 2000 years ago. In the early and mid-1900s, it was used as bio methane in gas distribution networks and compressed as vehicle fuel [34]. The technological developments in biogas production and the positive contribution to the reduction of greenhouse gases emissions have made the biogas popular again in the world although fossil fuels have lost their importance until the oil crisis in the 1970s due to the cheaper prices. America, the UK and Germany are the global players and more than 50% of the biogas plants in the world are located in these countries. It is estimated that the installed biogas capacity in the world will be 22,040 MW by 2025 [34].

Turkey's waste biomass potential is estimated to be approximately 8.6 million tons of equivalent oil (toe). The biogas potential to be produced from this waste is estimated to be 1.5-2 million toe [37]. However, this energy potential is not utilized at the desired level. The first attempt in biogas production was established by the Ministry of Energy and Natural Resources, where a pilot plant was used as a raw material for animal manure, but the facility was closed down in 1987[38]. According to report released by Turkey Energy Affair General Directorate, first commercial electricity production from landfill waste is produced by ITC-KA Company in 2007. While from 2007 to the first quarter of 2019, biogas investments are generally aimed at generating electricity from landfill waste, organic, industrial, agricultural, animal and forest products wastes related facilities were started to be established after 2010. Total electricity generation from bioenergy sources including solid biofuels, biogas, municipal waste and liquid biofuels reached 1300.2 MW in 2020 [39].

2.2 Electricity Generation from Animal Wastes

The treatment of livestock wastes in power plants contribute to the environment in a positive way. Animal waste produced from the animal husbandry is mostly used as fertilizer. The usage of fertilizer causes serious environmental impact such as leakage of nitrate and phosphate into soil and water. In addition, the storage of animal manure at waste sites increases the release of one of the most important greenhouse gases (methane) and has a negative impact on global warming. Instead of being used directly as a fertilizer or as a fuel source, these livestock wastes can be burned together with fossil resources to produce heat and electric energy and can be used to produce biogas via anaerobic digestion.

Biogas production from livestock wastes worldwide is becoming increasingly popular. For example, to achieve higher methane efficiency in large-scale biogas plants in Denmark, biogas is obtained via anaerobic digestion by mixing animal waste and organic industrial wastes. However, a small number of biogas plants in Denmark cannot provide more economic benefits from the non-digestible part of the animal waste in the liquid mixture, whose concentration in anaerobic digestion is increased, results in a low level of biodegradation. In order to increase

biogas efficiency in Denmark, it is recommended to use energy plants such as corn, sunflower, grass and water grass that increase biogas efficiency in Germany and Austria [40]. Thanks to the Austrian Green Electricity Act, incentives for the establishment of a plant producing biogas from agricultural and animal sources are encouraged. Biogas is an attractive material as a raw material, because animal waste density is sufficient in most regions of Austria.

It is an attractive raw material for the production of biogas, as animal waste is sufficient in most regions of Austria. In addition, biogas raw materials are used in biogas plants to increase the methane yield. These raw materials includes corn (36%), animal waste (24%), biological waste (12%), meadow silage (10%), agricultural wastes (9%), grain silage (7%) and other energy plants (2%) [41]. Portugal's annual heat and power output from livestock waste is 363 GWh and 725 GWh, respectively. However, in Portugal, the share of animal waste in biogas power generation is less than 1%, mainly due to inconsistent policies in waste management and in reducing the size of research that makes energy production impossible [42]. Spain is Europe's fourth largest animal waste producer with 118 million tons of waste. In Spain, only 0.69% of animal waste produced in 2011 was treated by anaerobic digestion.

Slow developments in the biogas industry stem from national policies in Spain. There is no specific support scheme for heat and power generation from biogas in Spain today; as a result, biogas energy does not attract investors' attention [43]. Germany has been promoting biogas production since 1990 and is the largest biogas producer in Europe [44]. According to the 2013 data, there are 9,035 biogas plants in Germany and the installed capacity of the plants is 3543 MW. 87% of these facilities use energy plants as raw materials while the remaining part consists of waste sludge, industrial wastes and bio-waste [44]. The Renewable Energy Act, which came into force in 2000, promotes electrical energy from biogas. However, with the law changed in 2012, biogas production from the primary raw material (such as corn and grain) was restricted and government incentives was provided to animal farms which produce biogas to increase biogas production in rural areas [44]. Italy, which ranks second in Europe in biogas production, accounts for 80% of its biogas production from agricultural resources,

about 18% from waste and the rest from waste sludge. However, in 2013, with the law changed, agricultural and animal wastes are encouraged for the plants smaller than 500 kW and the share of energy crops is tried to be reduced [44]. Compared to Germany and Italy, France has fewer biogas plants. The reason is that the amount of government incentives given is low compared to the other two countries. France meets most of its raw material needs from energy crops and other parts from waste and organic industrial wastes. In France, the energy incentive for the production of biogas from animal waste is limited to at least 300 kW and not more than 1,000 kW [44].

In order to reduce CH_4 emissions, the United States (US) promotes the production of biogas from livestock waste within the framework of the Agstar program. Within the framework of this program, more than 8,000 bovine farms produce energy at 16 million MWh per year [45]. Biogas has been used in the fields of electricity and combined heat and power production between 2000 and 2013. Heat and power production produced from farm animal waste continued to increase although electricity production decreased between 2013 and 2018 [45]. In Chile, farm-based anaerobic digestion technology has been progressed slowly. Total biogas production reached 0.4 PJ/year in 2011 [44]. Small-scale businesses using CM as raw materials have spread to different parts of Indonesia [44]. These biogas plants were not provided with adequate government support. Thailand's biogas potential is 70 TJ and the country uses biomass raw material as farm animal waste, agricultural industry waste and waste sludge. Although biogas is produced from agricultural wastes of 1,000 million m^3 annually, only 36% of biomass potential is utilized [46].

Animal wastes in Turkey are mostly used for heating purposes in rural areas, government incentives in recent years to the production of biogas and electricity purchase guarantee is to promote the production of biogas. Biogas production from agricultural and animal waste showed considerable increase after 2010 while biogas generation mainly obtained from landfill waste at the first stage. In 2019, the amount of installed power produced from biogas plants using these raw materials reached 218 MW [47]. According to the report of the International

Energy Agency, biofuels and energy derived from waste meets approximately 0.6% of Turkey's energy requirement [48].

2.3 Co-Firing Technology for Energy Generation

Instead of burning biomass directly and generating electricity, using co-firing technology to produce electricity is increasing its popularity all over the world [49]. Recent research conducted in Europe and the US showed that biomass burned along with fossil fuels had a positive effect on both the environment and the energy production economy [50]–[53]. As the net CO_2 production of biomass is zero, the CO_2 emissions of biomass are less than conventional coal-fired combustion plants. It has been seen that in many combustion tests performed, nitrogen oxide (NO_x) and sulfur dioxide (SO_2) emissions decreased due to biomass raw material [54]. It does not require large capital investment since co-firing technology uses the infrastructure of an existing coal-fired combustion plant, as a result, investments in infrastructure are saved and increase the supply of biomass. In addition, co-firing technology is a less risky option for renewable energy generation because the risks associated with raw material supply and large capital investment are less than those of other alternative uses of biomass [44]. As a result, thanks to all these advantages, biomass raw materials in various forms have been burned in existing coal and gas-fired boilers in the last decade and bioenergy has been obtained with co-firing technology [55].

Biomass co-firing process has a wide range of applications in many developed and developing countries [56]. More than 150 coal fired plants, woody biomass and other waste biomass raw materials, which is mostly in the 50 MWe-700 MWe range, have been tested or harmonized together with co-firing technology [57]. Co-firing technology has successfully adapted the use of powder-fired burners, fixed and fluidized bed burners and grate boilers [58]. Optimal co-firing rates for selected combustion mixtures of biomass and coal must be specified taking into account the costs and performances of the installation [59]. Co-firing of more than 20% of the biomass with coal on energy basis is technically feasible. Besides; the co-firing level in many commercial applications is up to 5% to 10% on energy basis [59]. In order to control furnace efficiency and production, biomass particle size,

biomass injection rate, thermal and fluid-dynamics behavior and burner design are important. Mostly, after adjusting the combustion efficiency for the new fuel mixture, little or no loss was detected in the overall efficiency of the boiler types used for co-firing of biomass [59]. The net electrical efficiency of the co-firing plant with a typical biomass ranges from 35% to 44% [60].

Co-firing technologies in different regions of the world have been studied in detail by various researchers. After 2002, several coal-fired power plants were adapted with the co-firing technology. In the UK, in 2002, 286 GWh of electrical energy was produced with co-firing technology and met 2.57% of the UK's renewable energy production. In 2011, electricity production rose to the highest level of 2,964 GWh and met 6.45% of the renewable energy generation. However, co-firing technology has lost its importance due to changes in the legal regulations on renewable energy sources after 2016 [44]. The Netherlands had been providing state support to the combined heat and power plants and the local producers for wholesale electricity prices for wood pellets, agricultural waste and mixed biomass raw materials before 2009. With the agreement between the Dutch government and the private sector after the second half of 2013, incentive for co-firing technology was increased by providing state-of-the-art support to co-firing plants with an annual capacity of 25 PJ. Then, with the Sustainable Energy Production Support Program covering the years 2015-2023, it will continue to provide money to this agreement [44]. In spite of these supports, many problems for the co-firing technology in the Netherlands are still up-to-date. For instance, wood pellets are often used with coal, and about 70% of this is imported in co-firing plants. Besides, transportation costs of biomass, low energy value and corrosion in the boilers, slag formation and contamination are among the problems of co-firing technology. There are 30 co-fired plants in Germany, of which 13 are operated with mixed fuel. The co-firing plant uses more than 50% sludge as biomass, as well as other important biomass sources, such as straws, waste wood and organic residues [44]. However, the reasons such as the supply problem of the raw material, the variability of the raw material depending on the season, the difficulty of the procedure required to obtain the operation license of the co-firing plants are seen as obstacles to the burning technology in Germany.

Denmark's goal for 2050 is to supply 100% of its energy from renewable energy. In line with this target, it planned to meet 30% of its energy from renewable energy up to 2020 and to reduce the greenhouse gas emissions to 20% and to achieve the emission level in 2005 [61]–[63]. To achieve this goal, wind and biomass resources are mostly used. There are 5 co-incineration plants in Denmark. The main raw material of these facilities is the straw, wood chip and wood pellet. Public Service Obligation provides state support to consumers' electricity bills, energy research, combined heat power cycle plants and energy systems development [64]. Among other European countries including Finland, Sweden, Russia, Belgium, Austria, Hungary Italy and Spain have also been used co-firing technology. In Finland, co-firing plants generally use wood and peat coal has a significant share. Belgium began to produce electricity from co-firing technology after the Green Certificate System came into force [44]. There are 5 co-incineration plants operating in Belgium, and olive pulp, wood chip and pellet are used as raw materials combustion technology first started in 1991 in Austria. There are a total of five co-firing plants, four of which work with direct combustion and one indirect operation, and usually pulverized coal and bark are used as raw materials. In Sweden, there are 9 co-firing plants, although there is little energy from coal-based plants. The electric energy produced from the co-firing plant in Hungary has reached 1,309.5 GWh in 2012 and it increased the electricity generation capacity to 2,688 GWh in 2020. In Italy and Spain, there are four co-firing plants in total [44].

40 of 560 coal co-firing plants have switched to co-firing technology, which tends to increase in the future although coal has the largest share in electricity generation in US [65]. The most important raw materials of co-firing plants are wood products and railway travers. In Canada, there are direct-type co-firing plants with a capacity of 2,500 MW. Domestic and municipal wastes, agricultural and forest products are used as biomass raw materials in co-firing plants [66]. Although Brazil is the largest agricultural producer in the world, there is only one co-firing plant with a capacity of 50 MW because existing facilities are far away from biomass raw material. Between the years 2013-2016, the Argentine Ministry of Agriculture and Federal Planning and the United Nations Food and Agricultural

Organization agreed on the conversion of forest, animal manure and agricultural waste. In this context, they planned to convert 12 million tons of biomass to bioenergy and to increase the electricity energy of Argentina from biomass to 10%. In Peru and Bolivia, although there is sufficient biomass raw material for the co-firing plant, there is no existing facility [44].

In Japan, there are 12 co-firing plants that are tested and operated in total. These plants primarily use forest residues at 2-3% to incinerate and co-fire with coal. The Japanese government estimates that by 2030, 27% of Japan's electricity production is expected to be supplied by coal and 3.7-4.6% by biomass. South Korea imposed 2% of the electricity produced from renewable energy sources in 2012. Furthermore, it planned to increase this rate to 10% by 2022. For this reason, South Korea focuses on co-firing technology and has set an annual biomass requirement of 10 million tons per year [44].

In different parts of the world, for example, China, Malaysia, Thailand and Taiwan have energy by burning wood bark, wood pellets, peat coal, vegetable oil and sludge in the co-firing plants. However, these facilities are generally small and medium-sized processes [44].

2.4 Solar Energy in Electricity Generation

Solar energy is one of the alternative clean energy sources compared to fossil energy sources. Studies on solar energy intensified in the 18th and 19th centuries, and the first solar energy company was established in the US in 1900 [67]. The energy crisis that started in the 1970s has increased the importance of solar energy and solar power plants have become widespread since the 1980s. The importance of solar energy has increased with the government incentives given to photovoltaic cell production and solar power plant installation [67]. Considerable amount increase in installed capacity of solar energy which is 41,600 MW has started around world in 2010 and it has reached to 716,153 MW in 2020 [68]. China has the world's largest capacity of solar plant with an installed power of 253,834 MW in 2020. The US, Japan, Germany and India which have 75,572 MW, 68,665 MW, 53,783 MW and 39,212 MW, respectively, are the other countries that possess high installed capacity of solar energy plant [68]. The installation of solar power

plants has been encouraged in Turkey with the support law for renewable energies, which entered into force in 2005. Installed capacity of solar plant in Turkey was 12 MW in 2012, however this capacity reached to 6,668 MW in 2020 [68].

Turkey has a high solar energy potential due to its geographical location. The average daily and annual sunshine duration is 7.2 hours and 2,640 hours, respectively, and the average total radiation intensity is 3.6 kWh/m^2 per day and 1,311 kWh/m^2 per year, respectively [69]. The sunniest period in Turkey is in July and the least in December, and the Central Anatolia and Southeast Anatolia regions are the most suitable places in terms of sunshine duration [69]. With the "Law on the Use of Renewable Energy Sources for the Purpose of Electric Power Generation", which was enacted in 2005, the share of solar power plants in total electricity production increased to approximately 4% in 2020 with the government incentives to solar energy [70]. As of the second half of 2021, the amount of incentives given to solar energy has been changed to Turkish lira and the duration of the incentive has been reduced from 10 to 5 years [71]. The decline in government subsidies may lead to a reduction in the installation of solar power plants and may encourage the installation of new generation plants such as hybrid systems.

2.5 Biomass and Solar Hybrid Energy System for Electricity Generation

Energy generation from biomass and solar energy sources offer many advantages however some issues such as low efficiency compared to conventional energy sources, higher capital cost, climatic conditions and reliability of supply affects construction of renewable energy plants [72]. Using biomass and solar resources alongside with conventional energy sources such as diesel and natural gas (NG) can provide partial solution to some of the issues associated with standalone energy systems [23]. Many governments promote utilization of renewable energy sources by supporting feed in tariffs, tax incentives and subsidies [73]. Turkey also provides subsidies for renewable energy sources by supporting lower feed in tariffs for producers to sell electricity to the national grid. Until 2021, Turkish

government's incentives for solar and biomass energy attracted significant number of investors. HRES often consist of one or more renewable energy sources together with a battery system or grid connected system. HRES can be used independently of the national grid to meet the energy demand in rural areas. Detailed analysis of the HRES design consisting of solar PV and biogas on a provincial basis (Turkey) is quite scarce in the literature. Therefore, there should be a need for detailed study on this thesis.

3
DATA AND METHODOLOGY OF MODULAR HYBRID SYSTEM DESIGN

3.1 Economic Parameters in HOMER

HOMER 3.13.7 Pro Edition software is applied for design, optimization and sensitivity analysis in this study. It provides sensitivity analysis option to understand changes that impact on NPC of the particular system [74]. The other economic indicators used for this study is explained in subsection below.

3.1.1 Initial Capital Cost

The initial capital cost represents total amount of component at the beginning of the project including equipment and installation cost. In the hybrid systems, civil work, installation cost, and electric connections and testing are the components of the initial capital cost [75].

3.1.2 Replacement Cost

The replacement cost means that if a component completes economic life, the new one is replaced. It differs from initial capital cost as only some part of the component may require replacement. It may differ from initial capital cost in terms of some reasons [74]:

- Some component of the hybrid system may not require replacement at the end of their life.
- The initial cost may be decreased or minimized by subvention while replacement cost may not be reduced.

3.1.3 Operation and Maintenance Cost

Operation and Maintenance (O&M) cost is the overall scheduled cost for life time operation and maintenance of the facility. O&M cost is mainly entered as an annual amount but some component is in hourly basis such as generators. O&M cost for the grid is annual power purchase from grid minus revenue from the sell electricity to the national grid. System fixed O&M cost, and penalties including

emission and capacity shortage is classified as the other O&M costs in HOMER. Other O&M cost can be calculated as using equation (3.1) [74]:

$$C_{om,other} = C_{om,fixed} + C_{cs} + C_{emissions} \tag{3.1}$$

$C_{om,other}$ (\$/yr) is the hybrid system fixed O&M cost, C_{cs} capacity shortage penalty (\$/yr) and $C_{emissions}$ (\$/yr) is emission penalty per year.

3.1.4 Salvage Value

This value represents remainder in a part of the energy system at the end of the project lifetime. HOMER presume that the salvage value which is calculated in equation (3.2) only subjects to replacement cost [74].

$$S = \frac{C_{rep} R_{rem}}{R_{comp}} \tag{3.2}$$

S (\$) represents salvage value of the hybrid system, C_{rep} (\$) is the replacement cost of component for hybrid system, R_{rem} is the component remaining life and R_{comp} (yr) defined as lifetime of the component.

3.1.5 Annualized Cost

HOMER associates the capital, replacement, maintenance, fuel costs and other costs with the revenues and salvage values of each component in order to calculate annualized costs of the components. This annual cost which is calculated in equation (3.3) is suppositional cost that if taken place every year of the project lifetime, it would give a NPC equivalent to that of all the individual costs and revenues combined with that component along the project lifetime [74].

$$C_{ann} = CRF\left(i, R_{proj}\right).C_{NPC} \tag{3.3}$$

C_{ann} (\$) is defined annualized cost, $CRF()$ is capital recovery factor, i is annual real interest rate (%), R_{proj} is project lifetime (yr), and C_{NPC} is net present cost.

3.1.6 Operating Cost

The operating cost which is calculated equation (3.4) covers the annualized value of all costs and revenues except the initial capital cost [74].

$$C_{operating} = C_{ann,tot} - C_{ann,cap} \quad (3.4)$$

$C_{operating}$ ($/yr) is defined as operating cost, $C_{ann,tot}$ ($/yr) is total annualized cost and $C_{ann,cap}$ total annualized capital cost ($/yr). Total annualized cost is equal to:

$$C_{ann,tot} = C_{ini,tot} \times CRF() \quad (3.5)$$

$C_{ini,tot}$ ($) is defined as total initial cost and $CRF()$ is capital recovery factor.

3.1.7 Cost of Energy

COE is defined as average cost per kWh of beneficial electrical energy generated by the system. COE is calculated in equation (3.6) via dividing annualized cost of producing electricity by the total electric load served [74].

$$COE = \frac{C_{ann,tot}}{(E_{prim} + E_{def} + E_{grid,sales})} \quad (3.6)$$

COE ($/kWh) is defined as cost of energy, $C_{ann,tot}$ is total annualized cost ($), E_{prim} is total amount of primary load (kWh/yr), E_{def} (kWh/yr) is total amount of deferrable load and $E_{grid,sales}$ (kWh/yr) is the amount of energy sold to the grid.

3.1.8 Net Present Cost

NPC of a power system is the difference between the present value of the costs incurred during the life of the system and present values of the revenues. Calculation of NPC is given in equation (3.7) [74].

$$NPC = C_{ann,tot}/CRF_{(i,Rproj)} \quad (3.7)$$

NPC ($) is defined as net present cost, $C_{ann,tot}$ ($) is the total annualized cost, i is annual real interest rate (%) (discount rate), R_{proj} is (yr) project lifetime and $CRF_{(i,Rproj)}$ () is the capital recovery factor (CRF). CRF is given in equation (3.8):

$$CRF(i,N) = \frac{i(1+i)^N}{[i(1+i)-1]} \quad (3.8)$$

i is annual real interest rate (%) and N (yr) is the number of years.

3.1.9 Return on Investment

ROI is the cost savings with respect to the initial investment. In other words, it is found by dividing the average difference in nominal cash flows over the duration of the project by the difference in capital cost[74]. The calculation of ROI is given in equation (3.9)[74].

$$ROI = \frac{\sum_{i=0}^{R_{proj}} C_{i,ref} - C_i}{R_{proj} - C_{Cap,ref}} \tag{3.9}$$

ROI(yr) is defined as return on investment, $C_{i,ref}$ ($) is nominal annual cash flow for base (reference) system, C_i ($) is nominal annual cash flow for current system, R_{proj} (yr) is project lifetime in years and C_{cap} ($) is Capital cost of the current system.

3.2 Solar Energy

Solar data of Konya (37° 51.6' N latitude and 32° 28.8' E longitude), Erzurum (39° 54' N latitude and 41° 16.2' E longitude) and İzmir (38° 25.4' N latitude and 27° 8.6' E longitude) are used in this study. The source of data is obtained from the National Aeronautics and Space Administration's (NASA) surface solar energy set using HOMER database [76]. Average annual daily radiation for Konya, Erzurum and İzmir are found as 4.64, 4.57 and 4.68 kWh/m^2/day, respectively [76]. Daily radiation and clearness index of Konya, Erzurum and İzmir are shown in Figure 3.1. Monthly solar source for Konya, Erzurum and İzmir are summarized in Table 3.1.

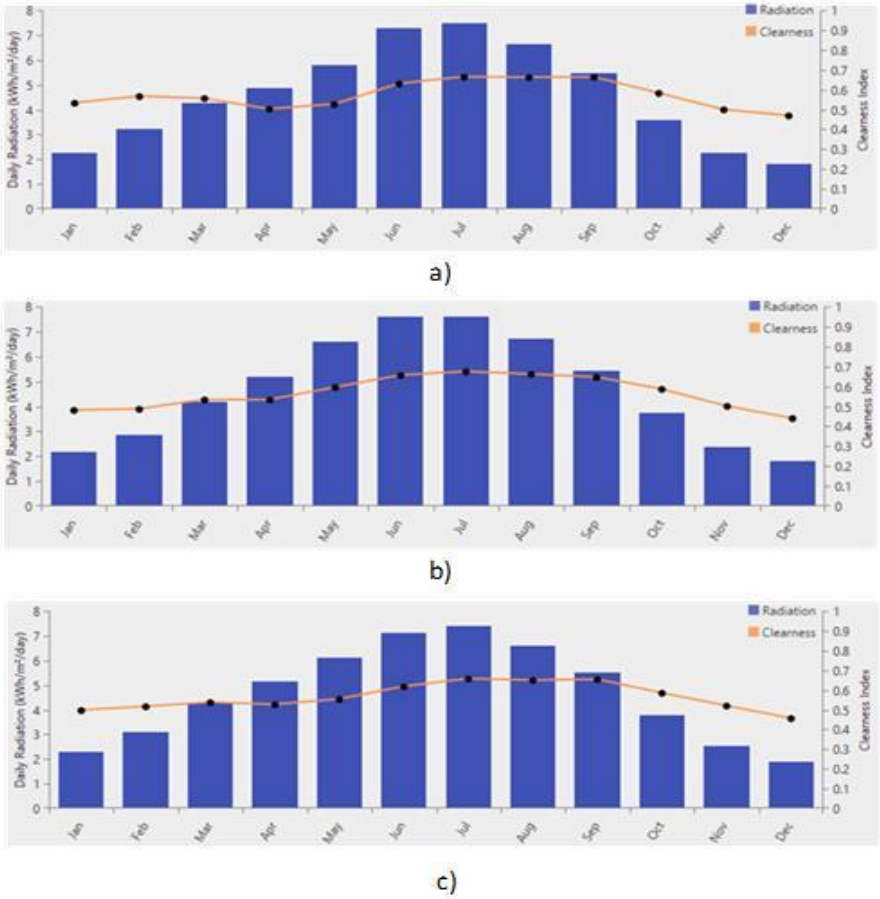


Figure 3.1 Daily radiation and clearness index of a) Konya, b) Erzurum and c) İzmir

Table 3.1 Monthly solar sources of Konya, Erzurum and İzmir

Konya			Erzurum			İzmir		
Month	**Clearness Index**	**Average Radiation** $\left(\frac{kWh}{m^2 day}\right)$	**Month**	**Clearness Index**	**Average Radiation** $\left(\frac{kWh}{m^2 day}\right)$	**Month**	**Clearness Index**	**Average Radiation** $\left(\frac{kWh}{m^2 day}\right)$
January	0.495	2.280	**January**	0.531	2.260	**January**	0.479	2.160
February	0.515	3.090	**February**	0.565	3.210	**February**	0.485	2.870
March	0.536	4.260	**March**	0.554	4.270	**March**	0.532	4.190
April	0.525	5.160	**April**	0.501	4.850	**April**	0.531	5.200

Table 3.1 Monthly solar sources of Konya, Erzurum and İzmir (continued)

May	0.552	6.120	**May**	0.525	5.800	**May**	0.594	6.580
June	0.616	7.130	**June**	0.628	7.280	**June**	0.654	7.580
July	0.656	7.390	**July**	0.662	7.460	**July**	0.673	7.580
August	0.647	6.590	**August**	0.660	6.650	**August**	0.660	6.700
September	0.652	5.510	**September**	0.662	5.450	**September**	0.645	5.410
October	0.583	3.770	**October**	0.581	3.580	**October**	0.585	3.730
November	0.519	2.520	**November**	0.498	2.250	**November**	0.499	2.380
December	0.455	1.900	**December**	0.468	1.790	**December**	0.439	1.790
Average	0.563	4.640	**Average**	0.570	4.570	**Average**	0.565	4.680

3.3 Biomass

In this study, CM is selected as the raw material (biomass) for biogas generation. In Turkey, there are nearly nine different breeds of dairy cattle [77]. The live weights of these animals differ according to their breeds. Daily manure generation (kg/day) is calculated based on the average of female live weight. Then, calculated average live weights are multiplied by 5.5% of their live weights. Adult live weights of these cattle and average daily manure generations are reported in Table 3.2. It is assumed that the average amount of CM produced per cattle per day is nearly 5-6% of its live weight [78].

Table 3.2 Adults live weights of dairy cattle and average daily manure generations [77]

Cattle breeds	Female live weight (kg)	Average daily manure generation (kg/day)
Anatolian Grey	375	23
Anatolian Black	200	13.7
South Anatolian Yellow	197	13.8
Simmental	1100-1400	55
Holstein	600	44
East Anatolian Red	323	19.7
South Anatolian Red	610	28.7
Brown Swiss	600	36
Jersey	330-400	21

3.4 Load Profile

Scaled data is used for computing primary load in HOMER in order to generate scaled data, HOMER multiplies each of the 8,760 baseline values by a common factor giving the annual average value. Scaled annual average is divided by

baseline annual average to find scaled data value. Even if the hourly load demand for a month is entered in HOMER, it calculates the average 24-hour load profile for the all year. This load profile can be more realistic-looking using random variability option. To find primary load data for different scale of dairy cattle barns, the electrical load of a typical farmhouse with 50 dairy cattle is based on. There are two electric loads for the farmhouse. Daily electricity loads are calculated as 9.081 kWh and 4.580 kWh for the house and barn, respectively [79]. Hourly load profiles of farmhouse and animal barn are shown in Table 3.3.

Table 3.3 A typical farmhouse daily electric load and dairy cattle barn electric load [79]

A Typical Farmhouse Daily Electric Consumption			
Household Electrical Appliances	**Power (W)**	**Daily Usage Hours**	**Energy Consumption (kW)**
Lamp (6 pcs)	23	4	0.552
Dishwasher	1800	0.5	0.9
Washing Machine	800	0.5	0.4
Refrigerator	40	24	0.96
Butter Machine	200	1	0.2
Vacuum Cleaner	1600	0.5	0.8
Iron	2200	0.5	1.1

Table 3.3 A typical farmhouse daily electric load and dairy cattle barn electric load (continued)

TV	100	4	0.4
Computer	100	4	0.4
Phone Charger	9	1	0.009
Electric Water Heater	2000	1	2
Oven	2000	0.1	0.2
Deep Freeze	40	24	0.96
Hair Dryer	1000	0.5	0.5
		Total Energy Consumption	**9.081 (kWh)**
Dairy Cattle Barn			
Barn Equipment	**Power(W)**	**Daily Usage Hours**	**Energy Consumption(kW)**
Lamp (10 pcs)	23	3	0.69
Water Pump (2 pcs)	745	2	1.49
Milking Machine (2 pcs)	600	2	1.2
		Total Energy Consumption	4.58 (kWh)

3.5 Modeling and Sizing of HRES

Three cities with the largest number of dairy cattle are selected for the solar and biomass hybrid system. With reference to these cities, solar and biomass hybrid energy potential of Turkey are theoretically estimated. To do this, different size of hybrid model configurations is demonstrated based on the size of the dairy cattle barns. The size of 50, 100, 500, 1000 and 5000 dairy cattle barns are considered in this proposed study. In this system, solar and biomass are selected as the primary energy sources. For animal health and welfare, it is recommended to have a maximum of 80 to 100 cattle in a barn [80], [81]. Therefore, a modular system design with 100 cattle in each barn is accepted for 500, 1000 and 5000 cattle barns. The load demands of animal barns containing more than 100 dairy cattle are obtained by multiplying them in direct proportion to the number of animals. The system is designed without energy storage as it is directly connected to national grid system. Working principle of the system is based on both sale power to grid and purchase from the grid if needed. Five different size of the system configuration including biomass generator, PV, converter, two electric load and grid components are illustrated in Figure 3.2. The cost of all components are in US dollars. Four different sensitivity input are used for five HOMER configurations. Amount of CMs are calculated taking average value of widely grown dairy cattle breeds in Turkey. These values are calculated as 0.7, 1.1, 1.5 and 2.5 tons for a barn with a capacity of 50 animals and multiples of this value are taken for barns with other barn capacity. Grid sale capacity are chosen based on the peak demand of the system configurations. Based on the inflation rate for December 2019 (11.87%), four different sensitivity variables (9.00%, 11.87%, 15.00% and 20.00%) are used for all HOMER configurations [82]. Similarly, based on the discount rate of December 2019 (12.50%), four different sensitivity variables (10.00%, 12.50%, 15.00% and 18.00%) are used for all HOMER configurations [83].

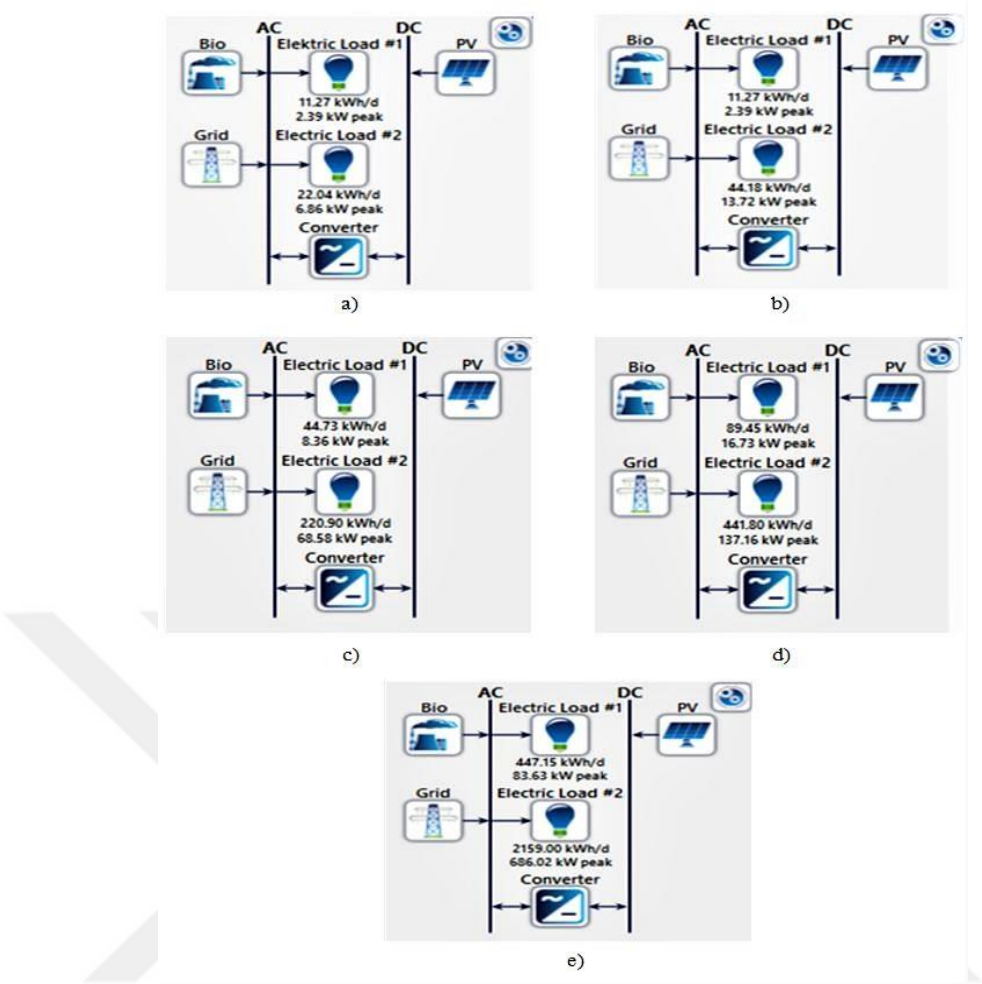


Figure 3.2 Five different size of the system configurations a) 50 b) 100 c) 500 d) 1000 e) 5000) including biomass generator, PV, converter, two electric load and grid components.

3.5.1 Photovoltaic Panel

The required capacity of PV panel for rooftops of the cattle barn are calculated using HOMER optimizer advanced option tab. In the advanced tab, lower and upper limit of PV capacity are chosen then HOMER calculates optimum required capacity of PV for both winning system architecture and base case architecture. Capital, O&M cost of PV per kW are calculated based on the feasibility studies published by Mevlana Development Agency. The per W capital cost of the PV panel is $ 3.140 and O&M cost is $ 0.021 [84]. Thus, capital cost and O&M of the PV panel are taken $ 3,140 and $ 21 per kW respectively [84]. Replacement cost of the PV panel is calculated based on the US National Energy Laboratory data. This cost is calculated by summing component part replacements (4.550 $/kW year), module replacement (0.820 $/kW year) and inverter replacement (10 $/kW

year) [85]. Total replacement cost of the PV is taken $15.370 per kW. The lifetime of the PV is taken 25 years (not considering tracking or concentrating system) and derating factor is assumed to be 80%. The ground reflectance is taken 20% and temperature effect is neglected.

3.5.2 Biomass Generator Inputs

Default biomass generator offered by HOMER is used in this study. Capital, replacement and O&M cost of the generator are taken 3,000 $/kW, 1,250 $/kW and 0.100 $/kW/op. hr respectively. Unlike other components, the lifetime of the generators is specified as operating hours. Minimum load ratio is taken 50 % and the lifetime of the generator is chosen as 20,000 hours. Search space tab is used to find optimum generator capacity.

3.5.3 Converter Inputs

Cost of the converter per kW taken from HOMER default cost system for both capital and replacement are $300 and O&M cost are taken zero. HOMER optimizer advanced option is used to calculate optimum capacity of converters. All converters size is arranged properly to satisfy peak demand of the farmhouse and dairy cattle barns. Lifetime and efficiency of the converters are taken as 15 years with 95% efficiency, respectively.

3.5.4 Grid Inputs

HOMER provides four different grid options namely simple rates, real time rates, schedule rates and grid extension. Scheduled rates option is chosen, and power price and sellback price is assumed to be constant. Working principle of the grid is arranged according to simulation of the system with and without the grid and net metering option, which is briefly energy purchased minus energy sold, is chosen. According to the “Law of the Ministry of Energy and Natural Resources on the Use of Renewable Energy Sources for Electrical Energy Production,” the government's purchase support per kW for biomass and solar energy is $ 0.133 [86]. Electric purchase price from grid for 2019 is taken $0.088 [87]. Grid extensions cost and distributed generation costs are neglected. Sensitivity variables are considered to find most feasible grid sale and purchase capacity for different system configurations.

3.6 Basic Terms in Regression Models

In understanding regression models, there are certain criteria to determine the performance of the model. These can be listed as train and test data set, overfitting, underfitting, bias, variance, RMSE, coefficient of determination (R^2) and regularization techniques.

3.6.1 Train and Test Data Set

In supervised machine learning, there is a target variable and a dependent variable that is used to predict one or more target domains. It is aimed to find the most suitable machine learning algorithm by making basic modeling experiments on the Train data set [88]. The Train dataset consists of the most sampled observations. Depending on the number of observations or data, between 50% and 80% of the total data set can commonly be reserved for the train data set [89]. Data for the validation section is selected from the train data set. The model is tried to be improved by validating the algorithm created by choosing the most suitable model on the train set.

The test dataset can be called the remainder of the train dataset. This section compares estimates and actual data. The machine learning model learned from the train dataset is applied on the test dataset. During the application, the target variable in the test data set is removed and then the variables in the test data are added to the established model and the target variable is expected to be estimated from the model. Then, the predicted variables are confronted with the target variable, which was formerly selected from the data set, and measurement of model performance is applied [88], [89].

3.6.2 Overfitting and Underfitting

When a regression model is constructed they use selected data set to train the model. However, when the model is overtrained or contains high complexity it can attempt to learn irrelevant information within the selected dataset [90]. Then, the model commit to memory noise and adapt firmly to train data set and it becomes overfitted. If the model has low error and high variance it means that overfitting occurs [90].

Underfitting is a phenomenon in a regression model where the model is incapable to apprehend the relationship between input and variables precisely. It leads to high error rate on the training set and occurs in simple model which requires more training and input features or less regularization [91]. If the model has low variance and high bias it means that underfitting occurs [91].

3.6.3 Bias and Variance

Bias is defined as difference between average prediction of a model and correct value. The model including high bias little attend to the training data and oversimplified the model. Bias always causes high error on train and test data set.

Variance occurs when a model performs well on the training set, but not on a test data set or validation set. Variance is an indicator of how dispersed the estimated value from the true value is. The variance in such models result in well performance on training but it leads to high error rates on test data [92].

Relation between bias and variance is outlined in bulls-eye diagram considering underfitting and overfitting performance of the model.

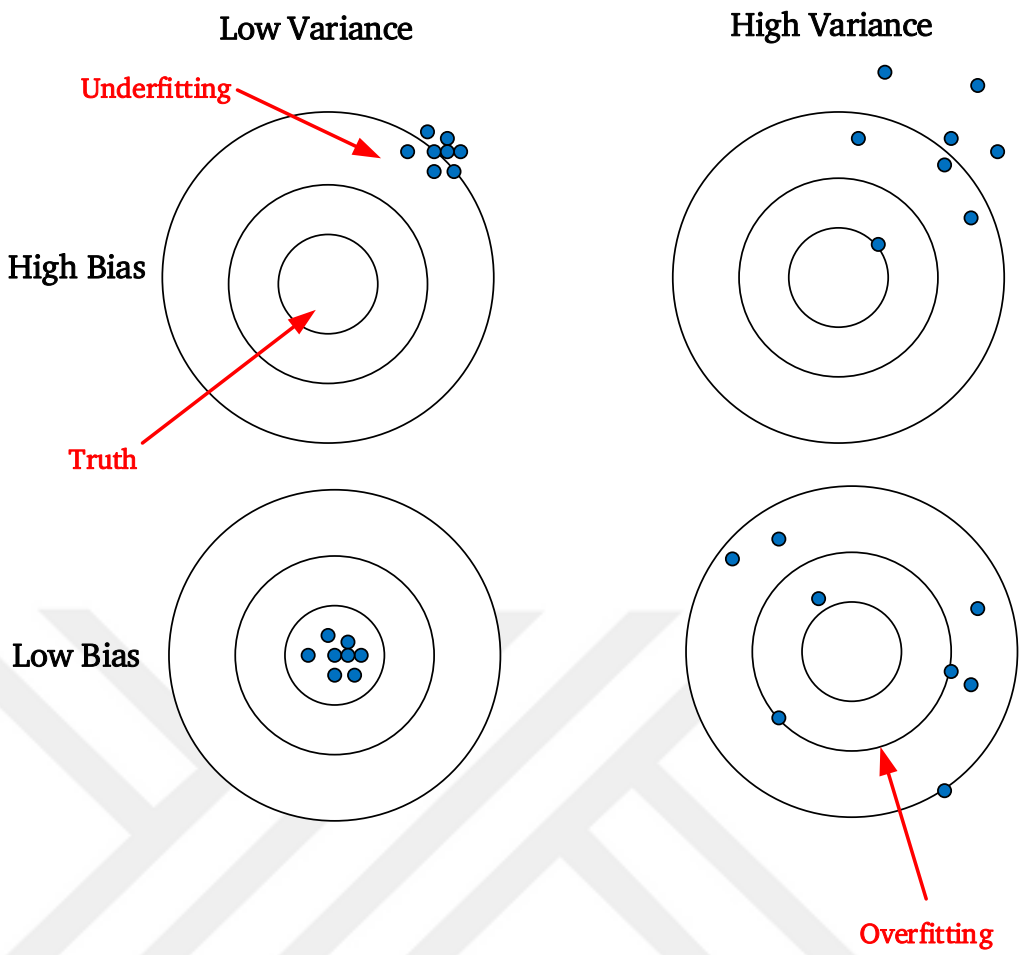


Figure 3.3 Representation of bias and variance tradeoff considering underfitting and overfitting using bulls-eye diagram [93]

3.6.4 Root Mean Squared Error (RMSE)

RMSE is a quadratic metric that measures the size of the error and finds the distance between the predicted values and the actual values in a machine learning model. The RMSE is the standard deviation of the estimation errors or residuals. The RMSE value can take values between zero and infinity [94]. Negatively oriented or lower value estimators perform better. The RMSE value of zero is difficult in practice and means that the model makes no errors [94]. The calculation of RMSE is given in equation (3.10).

$$RMSE = \sqrt{\frac{\sum_{i=1}^{N} ||y(i) - \hat{y}(i)||^2}{N}} \tag{3.10}$$

N represents number of data points, $y(i)$ is ith measurement, and $\hat{y}(i)$ is the predicted value.

3.6.5 Coefficient of Determination (R^2)

The coefficient of determination (R2) in a regression model examines how the proportion of the variance in the dependent variable that can be described by the independent variable. R^2 is also known as goodness of fit which is represented between of 0 and 1 and percentage form between 0% and 100%. While a value is 1 or 100% means highly reliable model and indicates a perfect fit, the value is 0 or 0% means that calculation does not achieve accurately model the data at all [95]. The calculation of R^2 is given in equation (3.11).

$$R^2 = \left[\frac{N\sum xy - \sum x \sum y}{\sqrt{[N\sum x^2 - (\sum x)^2][N\sum y^2 - (\sum y)^2]}}\right] \tag{3.11}$$

R^2 is denoted as coefficient of determination, N is number of samples given, $\sum xy$ is sum of paired product, $\sum x$ is x sample sum, $\sum y$ is y sample sum, $\sum x^2$ square of x sample sum and $\sum y^2$ square of y sample sum.

R^2 is also written as which is given in equation (3.12) [96]:

$$R^2 = 1 - \frac{SS_{regression}}{SS_{total}} \tag{3.12}$$

$SS_{regression}$ measures how well a regression model performs the data that is used for modeling. SS_{total} explains the variation in the observed data.

3.6.6 Regularization

Regularization is defined as a pattern of regression that arranges or shrinks the coefficient predicts towards zero. It also eludes learning more complex/flexible model, due to occurring the risk of overfitting [97]. Regularization can significantly reduce the variance of regression model without increasing its bias substantially. Lambda (λ) or tuning parameter is used in the regularization techniques in order to control or regularize the impact on bias and variance [98]. In other words, regularization operates by adding penalty or shrinkage term with

residual sum of squares to the complex model to achieve optimum bias and variance.

3.6.7 Validation

Models suitable for datasets can be obtained using machine learning methods. Evaluating in the regression model helps in choosing the most appropriate model and in understanding how well the learning model will work in the future hold-out or cross validation method can be applied to eliminate overfitting [99].

One of the simplest methods of resampling data is hold out. This method randomly patterns some cases from the learning set for test and creates the training set of the remaining cases. In general, the training set includes about 70% to 90% of the data, while the test set includes 10% to 30% of the data. In some cases, 80% training set and 20% test set can also be used. If the data set composing the training and test set is large, the observed test error can be a reliable estimate of the model's true error for new or unseen cases.

Cross-validation or "k-fold cross validation" is the process of randomly splitting the data set into 'k' groups. One of the groups is used as the test set and the other as the training set [100]. By repeating each group in this manner, the model is trained and tested with the other group. Thus, the model is trained with all the data and this process is very necessary for the accuracy of the model. The cross validation method is a more commonly used model as it provides your model the possibility to train with more than one training-test group. Thus, it is measured whether the model will perform on unseen data well or not. Compared to the hold out model with cross validation, this model only depends on a training-test split, and the success rate of the model depends on how the data are divided into training and test sets. For 5-fold cross validation which is shown in Figure 3.4, the dataset is divided into 5 groups and the model will be trained and tested 5 times, therefore each group has a chance to become a test set.

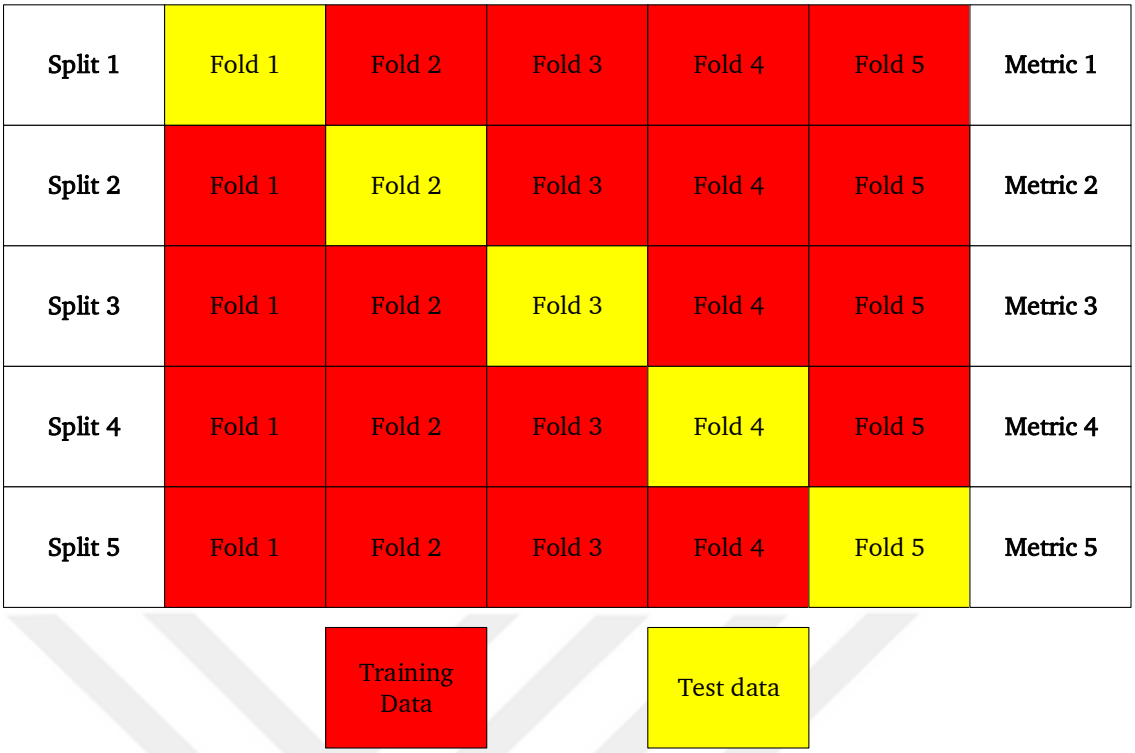


Figure 3.4 Representation 5-fold cross validation [101]

3.6.8 Multicollinearity

The multicollinearity problem between the independent variables causes deviations from the assumptions about the multiple regression model. The standard errors of parameter estimate that determine the relationship between variables take a large value in case of multicollinearity [102], [103]. As a result, the direction and value of the true correlation coefficient may differ significantly. Minimizing the multicollinearity problem in the multiple regression model is important for healthy decision making.

The variances of parameter estimation are most affected by multicollinearity. The covariance matrix of the ordinary least squares (OLS) estimator $\hat{\beta}$ is shown below [104].

$$Cov(\hat{\beta}) = \sigma^2(X'X)^{-1} \tag{3.13}$$

$(X'X)^{-1}$ is with j th diagonal element c_{jj}, and

$$Var\hat{\beta}_j = \sigma^2 c_{jj} = \sigma^2\left(1 - {R_j}^2\right)^{-1} \quad (3.14)$$

${R_j}^2$ denoted as the coefficient of determination, which is the coefficient of determination of the regression equation obtained when each of the independent variables is treated as a dependent variable and σ^2 is variance of parameter estimates.

If coefficient of determination between independent variables is ${R_j}^2 = 0$, $Var\hat{\beta}_j$ is equal to σ^2. When ${R_j}^2$ is different from 0, $Var\hat{\beta}_j$ is greater than σ^2. The multicollinearity problem reduces the consistency of the estimation of the dependent variable. Since the regression coefficient is very different from the true coefficients in terms of direction and size, it also affects the dependent variables, so the standard errors of these variables are large.

Correlation matrix, variance inflation factor (VIF), and examination of eigenvalues and eigenvectors methods can be used to identify the multicollinearity problem in the multiple regression model.

- Determination by Pearson correlation matrix: It was determined that if the simple correlation coefficient between two independent variables was highly significant (r>75%), this could lead to a multicollinearity problem. Similarly, if the absolute value of the correlation coefficient is greater than 0.8, it is shown in various studies in the literature that there is a multicollinearity [105].
- Determination of multicollinearity with VIF: The j diagonal element of the correlation matrix cjj gives the VIF for the j th independent variable. The VIF value is well measured in identifying more than two correlations. The VIF value above 10 indicates strong multicollinearity in the regression model [104].
- Examination of Eigenvalues and Eigenvectors: Eigenvalues of $(X'X)$ are $\lambda_1 \geq \lambda_2 \geq \lambda_3 \geq \cdots \geq \lambda_j > 0$ and their corresponding unit orthogonal eigenvectors are $V_1, V_2, \ldots . V_j$ and, the representation of λj is given in equation (3.15):

$$\lambda j = V_j' XXV_j = (XV_j)'(XV_j) \quad (3.15)$$

$$j = 1, 2, \ldots, k$$

Small eigenvalues and corresponding eigenvectors determine internal relationships. If the last r eigenvalues of $(X'X)$ are small enough, the expression $(XV_j)'(XV_j)$ becomes about 0 as XV_j is about 0 $(XV_j = \approx 0)$. When the eigenvalues of the correlation matrix $(X'X)$ are examined to determine the multicollinearity, there is little correlation between the independent variables if the $max|\lambda_j|/\min|\lambda_j|$ ratio is less than 10. However, this ratio greater than 30 indicates the existence of a strong relationship [104].

3.7 Definition of Regression Models

3.7.1 Linear Regression

In simple linear regression model, the purpose is to predict n observations of the dependent variable, with a linear combination of independent or explanatory variables, and error term with variance [106]:

$$y = X\beta + \varepsilon \quad \text{and} \quad \varepsilon \sim N(0, \sigma^2) \quad (3.16)$$

In the equation (3.16), Y is denoted as the dependent or response variable, X is independent or explanatory variables, ε and σ^2 are normally distributed error term and variance, respectively. In the OLS method, β_{OLS}, is regression coefficients of OLS, estimated as $\hat{\beta}_{OLS}$ thereby that of sum of squares of residuals is tried to be as small as possible. That is to say, linear regression loss function $(L_{OLS}(\hat{\beta}))$ is minimized shown in equation (3.17).

$$L_{OLS}(\hat{\beta}) = \sum_i^n (Y_i - X'_i\hat{\beta})^2 = \left\|Y - X\hat{\beta}\right\|^2 \quad (3.17)$$

To get $\hat{\beta}_{OLS}$ (OLS estimator of β_{OLS}), the equation (3.18) is used:

$$\hat{\beta}_{OLS} = (X'X)^{-1}(X'Y) \quad (3.18)$$

When measuring estimation quality of regression model, two critical characteristics of estimators are taken into consideration. These are the bias and variance term. While the bias, which is difference between true parameters and expected predictors, measures the accuracy of the estimates, variance measures the dispersion and uncertainty. OLS approach gives reasonable prediction in unbiased cases, however it causes large variance problem which is taken place in two conditions [107], [108]:

- Multicollinearity problem occurs in the independent/predictor variables.
- In the case of a large number of independent variables, if the independent variables (m) approach the observations (n), the variances approach infinity.

In order to overcome these problems in linear regression, regularization techniques are applied to reduce high variance by introducing some bias.

3.7.2 Ridge Regression

The notion of ridge regression (RR) is first acquainted by Hoerl and Kennard [109]. RR is a method to analyze multi regression data that affect from multicollinearity. In the presence of multi regression, large variances occur although estimation of least squares is unbiased. Thus deviation from true value takes place. To eliminate standard errors caused by ordinary least squares, RR adds some degree of bias for regression estimation. Multicollinearity is defined as close-linear relationships amongst the independent variables. Multicollinearity negatively impact on imprecise estimation of the regression coefficients (RC), increase the standard errors of the RC, decrease the partial t-tests for the RC, cause false unimportant p-values, and reduce the predictability of the regression model. Enhancement of ridge loss function (L_{ridge}) in the RR provides minimizing the sum of squared residuals and adding penalty term to the size of parameter estimates to shrink them towards zero. Equation (3.19) for RR is given below [107], [108]:

$$L_{ridge}(\hat{\beta}) = \sum_{i=1}^{n}\left(Y_i - X'_i\hat{\beta}\right)^2 + \lambda\sum_{j=1}^{m}\hat{\beta}_j^{\,2} = \left\|Y - X\hat{\beta}\right\|^2 + \lambda\left\|\hat{\beta}\right\|^2 \qquad (3.19)$$

Solving $\hat{\beta}_{ridge}$ with the equation (3.20) given below allows finding ridge RR estimates.

$$\hat{\beta}_{ridge} = (X'X + \lambda I)^{-1}(X'Y) \tag{3.20}$$

Lambda (λ) is denoted as regularization penalty and I is identity matrix. The lambda value can take value from zero to infinity. If the λ value approaches zero, $\hat{\beta}_{ridge}$,which is denoted as ridge regression coefficient, approaches to $\hat{\beta}_{OLS}$. On the other hand, if λ value approaches to infinity, $\hat{\beta}_{ridge}$ approaches zero.

3.7.3 Lasso Regression

Least absolute shrinkage and selection operator regression (LR) has nearly same concept with RR. However, the key difference between RR and LR is that RR reduces the slope only asymptotically close to zero, whereas LR can reduce the slope of superfluous variables to zero. In other words, it is more useful than RR when reducing variance in models with such superfluous variables since LR can remove superfluous variables from equations. The equation (3.21) shows how to minimize lasso loss function ($L_{lasso}(\hat{\beta})$) [107], [108]:

$$L_{lasso}(\hat{\beta}) = \sum_{i=1}^{n}(y_i - x'_i\hat{\beta})^2 + \lambda \sum_{j=1}^{m}|\hat{\beta}_j| \tag{3.21}$$

3.7.4 Elastic Net Regression

Elastic net regression (ENR) combines of RR and LR penalty to obtain strength of the both methods. Elastic net minimizes elastic net loss function ($L_{elastic\ net}(\hat{\beta})$) given in equation (3.22)[107], [108]:

$$L_{elastic\ net}(\hat{\beta}) = \sum_{i=1}^{n}(y_i - x'_i\hat{\beta})^2/2n + \lambda\left(\frac{1-\alpha}{2}\sum_{j=1}^{m}\hat{\beta}_j^{\,2} + \alpha\sum_{j=1}^{m}|\hat{\beta}_j|\right) \tag{3.22}$$

Actually, RR and LR use their own penalties term and cross validation method uses different combination to find best penalties for RR and LR. However, in R programming, it uses as mixing parameter α term between ridge ($\alpha = 0$) and lasso ($\alpha = 1$).

3.7.5 Econometric Prediction Methods

Forecasting improvement of renewable energy utilizing econometric models can help to renewable energy sector and its supply chain. Lee, (2017) rigorously conducted comparison of econometric assessment for nine different model [110]. He concluded that regression model can be most suitable econometric model for the bioenergy industry. With reference to Lee (2017), four different regression model including classical linear regression, RR, LR and elastic ENR are considered for econometric assessment of solar and biomass HRES. The contribution of electricity generation to GDP is determined as dependent variable and the relationship between dependent/independent variables are estimated by selecting thirteen independent variables and different regression models. Dependent and independent variables and their notations used in the R program are shown in Table 3.4. The values are started from 2010 as renewable energy production trend has increased dramatically since 2010. It is assumed that the increase in human population and total fertilizer consumption and reasonable decrease in milk feed prices may affect the increase in milk consumption and dairy cattle number. The rise in milk consumption and the number of dairy cattle may trigger more CM production, and as a result, encourage the establishment of more biogas plants. The trend in world biogas energy production and the change in the cost of installation of biogas can be directly or indirectly associated with the production of electricity from biogas. Moreover, Turkey's biogas installed capacity and AW of hybrid power plant may be related with in biogas production. Rise in installed solar energy capacity of Turkey and the world, and decline in solar energy installation cost in the world can remarkable impact on increasing of electric production from renewable energy. Taking into account the possible implications, the impact of these parameters on the share of electricity generation in GDP is measured. Schematic diagram of possible inferences to be used with regression methods is illustrated in Figure 3.5.

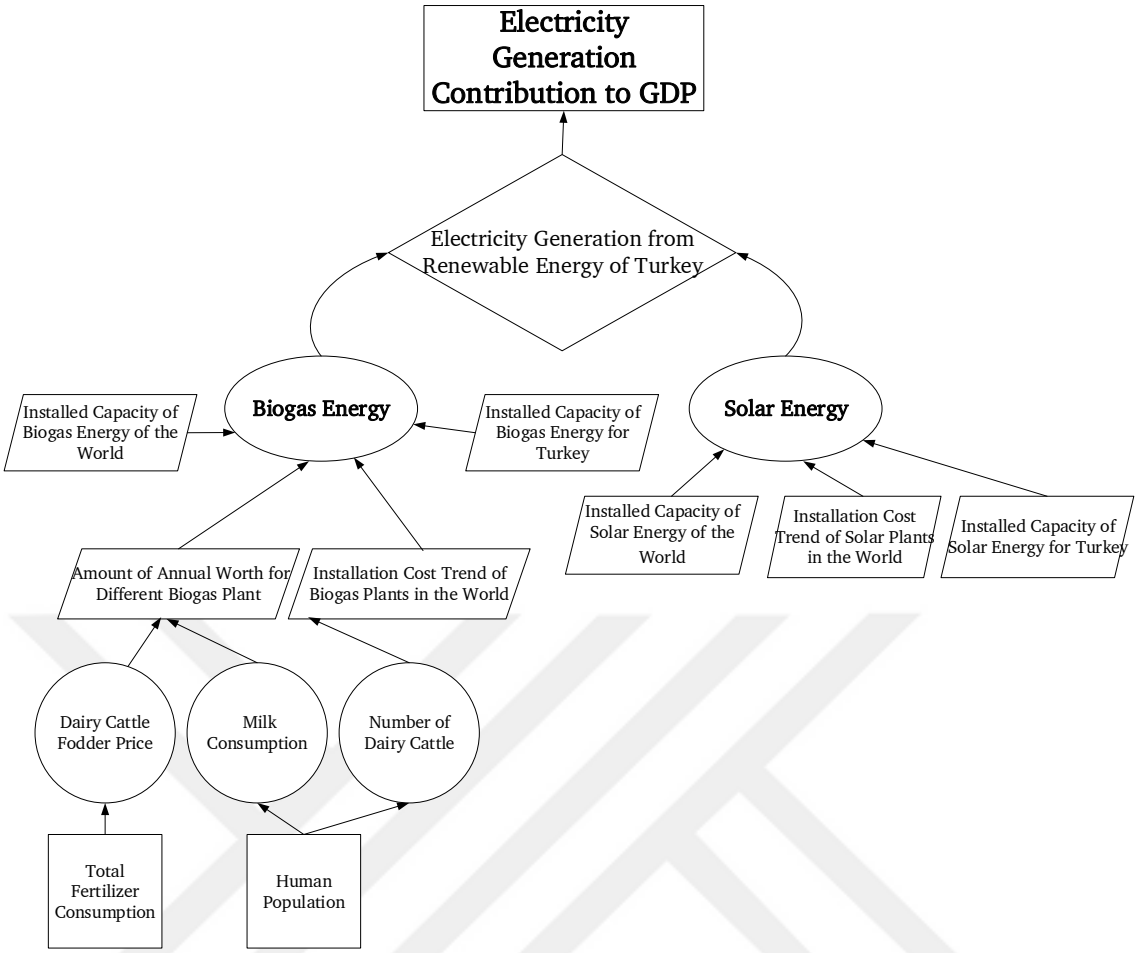


Figure 3.5 Schematic diagram of possible inferences to be used with regression methods

Table 3.4 Mean and standard deviation of dependent and independent variables and their notations [111]–[114]

Independent variable and dependent variables	Mean	Standard Deviation
Electricity Generation Contributed to GDP (Y)	9.081	1.54
Human Population (X1)	16.48	2.30
Cow Milk Consumption (X2)	18.15	3.17
Total Amount of AW for Different Animal Barns (X3)	868.56	286.76

Table 3.4 Mean and standard deviation of dependent and independent variables and their notations (continued)

Solar Installed Capacity of Turkey (X4)	1072.77	1862.68
Biogas Installed Capacity of Turkey (X5)	226.77	131.37
Electricity Generation from Renewable Energy in Turkey (X6)	16.54	11.86
Total Amount of Fertilizer Consumption (X7)	3787.33	694.67
World Biogas Energy Production (X8)	14550.56	2855.09
World Solar Energy Production (X9)	210.66	149.13
World Total Installed Cost of Solar Energy (X10)	2480	1152.95
World Total Installed Cost of Biogas Energy (X11)	2304	620.28
Dairy Cattle Fodder Price (X12)	0.79	0.22
Number of Dairy Cattle (X13)	14.15	1.68

R version 3.6.2 free software are used to build regression algorithms for estimating four different regression models. “plyr”, “readr”, “dplyr”, “caret”, “ggplot2” and “repr” packages are required for both linear regression and other methods for regularization [115]–[119]. After packages are installed, data partitioning is applied to divide dataset in two parts: train and test data. Train data set is used for constructing the regression model whereas the test data set is applied for regression model validation. The next step is to scale numeric features using “preProcess” and “predict” functions. Lastly, linear modelling function “lm” is used to create linear regression model. Unlike the linear regression, “glmnet” package is needed for regularized regression models [120]. The “glmnet function does not operate with dataframes thus numeric matrix is created for training features vector’s target values. “dummyVars” function which is included in the “caret”

library, is used for model matrix. Then, “predict” function is applied to create numeric model matrices for both train and test data. After regularization step is completed, RR, LR and ENR are applied respectively. Train and test data matrices are separately created for dependent variable (Y) and independent variables (X). Before creating RR model, cross validation method is applied with the function of “cv.glmnet” to find optimum lambda value by trying a list of lambda values. Then RR model is created with “glmnet” function. In LR, generally same procedure is repeated with RR. However, unlike the RR, alpha value for LR is set to one instead of zero. Also, LR forces some trivial values to zero in order to provide other coefficients to be non-zero values, RR squares all of the coefficients. In ENR model, “caret” package is used to find optimal values of alpha and lambda automatically. “TrainControl” function specifies how to repetitive cross validation will occur.

4
METHODOLOGY OF HYBRID SYSTEM DESIGN WITH CO-FIRING

4.1 HRES Design Scenarios in HCP

Solar and biomass based HRES design have been used for biological and thermal gasification processes with and without co-firing in order to estimate electricity generation potential of different biomass sources [74]. There are a few studies focusing on biomass co-firing with fossil fuels such as diesel and NG. In this study, co-firing of hazelnut shells with NG and solar PV electricity generation potentials are estimated for Ordu province. A HCP is simulated to estimate co-firing potential of hazelnut shells using a grid–connected system. In this study, technical and economic analysis of the proposed HCP is analyzed based on different subsidies for solar and biomass energy before and after 2021 due to the newly enacted renewable energy legislation. In this paper, Option A and B represents feed in tariff rates, which are 0.133 $/kWh before 2021 and 0.080 $/kWh after 2021, respectively [86], [121]. Sensitivity analysis is used to compare two cases that correspond to NPC and COE. In addition, four different scenarios: Scenario-1 (NG with biomass co-firing-grid), Scenario-2 (PV and NG without co-firing-grid), Scenario-3 (NG without biomass co-firing-grid), and Scenario-4 (PV and NG with biomass co-firing-grid) are considered in order to compare renewable resources and conventional sources mainly in terms of NPC, COE and emission analysis. Configuration of the PV panel, NG generator with biomass co-firing, converter and grid system are included and analyzed using HOMER pro 3.14 developed by the National Renewable Energy Laboratories (NREL).

4.1.1 Selected Region of HRES

The simulated HCP for solar and biomass HRES is located in Ordu province of Turkey. Hazelnuts are collected from local producers. The latitude and longitude of the facility for the proposed study are 40°56.6'N and 37°53.3'E. Annual production of hazelnut shells in this facility is about 10,000 tons.

4.1.2 Hazelnut Shell for Electricity Generation via Co-firing

Electricity generation from biomass in HOMER is performed by thermochemical or biological processes. In this study, thermo-chemical and gasification processes are applied to hazelnut shell in order to generate electricity. Biogas term in HOMER is entitled to gasified biomass (hazelnut shell) and product of gasification mainly constitute (CO), hydrogen (H), CO_2 and considerable amounts of nitrogen (N) when thermal gasification is applied in the presence of air. From here onwards, the term biogas is used to represent gasified hazelnut shells. CH_4 and water vapor is generated in minor quantities from thermal gasification. Gasified biomass or biogas has lower calorific value compared to fossil fuels if it includes higher amount of nitrogen. However, it offers significant benefits to fossil fuels such as cleaner combustion, higher efficiency and better control [74].

In this study, hazelnut shell is co-fired with natural gas in certain amounts. At every step, required output of the generator and related mass flow rates of biogas and fossil fuels are calculated by using HOMER. Some key assumptions used in these calculations are as follows [74].

- The biogas substitution rate refers to z_{gas}, which is a constant and it is not depended on engine output power or fuel mixture.
- Co-firing operation is constantly tried maximize biogas utilization and minimize fossil fuel consumption.
- The fossil fraction must be above a specific minimum value.
- The derating factor coupled with operating in dual-fuel mode is lower than 100%, the generator can generate up to 100% of its rated capacity if the fossil fraction is adequate.

Co-fired generator fuel consumption is considered in pure fossil mode in order to generate the fuel curve. Fossil fuel consumption in pure fossil mode is represented by equation (4.1). Mass balance equations used in the calculations are given equations (4.1-4.10). The symbols used in equations (4.1-4.10) are explained in Table 4.1 with proper units and descriptions.

$$\dot{m}_0 = \rho_{fossil}\left(F_0 \cdot Y_{gen} + F_1 \cdot P_{gen}\right) \tag{4.1}$$

$$\dot{m}_0 = \dot{m}_{fossil} + \frac{\dot{m}_{gas}}{z_{gas}} \text{ and } \dot{m}_{gas} = z_{gas}\left(\dot{m}_0 - \dot{m}_{fossil}\right) \tag{4.2}$$

$$x_{fossil} \equiv \frac{\dot{m}_{fossil}}{\dot{m}_0} \tag{4.3}$$

By rearranging equation (4.2) and (4.3),

$$\dot{m}_{gas} = z_{gas}\left(\dot{m}_0 - x_{fossil} \cdot \dot{m}_0\right) \text{ and } \dot{m}_{gas} = z_{gas} \cdot \dot{m}_0\left(1 - x_{fossil}\right) \tag{4.4}$$

When the fossil fraction $\left(x_{fossil}\right)$ is unknown, it is not possible to calculate P_{bio}. Therefore, biogas fuel rate $\left(\dot{m}_{gas}\right)$ is maximized in order to minimize x_{fossil} and it is assumed that $x^*_{fossil} \leq x_{fossil} \leq 1$.

Minimum fossil fraction is defined as x^*_{fossil} that is required for ignition, and target value of biogas flow rate is $\dot{m}^l_{gas}$ as shown in equation (4.5).

$$\dot{m}^l_{gas} = z_{gas}\dot{m}_0\left(1 - x^*_{fossil}\right) \tag{4.5}$$

Actual value of $\dot{m}_{gas}$ has two independent upper limits. Generator output is limited to Y^*_{gen}, when x_{fossil} is at minimum fossil fraction as shown in equation (4.6).

$$Y^*_{gen} = \tau \cdot Y_{gen} \tag{4.6}$$

Where, τ is defined as derating factor, which is between 0 to 1. Using equation (4.1) and (4.4) maximum value of biogas flow rate is calculated in equation (4.7).

$$\dot{m}^*_{gas} = z_{gas} \cdot \rho_{fossil}\left(F_0 \cdot Y_{gen} + F_1 \cdot Y^*_{gen}\right)\left(1 - x^*_{fossil}\right) \tag{4.7}$$

The upper limit mentioned above can be regarded as a physical constraint, which is the maximum rate where biogas can be taken into engine. The current biomass resource a_{gas} forms the upper limit on $\dot{m}_{gas}$. Thus, the actual value of $\dot{m}_{gas}$ is equal to minimum (MIN) of $\dot{m}^*_{gas}$ and a_{gas} as shown in equation (4.8).

$$\dot{m}_{gas} = MIN\left(\dot{m}^l_{gas}, \dot{m}^*_{gas}, a_{gas}\right) \tag{4.8}$$

After determining the value of $\dot{m}_{gas}$, x_{fossil} can be calculated using equation (4.4)

$$x_{fossil} = 1 - \frac{\dot{m}_{gas}}{z_{gas} \cdot \dot{m}_0} \tag{4.9}$$

And, using equation (4.3):

$$\dot{m}_{fossil} = x_{fossil} \cdot \dot{m}_0 \tag{4.10}$$

Thus, using equation (4.8) and (4.10), the value of fossil fuel flow rate and biogas flow rate can be found.

Table 4.1 Symbols units and descriptions of operations of co-fired generator

Symbol	Units	Description
ρ_{fossil}	kg/L	Density of fossil fuel
τ	%	Generator derating factor
P_{bio}	kg/hr	Biogas flow rate
a_{gas}	kg/hr	Available biogas flow rate
$\dot{m}_0$	kg/hr	Fossil fuel flow rate (in pure fossil mode)
$\dot{m}_{fossil}$	kg/hr	Fossil fuel flow rate (in dual –fuel fossil mode)
$\dot{m}_{gas}$	kg/hr	Biogas flow rate (in dual-fuel mode)

Table 4.1 Symbols units and descriptions of operations of co-fired generator (continued)

$\dot{m}_{gas}^{*}$	kg/hr	Maximum value of biogas flow rate
$\dot{m}_{gas}^{l}$	kg/hr	Target value of biogas flow rate
x_{fossil}	%	Fossil fraction
x_{fossil}^{*}	%	Minimum fossil fraction
z_{gas}	none	Biogas substitution ratio
F_0	L/hr/kW	Generator fuel curve intercept coefficient
F_1	L/hr/kW	Generator fuel curve slope
P_{gen}	kW	Power output of the generator
Y_{gen}^{*}	kW	Maximum output of generator at minimum fossil fraction
Y_{gen}	kW	Rated capacity of the generator

4.1.3 Solar Energy Potential of Selected Region

Solar irradiation potential of selected area is obtained from the NASA Surface Meteorology and Solar Energy Database. HOMER can tabulate daily radiation and clearness index monthly. Average daily radiation and average clearness index of the studied area are 3.940 kWh/m^2/day and 0.497, respectively [76]. Clearness index and daily radiation data per month are given in Table (4.2). Daily radiation from May to September is high enough for solar energy generation but the values in December and January may not be sufficient for desired electricity generation. HOMER is used to calculate energy generation from PV array as shown equation (4.11):

$$P_{PV} = Y_{PV} \cdot f_{PV} \left(\frac{G_T}{G_{T,STC}}\right)\left[1 + a_p\left(T_c - T_{c,STC}\right)\right] \tag{4.11}$$

In equation (4.11), P_{PV} (kW) denotes energy generation from PV array. Y_{PV} represents PV array rated capacity which is in standard test conditions. f_{PV} (%) denotes derating factor of PV which corresponds to possible losses including wiring, snow cover aging etc. G_T (kW/m^2) represents solar radiation incident on the PV array in the current time step. $G_{T,STC}$ (1 kW/m^2) is the measurement of incident radiation at standard test condition. Temperature effect on the power output of the PV array is neglected. Therefore, it is not considered in the calculation steps.

Table 4.2 Clearness index and daily radiation data per month [76]

Month	Clearness Index	Daily Radiation (kWh/m^2/day)
January	0.446	1.820
February	0.461	2.530
March	0.483	3.620

Table 4.2 Clearness index and daily radiation data per month (continued)

April	0.460	4.390
May	0.488	5.370
June	0.543	6.300
July	0.549	6.190
August	0.559	5.630
September	0.569	4.660
October	0.516	3.130
November	0.479	2.100
December	0.416	1.520
Average	0.497	3.940

4.1.4 Load Profile of HCP

Electricity demand of the HCP is mostly supplied from the national grid, and energy is generated NG. Daily load demand of this facility is about 2,673 kWh and this demand mainly stems from three phase motors and rooftop air-conditioners. Electric power demand load varies based on seasonal change thus load profile of the facility arranged according to these changes. Arranged load profile of the HCP is given Table (4.3). The peak hours of electricity demand are between 08:00-16:00 (local time) and 16:00-24:00 (local time) because the HCP operates in two shifts throughout the year. Daily load profile obtained from HCP is processed by HOMER to generate hourly load data depending upon monthly average daily load profiles. Random variability option is selected to achieve more realistic load profile using daily 10% and hourly 20% random noise, respectively.

Table 4.3 Daily load profile of HCP

Electric Appliances	Number of Units	Power per Hour (Watts)	Average Usage (hour/day)	Total Usage per Day (Watt)	Total Usage per Day (Kilowatt)
Armature Lamp (18 Watt) (All is turned on)	166	18	6	17,928	17.928
Armature Lamp (18 Watt)	40	18	8	5,760	5.760
Armature Lamp (40 Watt) (All is turned on)	36	40	6	8,640	8.640
Armature Lamp (40 Watt)	9	40	8	2,880	2.880
Three-Phase Motor (1500 Watt)	18	1,500	12	324,000	324.000
Three-Phase Motor (3000 Watt)	26	3,000	12	936,000	936.000
Refrigerator (300W)	5	300	24	36,000	36.000
Refrigerator (500W)	1	500	24	12,000	12.000
Commercial Dish Washer	1	6,000	3	18,000	18.000
Deep-Freezer	1	500	24	12,000	12.000
Toast Machine	1	3,000	2	6,000	6.000
Tea Maker	1	3,000	12	36,000	36.000
Electric Water Fountain	2	100	24	4,800	4.800
Black Light	6	36	12	2,592	2.592

Table 4.3 Daily load profile of HCP (continued)

Air-Conditioner	2	2,000	8	32,000	32.000
TV	1	150	4	600	0.600
Monitor System	1	800	24	19,200	19.200
Computer	7	200	8	11,200	11.200
Projector	1	400	1	400	0.400
Printer	5	300	8	12,000	12.000
Coffee Machine	1	300	8	2,400	2.400
Sodium Vapor Lamp	2	500	8	8,000	8.000
Fire Detection System	1	500	24	12,000	12.000
Conveyor	6	2,000	12	144,000	144.000
Commercial Hazelnut Weighing Machine	10	300	12	36,000	36.000
Automatic Door System	1	600	4	2,400	2.400
Roof-top Fan	5	200	24	24,000	24.000
Rooftop Air-Conditioner	1	45,000	12	540,000	540.000
Total				**2,266,800**	**2,266.800**

4.2 Hybrid Energy System Components

In this study, electricity generation potential based on hazelnut shell using biomass gasification in HOMER is applied to the HCP. HRES system configuration is considered depending upon the feed in tariffs before and after 2021. Primary load profile, biomass generator co-fired with NG, flat PV without temperature effect, system convertor for converting direct current (DC) bus to alternative current (AC) and grid system are the main components of HOMER configuration. The system does not have any energy storage device since it is planned to be directly connected to the national grid system. HRES configuration of HCP is shown in Figure 4.1. Both purchase from national grid and sale to national grid are applicable in HOMER thus net metering, which is calculated monthly is selected.

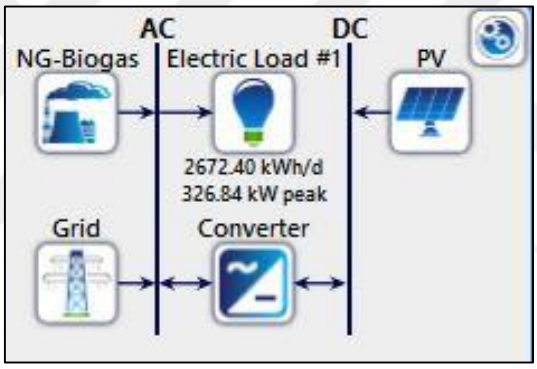


Figure 4.1 HRES configuration of HCP

4.2.1 Photovoltaic Panel

HOMER optimizer is used to calculate optimum PV capacity for the proposed HRES design. Capital and O&M cost of PV is calculated using feasibility report of Mevlana Development Agency. Capital and O&M cost of solar panel per kW is found $3,140 and $21, respectively[84]. Replacement cost including component part, module and inverter is obtained from NREL report, and total replacement cost is found to be $15.37 per kW[85]. Generic flat plate PV having 250 kW rating capacity, 80% of derating capacity and 20% of ground reflectance are assumed for the PV module. Temperature effect on the PV panel is neglected thus it is not considered in calculation.

4.2.2 Biomass Generator

Generic natural gas fueled generator with capability of co-firing is used in the systems design. Capital, replacement and O&M of the biomass generator are $1,700, $1,300 and 0.010 ($/op. hr), which are determined by HOMER. In order to find optimum generator size, search tab is selected. Generator size of 1,500 kW and 2,000 kW are chosen in the search tab. At the time of calculations, natural gas price was $0.280 per m^3 and hazelnut shell price per ton was $76.00. Minimum fossil fraction (%) and derating factor (%) are 20.00% and 70.00%, respectively. The hourly hazelnut shell production is calculated as 27.40 tons per hour since hazelnut supply of the HCP is continuous throughout the year.

4.2.3 Converter

System converter is selected for this proposed design, and cost of capital, replacement and O&M are obtained from HOMER. Capital and replacement cost of the converter are $300 per kW and O&M cost is assumed to be zero. Upper and lower limit are used to define optimum converter size with the value of 1,250 kW and 0. Lifetime of the converter is selected as 15 years and efficiency of inverter input is selected as 95%.

4.2.4 Grid

HRES design in this study is planned as grid-connected. Among the four different advanced grid options namely simple rates, real time rates, scheduled rates and grid extension in HOMER, schedule rates are chosen for this design to find net metering, which calculates net purchases monthly or annually using grid power price (0.088 $/kWh) and grid sellback price (0.133 $/kWh). Grid sellback price is determined according to the government incentive that was published in the “Law of the Ministry of Energy and Natural Resources on the Use of Renewable Energy Sources for Electrical Energy Production” [86]. Grid capital cost in HOMER is equal to interconnection charge when HRES is connected to the grid and it includes some other power devices namely PV array or biomass generator. According to the “Article 21 of the Electricity Market Connection and System Use Regulation”, interconnection charge is not charged during the establishment of electricity generation facilities after 2017 therefore grid capital cost of HRES

system is zero [122]. The stand-by fee is determined by the EMRA, which is $9,477 per year [123].

4.3 Economic Parameters and Formulation in HOMER

Technical and economic analysis in HOMER are based on the simulation, optimization and sensitivity analysis. Every system configuration in HOMER that one wants to take into consideration is performed with energy balance calculation. Then, HOMER optimizes whether configuration of the system is feasible or not by estimating the capital and operating costs of the system over the lifetime of the project [30]. Sensitivity case is optional in HOMER, however it is quite useful depending on the changing conditions such as fuel price, discount, interest rate etc. In general, NPC and COE are the main economic metrics while determining feasibility of the project since they are more trustworthy than other economic estimation methods [124]. Inflation rate and discount rate of the proposed HRES design is obtained from the Central Bank of Turkey [82]. Sensitivity option is used in determining optimum inflation and discount rate in order to cover as economic indicators in Turkey. Inflation and discount rates and project lifetime are 11.85%, 10.00% and 25 years, respectively.

5
RESULTS AND DISCUSSION

5.1 Cost Analysis Results for Modular HRES Design

Optimization results of the solar biomass hybrid systems with grid-connected for the cities of Konya, Erzurum and İzmir have similar NPC value and AW. The main reason for this, these cities have nearly same average radiation and the amount of biomass resource for all HOMER configurations is assumed constant in all cities. Konya is chosen as reference city for all the results of these studies except Table (5.1) results. The results in Table (5.1) show the most important economic metrics values for all hybrid system configurations. HOMER represents overall and categorized results in the form of table. Most feasible system results are shown in categorized section whereas overall results are used to see all system configuration. In some condition sensitivity cases helps to find most optimum option. HOMER compares winning system architecture and base case architecture with the economic metrics options. In addition, simulation details tab shows all the details about the system including cost summary, cash flow, compare economics, electrical, fuel summary, biogas genset, renewable penetration, PV, grid, converter and emissions. HOMER generally takes into consideration NPC value to evaluate whether system is feasible or not. Nevertheless, ROI, internal rate of return (IRR), and AW are also considered for the assessment of the systems. ROI of the all configurations have positive value and payback period of the systems have very short. In addition, this method is preferred since the AW method calculates the return of the hybrid systems annually. Table (5.2) shows the number of 50, 100, 500, 1000 and 5000 dairy cattle farms, their AWs and their total annual returns. Numbers and shares of dairy cattle production by years and scales are obtained from National Milk Council's 2018 and Agricultural Engineers Chamber's 2018 reports [125], [126]. The total AW of all hybrid configurations are also used as an independent variable in regression analysis.

Table 5.1 Most important econometric values for all hybrid system configurations

50 Cattle Capacity Hybrid System				
Economic Parameters		**Konya**	**Erzurum**	**İzmir**
Winning System Architecture	Grid (kW)	15	15	15
	Bio (kW)	12	12	12
	PV (kW)	17.50	17.30	16.70
	Converter (kW)	10.90	11	10.70
AW ($/yr)		16,393	16,401	16,497
ROI (%)		27.20	27.50	28.80
IRR (%)		28.30	28.60	29.60
Simple Payback Period (yr)		3.69	3.64	3.46
Discounted Payback Period (yr)		3.50	3.46	3.28
100 Cattle Capacity Hybrid System				
Economic Parameters		**Konya**	**Erzurum**	**İzmir**
Winning System Architecture	Grid (kW)	15	15	15
	Bio (kW)	21	21	21
	PV (kW)	33.80	33.60	33.20

Table 5.1 Most important econometric values for all hybrid system configurations (continued)

	Converter (kW)	21	20.80	21
AW ($/yr)		29,021	28,895	29,021
ROI (%)		24.90	23.80	25.30
IRR (%)		26.40	27.20	26.80
Simple Payback Period (yr)		4.03	3.96	3.99
Discounted Payback Period (yr)		3.86	3.75	3.79
500 Cattle Capacity Hybrid System				
Economic Parameters		**Konya**	**Erzurum**	**İzmir**
Winning System Architecture	Grid (kW)	80	80	80
	Bio (kW)	120	120	120
	PV (kW)	168	168	164
	Converter (kW)	104	106	104
AW ($/yr)		167,100	167,163	167,100
ROI (%)		29.00	29.00	29.60
IRR (%)		29.80	29.80	30.40
Simple Payback Period (yr)		3.42	3.43	3.33
Discounted Payback Period (yr)		3.25	3.26	3.17

Table 5.1 Most important econometric values for all hybrid system configurations (continued)

1000 Cattle Capacity Hybrid System				
Economic Parameters		**Konya**	**Erzurum**	**İzmir**
Winning System Architecture	Grid (kW)	120	120	120
	Bio (kW)	250	250	250
	PV (kW)	254	258	257
	Converter (kW)	159	164	162
AW ($/yr)		343,061	343,136	343,104
ROI (%)		39.70	39.00	38.60
IRR (%)		38.50	38.00	38.20
Simple Payback Period (yr)		2.68	2.71	2.65
Discounted Payback Period (yr)		2.63	2.66	2.60

Table 5.1 Most important econometric values for all hybrid system configurations (continued)

5000 Cattle Capacity Hybrid System				
Economic Parameters		**Konya**	**Erzurum**	**İzmir**
Winning System Architecture	Grid (kW)	600	600	600
	Bio (kW)	1,250	1,250	1,250
	PV (kW)	1,518	1,523	1,517
	Converter (kW)	949	957	943
AW ($/yr)		1,731,566	1,732,229	1,731,492
ROI (%)		33.30	33.20	33.50
IRR (%)		33.50	33.40	33.50
Simple Payback Period (yr)		2.94	2.95	2.94
Discounted Payback Period (yr)		2.88	2.89	2.88

Table 5.2 The number of 50, 100, 500, 1000 and 5000 dairy cattle farms, their AWs and their total annual returns [125], [126]

Time	Number of Dairy Farms Having 50 Cattle in Turkey	AW of 50 Cattle ($) in Total	Number of Dairy Farms Having 100 Cattle in Turkey	AW of 100 Cattle ($) in Total	Number of Dairy Farms Having 500 Cattle in Turkey	AW of 500 Cattle ($) in Total	Number of Dairy Farms Having 1000 Cattle in Turkey	AW of 1000 Cattle ($) in Total	Number of Dairy Farms Having 5000 Cattle in Turkey	AW of 5000 Cattle ($) in Total	Total AW of All Farms ($)
2010	10,336	169,820,480	2,425	71,239,225	718	121,456,162	300	103,572,900	40	69,270,480	535,359,247
2011	11,511	189,125,730	2,701	79,347,277	800	135,327,200	334	115,311,162	44	76,197,528	595,308,897
2012	12,685	208,414,550	2,976	87,425,952	882	149,198,238	368	127,049,424	48	83,124,576	655,212,740
2013	13,979	229,674,970	3,280	96,356,560	972	164,422,548	406	140,168,658	53	91,783,386	722,406,122
2014	15,405	253,104,150	3,615	106,197,855	1,071	181,169,289	447	154,323,621	59	102,173,958	796,968,873
2015	16,551	271,932,930	3,778	110,986,306	1,041	176,094,519	484	167,097,612	82	142,004,484	868,115,851

Table 5.2 The number of 50, 100, 500, 1000 and 5000 dairy cattle farms, their AWs and their total annual returns (continued) [125], [126]

2016	18,917	310,806,310	4,036	118,565,572	1,335	225,827,265	638	220,265,034	115	199,152,630	1,074,616,811
2017	21,282	349,663,260	4,540	133,371,580	1,502	254,076,818	718	247,884,474	129	223,397,298	1,208,393,430
2018	23,942	393,367,060	5,108	150,057,716	1,690	285,878,710	807	278,611,101	146	252,837,252	1,360,751,839

5.1.1 Hybrid System with 50, 100, 500, 1000 and 5000 Cattle

Table (5.3) indicates categorized results of the all hybrid system configurations attained from HOMER. The difference between NPC, COE and the AW of the hybrid system configuration are not significant. HOMER always ranks starting from the lowest NPC value. Combination of PV and biomass with connected to grid in the categorized summary have lowest NPC value with the 15 kW, 15 kW, 80 kW, 120 kW and 600 kW grid capacity respectively. Government subsidies, tax breaks and governmental tariffs help to reduce COE value [127]. Turkish government promotes for feed in tariff and domestic production PV panel and converter support for renewable energy investor. Therefore, the contribution of PV and grid connected system provide much lower COE values compared to standalone biomass system. The COE has lowest value in the 100 cattle capacity system with 0.029 $/kWh however the highest value for COE in the 1000 cattle capacity system with 0.046 $/kWh.

Table 5.3 Categorized results of a) 50 b) 100 c) 500 d) 1000 e) 5000 cattle barns' hybrid system configurations

PV (kW)	Bio (kW)	Grid (kW)	Converter (kW)	NPC ($)	COE ($)	Operating Cost ($/yr)	Initial Capital ($)
17.5	12	15	10.9	36,942	0.037	1,827	94,231
null	12	15	null	46,875	0.123	346.82	36,000
14.1	12	null	1.7	477,191	1.250	12,645	80,705
null	12	null	null	550,965	1.450	16,423	36,000
a)							

Table 5.3 Categorized results of a) 50 b) 100 c) 500 d) 1000 e) 5000 cattle barns' hybrid system configurations (continued)

PV (kW)	Bio (kW)	Grid (kW)	Converter (kW)	NPC ($)	COE ($)	Operating Cost ($/yr)	Initial Capital ($)
null	21	15	null	79,763	0.125	534.59	63,000
33.8	21	15	21	54,219	0.029	3,866	175,443
20.6	21	null	2.8	804,964	1.270	21,570	128,622
null	21	null	null	964,188	1.520	28,741	63,000
b)							
PV (kW)	Bio (kW)	Grid (kW)	Converter (kW)	NPC ($)	COE ($)	Operating Cost ($/yr)	Initial Capital ($)
168	120	80	104	270,119	0.029	20,681	918,594
null	120	80	null	399,900	0.131	1,273	360,000
91.8	120	null	12.8	4.49M	1.480	122,548	652,070
null	120	null	null	5.51M	1.810	164,233	360,000
c)							

Table 5.3 Categorized results of a) 50 b) 100 c) 500 d) 1000 e) 5000 cattle barns' hybrid system configurations (continued)

PV (kW)	Bio (kW)	Grid (kW)	Converter (kW)	NPC ($)	COE ($)	Operating Cost ($/yr)	Initial Capital ($)
null	250	150	null	817,983	0.134	2,168	750,000
254	250	120	159	721516	0.046	27,852	1.59M
186	250	null	22.7	9.33M	1.530	254,812	1.34M
null	250	null	null	11.50M	1.890	342,153	750,000
d)							
PV (kW)	**Bio (kW)**	**Grid (kW)**	**Converter (kW)**	**NPC ($)**	**COE ($)**	**Operating Cost ($/yr)**	**Initial Capital ($)**
null	1250	750	null	4.04M	0.135	9,221	3.75M
1,518	1250	600	949	3.10M	0.035	181,851	8.80M
928	1250	null	129	46.60M	1.560	1.27M	6.70M
null	1250	null	null	57.40M	1.920	1.71M	3.75M
e)							

Effects of costs including capital, operating, replacement and salvage on the components obtained from HOMER are shown in the Figure (5.1). Capital cost of the PV, which is $54,950, $106,134, $527,421, $797,265 and $8,801,000, respectively, in the hybrid systems have highest impact for all configurations and lowest impact is converter, which is $3,281, $6,307, $31,171, $47,578 and $284,565, respectively. Grid revenue for all configurations gradually increases

starting from year 1 to year 25. Replacement of converter is applied in year 15 and replacement cost of the converter is $4,225, $8,122, $31,171, $47,578 and $366,434, respectively. Total salvage values of the components are $23,948, $42,512, $243,599, $429,615 and $2,243,236, respectively. Costs in the form of annualized costs are also calculated using HOMER. Table (5.4) summaries the annualized costs of the components. In order to calculate annualized cost, NPC value is firstly calculated then it multiplies by the CRF. Annualized initial capital of the systems is $3,005, $5,595, $29,295, $50,862 and $280,682, respectively. The initial cost contains mainly PV costs approximately 58%, 60%, 57%, 50% and 54%, respectively. However, only 3.5%, 3.7%, 3.3%, 2.9% and 3.2% of the cost is generated by the converters.

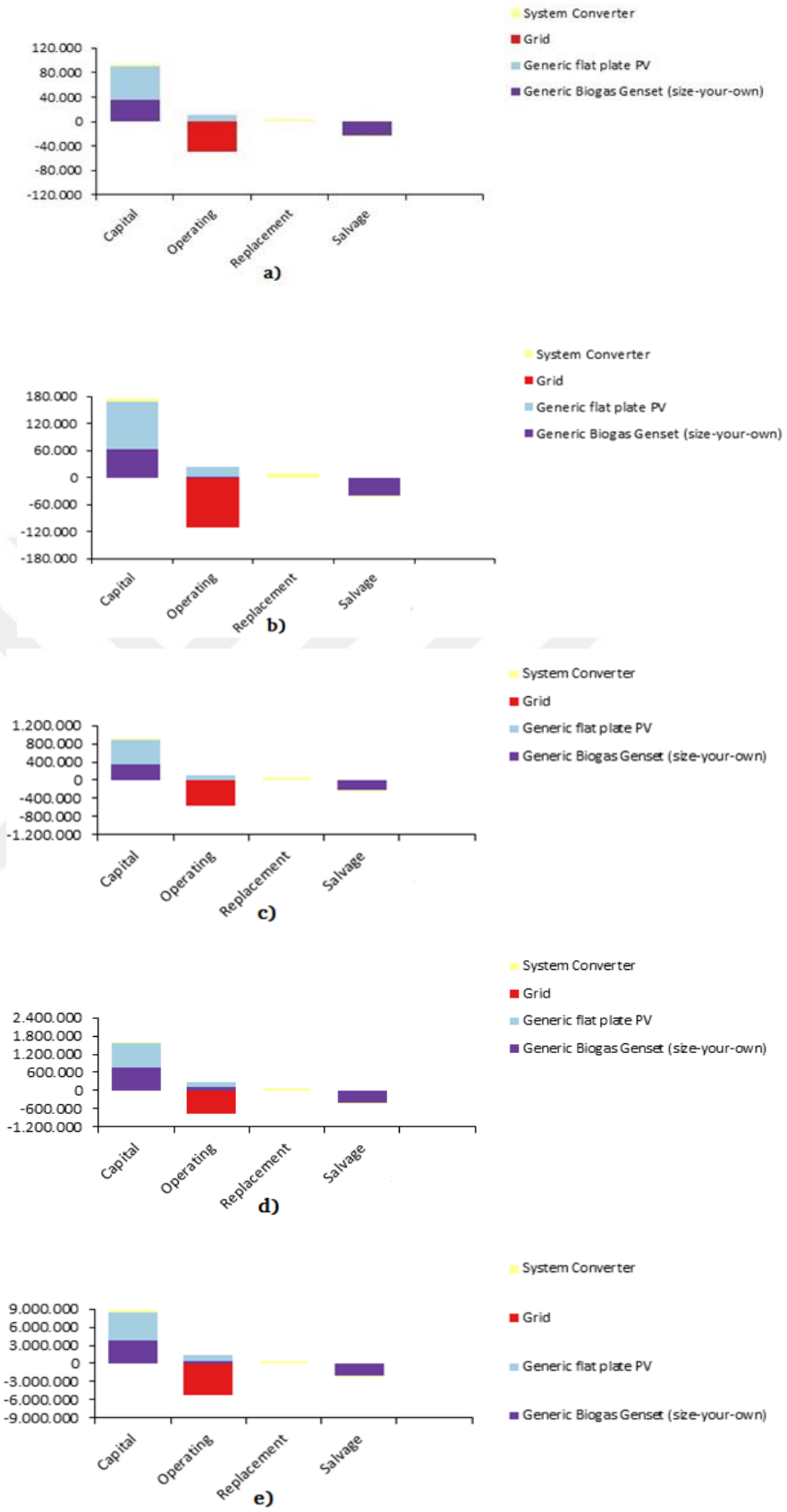


Figure 5.1 Effects of capital costs on the components for a) 50 b) 100 c) 500 d) 1000 e) 5000 dairy cattle barns

Table 5.4 Annualized costs of the hybrid system components

Annualized Costs of 50 capacity Animal Barns						
Component	**Capital ($/yr)**	**Replacement ($/yr)**	**O&M ($/yr)**	**Fuel ($/yr)**	**Salvage ($/yr)**	**Total ($/yr)**
Biogas Genset	1,148	0	0	0	-710	438
PV	1,752	0	367	0	0	2,119
Grid	0	0	-1,565	0	0	-1,565
Converter	104	134	0	0	-53	185
System	3,004	134	-1,198	0	-764	1,177
Annualized Costs of 100 capacity Animal Barns						
Component	**Capital ($/yr)**	**Replacement ($/yr)**	**O&M ($/yr)**	**Fuel ($/yr)**	**Salvage ($/yr)**	**Total ($/yr)**
Biogas Genset	2,009	0	29	0	-1,253	784
PV	3,384	0	709	0	0	4,094
Grid	0	0	-3,508	0	0	-3,508
Converter	201	259	0	0	-102	358
System	5,594	259	-2,770	0	-1,355	1,728

Table 5.4 Annualized costs of the hybrid system components (continued)

Annualized Costs of 500 capacity Animal Barns						
Component	**Capital ($/yr)**	**Replacement ($/yr)**	**O&M ($/yr)**	**Fuel ($/yr)**	**Salvage ($/yr)**	**Total ($/yr)**
Biogas Genset	11,481	0	36	0	-7,263	4,253
PV	16,820	0	3,527	0	0	20,347
Grid	0	0	-17,755	0	0	-17,755
Converter	994	1,280	0	0	-505	1,769
System	29,295	1,280	-14,192	0	-7,768	8,614
Annualized Costs of 1000 capacity Animal Barn						
Component	**Capital ($/yr)**	**Replacement ($/yr)**	**O&M ($/yr)**	**Fuel ($/yr)**	**Salvage ($/yr)**	**Total ($/yr)**
Biogas Genset	23,919	0	2,975	0	-12,930	13,964
PV	25,426	0	5,332	0	0	30,758
Grid	0	0	-24,411	0	0	-24,411
Converter	1,517	1,953	0	0	-770	2,700
System	50,862	1,953	-16,104	0	-13,701	23,010

Table 5.4 Annualized costs of the hybrid system components (continued)

Annualized Costs of 5000 capacity Animal Barn						
Component	**Capital ($/yr)**	**Replacement ($/yr)**	**O&M ($/yr)**	**Fuel ($/yr)**	**Salvage ($/yr)**	**Total ($/yr)**
Biogas Genset	119,595	0	11,875	0	-66,930	64,540
PV	152,011	0	31,877	0	0	183,888
Grid	0	0	-165,787	0	0	-165,787
Converter	9,075	11,686	0	0	-4,610	16,151
System	280,681	11,686	-122,035	0	-71,540	98,792

Grid sale capacity of hybrid system consists of three sensitivity variables. When the sale capacity is 5 kW, 10 kW, 50 kW, 100 kW and 750 kW, the hybrid system does not give feasible solution. However, 10 kW, 20 kW, 100 kW, 150 kW and 900 kW sale capacities give lowest NPC ($36,942, $54,219, $270,119, $721,516, $, 3,097,716) and highest ROI (27.20%, 24.90%, %29.00, 39.70%, 33.30%) values. The most optimum value of the nominal discount rate and expected inflation rate for all configurations are 10.00% and 11.87%, respectively. Net metering function in HOMER is used to measure surplus power selling to the grid if it is possible. HOMER provides billing period either monthly or annually is used to indicate net purchases. If the net purchases negative meaning that it is sold more power than purchase. Table (5.5) shows grid outputs of the all hybrid system configurations. All system grid outputs give negative net energy purchase. Peak energy sold to grid in all configurations occur between May to September. However, most energy purchase from the grid occurs in November, December and January. Net energy purchase for all systems are -11,769 kWh, -26,380 kWh, -133,503 kWh, -183,548 kWh and -1,246,521 kWh, respectively.

Table 5.5 Grid outputs of the all hybrid system configurations

Grid Output of 50 Cattle Capacity Hybrid System						
Month	**Energy Purchased (kWh)**	**Energy Sold (kWh)**	**Net Energy Purchased (kWh)**	**Peak Load (kW)**	**Energy Charge ($)**	**Demand Charge ($)**
January	725	1,251	-526	8	0	0
February	625	1,289	-664	7	0	0
March	643	1,656	-1,013	8	0	0
April	604	1,644	-1,039	8	0	0
May	561	1,759	-1,199	7	0	0
June	546	1,868	-1,322	7	0	0
July	577	2,077	-1,500	9	0	0
August	641	2,006	-1,365	8	0	0
September	615	1,901	-1,286	8	0	0
October	645	1,651	-1,005	9	0	0
November	695	1,220	-525	7	0	0
December	739	1,064	-325	9	0	0
Annual	7,616	19,385	-11,769	9	1,565	0

Table 5.5 Grid outputs of the all hybrid system configurations (continued)

Grid Output of 100 Cattle Capacity Hybrid System						
Month	**Energy Purchased (kWh)**	**Energy Sold (kWh)**	**Net Energy Purchased (kWh)**	**Peak Load (kW)**	**Energy Charge ($)**	**Demand Charge ($)**
January	1,262	2,523	-1,260	13	0	0
February	1,083	2,592	-1,509	13	0	0
March	1,090	3,330	-2,240	12	0	0
April	986	3,312	-2,326	13	0	0
May	917	3,537	-2,620	13	0	0
June	881	3,762	-2,880	12	0	0
July	884	4,189	-3,305	12	0	0
August	1,021	4,046	-3,025	13	0	0
September	1,006	3,823	-2,818	12	0	0
October	1,096	3,318	-2,221	14	0	0
November	1,156	2,476	-1,319	13	0	0
December	1,293	2,149	-856	13	0	0
Annual	12,676	39,056	-26,380	14	3,508	0

Table 5.5 Grid outputs of the all hybrid system configurations (continued)

Grid Output of 500 Cattle Capacity Hybrid System						
Month	**Energy Purchased (kWh)**	**Energy Sold (kWh)**	**Net Energy Purchased (kWh)**	**Peak Load (kW)**	**Energy Charge ($)**	**Demand Charge ($)**
January	6,392	12,529	-6,138	71	0	0
February	5,466	12,886	-7,420	70	0	0
March	5,426	16,592	-11,166	70	0	0
April	4,881	16,524	-11,643	71	0	0
May	4,304	17,772	-13,468	62	0	0
June	4,071	18,938	-14,867	55	0	0
July	4,179	21,017	-16,838	69	0	0
August	4,867	20,268	-15,400	68	0	0
September	4,808	19,149	-14,341	69	0	0
October	5,289	16,619	-11,330	66	0	0
November	5,758	12,371	-6,613	72	0	0
December	6,437	10,716	-4,279	64	0	0
Annual	61,878	195,380	-133,503	72	17,755	0

Table 5.5 Grid outputs of the all hybrid system configurations (continued)

Grid Output of 1000 Cattle Capacity Hybrid System						
Month	**Energy Purchased (kWh)**	**Energy Sold (kWh)**	**Net Energy Purchased (kWh)**	**Peak Load (kW)**	**Energy Charge ($)**	**Demand Charge ($)**
January	11,917	19,669	-7,751	108	0	0
February	10,321	19,998	-9,677	109	0	0
March	10,662	25,469	-14,807	108	0	0
April	9,121	25,825	-16,704	104	0	0
May	8,828	26,966	-18,138	103	0	0
June	8,413	28,737	-20,324	105	0	0
July	8,285	32,504	-24,218	106	0	0
August	8,653	32,385	-23,731	103	0	0
September	9,367	29,363	-19,996	104	0	0
October	10,501	24,999	-14,498	109	0	0
November	10,647	19,623	-8,976	108	0	0
December	12,169	16,896	-4,727	109	0	0
Annual	118,886	302,434	-183,548	109	24,411	0

Table 5.5 Grid outputs of the all hybrid system configurations (continued)

Grid Output of 5000 Cattle Capacity Hybrid System						
Month	**Energy Purchased (kWh)**	**Energy Sold (kWh)**	**Net Energy Purchased (kWh)**	**Peak Load (kW)**	**Energy Charge ($)**	**Demand Charge ($)**
January	58,750	116,652	-57,902	541	0	0
February	50,267	119,265	-68,998	545	0	0
March	50,415	153,473	-103,058	538	0	0
April	42,661	154,255	-111,594	519	0	0
May	40,653	162,261	-121,609	513	0	0
June	38,387	172,802	-134,415	522	0	0
July	37,642	194,735	-157,093	530	0	0
August	41,362	191,258	-149,896	517	0	0
September	43,683	176,974	-133,291	522	0	0
October	49,763	151,097	-101,335	543	0	0
November	51,276	117,529	-66,253	542	0	0
December	59,526	100,603	-41,077	543	0	0
Annual	564,384	1,810,905	-1,246,521	545	165,787	0

5.1.2 Linear Regression Results

Linear regression model considers two metrics including RMSE and R^2 in order to evaluate performance of the model. As a rule of thumb, lower value of RMSE and higher value of R^2 are indicator of an ideal model. As a result of running the linear regression model under normal conditions, the coefficients, p value, standard error, degree of freedom and F statistic values of 13 independent variables are summarized in the R program. However, only the coefficients of 5 variables are calculated as 8 of the independent variables having singularity problem. This is due to the high degree of multicollinearity problem between the independent variables. When 8 independent variables are eliminated to estimate the dependent variable, linear regression does not again give an accurate RMSE and R^2 value since the data given by these variables has already presented in other variables, thus it is unnecessary. The possible result for linear model created in R programming is shown in Table (5.6).

Table 5.6 The possible result for linear model created in R programming

Coefficients	Estimate	Standard Error	t value	Pr (>|t|)
Intercept	9.604	NA	NA	NA
X1	-6.943	NA	NA	NA
X2	-0.138	NA	NA	NA
X3	7.281	NA	NA	NA
X4	-2.946	NA	NA	NA
X5	1.237	NA	NA	NA
X6	NA	NA	NA	NA
X7	NA	NA	NA	NA

Table 5.6 The possible result for linear model created in R programming (continued)

X8	NA	NA	NA	NA
X9	NA	NA	NA	NA
X10	NA	NA	NA	NA
X11	NA	NA	NA	NA
X12	NA	NA	NA	NA
X13	NA	NA	NA	NA

The strong correlation between the coefficients in the linear regression model leads to singularity problem and R^2 are found as 1.00. This value can be an indicator of multicollinearity problem between the independent variables. In the presence of multicollinearity, the standard errors of the parameter estimate that determine the relationship between the variables are large, which leads to a significant difference in the direction and value of the true correlation coefficient. In determining this problem, correlation matrix of multicollinearity, VIF, eigenvalue and eigenvectors methods are used. Studies in the literature suggest that if the simple correlation coefficient between two independent variables is highly significant, that is, greater than 75%, this may lead to a multicollinearity problem [105]. The existence of the multicollinearity problem between the independent variables is determined by the correlation matrix method shown in Table (5.7). Binary relation between independent variables have positive correlation means that they vary in the same direction. However, only *X10* is negative correlation and it is opposite direction. According to the literature, if the value of the VIF is greater than 5, it can be mentioned that there is a multicollinearity problem. When VIF analysis was performed in the R program, it is seen that the program gives excellent multicollinearity problem results ("aliased coefficient in the model" which arises singularity problem in the regression). Thanks to this method, it is seen that the linear regression method is not a suitable

regression analysis method. Finally, the ratio of the maximum to minimum values of the correlation matrix can be used to determine whether this problem exists in order to determine multicollinearity. If this ratio is less than 10, there is little relationship between the independent variables, but if this ratio is greater than 30, it indicates the existence of a strong relationship [105]. This value in the linear regression analysis is 675 which much higher than 30 means that multicollinearity occurs [105]. The existence of this problem is proved by the other three methods applied. Although the existence of the multicollinearity problem is determined by the emergence of the singularity problem. As a result, since an accurate regression model cannot be established with the linear regression method, regularization regression methods should be used.

Table 5.7 Multicollinearity problem between the independent variables determined by the correlation matrix method

	X1	*X2*	*X3*	*X4*	*X5*	*X6*	*X7*	*X8*	*X9*	*X10*	*X11*	*X12*	*X13*	*Y*
X1	1.000	0.933	0.979	0.804	0.986	0.965	0.788	0.982	0.974	-0.958	0.245	0.934	0.902	-0.953
X2	0.933	1.000	0.984	0.761	0.918	0.878	0.663	0.961	0.902	-0.950	0.249	0.936	0.986	-0.840
X3	0.979	0.894	1.000	0.893	0.994	0.995	0.818	0.935	0.997	-0.891	0.169	0.953	0.891	-0.969
X4	0.804	0.761	0.893	1.000	0.889	0.921	0.642	0.718	0.915	-0.642	0.037	0.913	0.825	-0.873
X5	0.986	0.918	0.994	0.889	1.000	0.992	0.776	0.946	0.997	-0.908	0.205	0.962	0.909	-0.972
X6	0.965	0.878	0.995	0.921	0.992	1.000	0.778	0.910	0.998	-0.861	0.138	0.962	0.883	-0.978
X7	0.788	0.663	0.818	0.642	0.776	0.778	1.000	0.750	0.781	-0.738	0.323	0.651	0.659	-0.725
X8	0.982	0.961	0.935	0.718	0.946	0.910	0.750	1.000	0.927	-0.992	0.233	0.911	0.919	-0.898
X9	0.974	0.902	0.997	0.915	0.997	0.998	0.781	0.927	1.000	-0.881	0.162	0.968	0.904	-0.973
X10	-0.958	-0.950	-0.891	-0.642	-0.908	-0.861	-0.738	-0.992	-0.881	1.000	-0.269	-0.862	-0.897	0.859

Table 5.7 Multicollinearity problem between the independent variables determined by the correlation matrix method (continued)

X11	0.245	0.249	0.169	0.037	0.205	0.138	0.323	0.233	0.162	-0.269	1.000	0.072	0.196	-0.059
X12	0.934	0.936	0.953	0.913	0.962	0.962	0.651	0.911	0.968	-0.862	0.072	1.000	0.954	-0926
X13	0.902	0.986	0.891	0.825	0.909	0.883	0.659	0.919	0.904	-0.897	0.196	0.954	1.000	-0.829
Y	-0.953	-0.840	-0.969	-0.873	-0.972	-0.978	-0.725	-0.898	-0.973	0.859	-0.059	-0.926	-0.829	1.000

5.1.3 Ridge Lasso and Elastic Net Regression Results

A penalty parameter is added to the OLS equation in RR, LR and ENR to minimize the problems in the linear regression model and to make a more accurate model estimation. This approach helps to significantly reduce the variance by reducing the predicted coefficients to 0 relative to the least squares estimates, i.e. fitting a model with all predictors using a method that adjusts or shrinks the coefficients towards 0. Lambda parameter is determined using cross validation technique in all regression methods. This technique is run with "cvglmnet" function by using 5-fold method with five repetitions. This results in optimum lambda value for the regression. In RR, the value of lambda is found to be 2.512 and 0.512 for the train and the test data. RMSE and R^2 value in RR is calculated for train and test data. While the value of RMSE and R^2 for train data is 0.43 (million $) and 0.82, these values for test data is found to be 0.46 (million $) and 0.92 respectively. RMSE for train and test data is reasonably good result as these values close to zero. Moreover, R^2 value of the test data shows 92% correlation with the actual dependent variable. This value can be relatively acceptable value. The intercept and coefficients of RR model is demonstrated in Table (5.8).

Table 5.8 The intercept coefficients of RR models

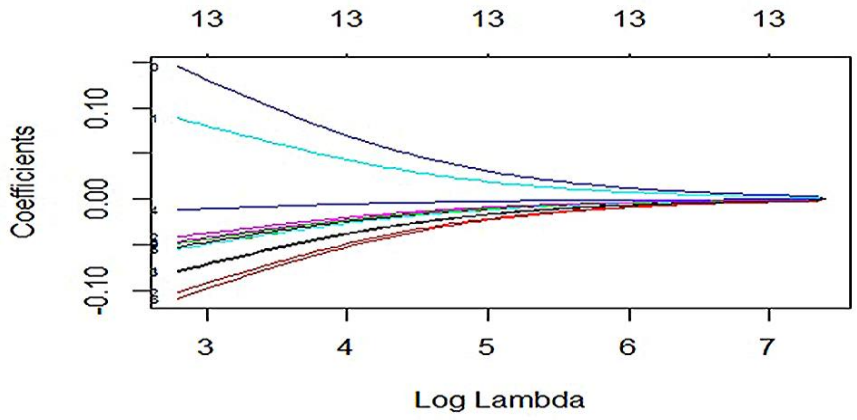
Coefficient	Estimate	Scaled Estimate	Std. Error (scaled)	t value (scaled)	Pr (>|t|)
Intercept	9.957	NA	NA	NA	NA
X1	-0.120	-0.198	0.030	6.574	4.890×10^{-11} ***
X2	-0.125	-0.194	0.029	6.567	5.140×10^{-11} ***
X3	-0.084	-0.198	0.029	6.682	2.360×10^{-11} ***

Table 5.8 The intercept coefficients of RR models (continued)

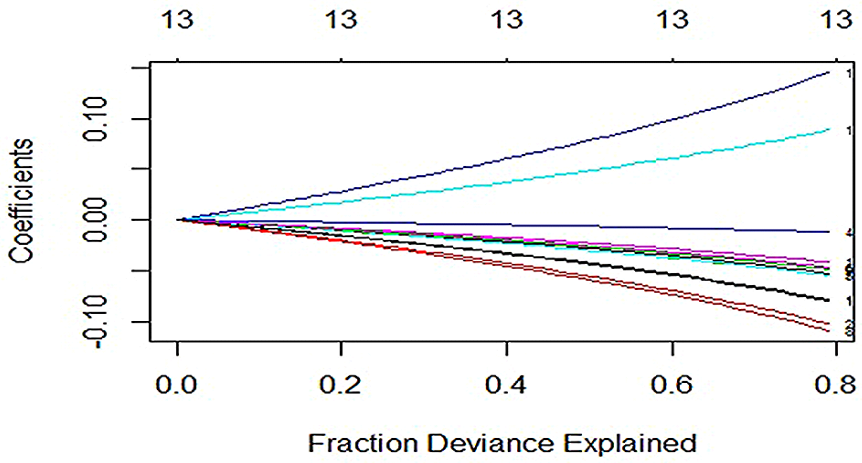
X4	-0.017	-0.196	0.028	6.873	$6.200\ 7\times10^{-12}$ ***
X5	-0.083	-0.197	0.028	6.851	7.340×10^{-12} ***
X6	-0.071	-0.196	0.028	6.899	5.230×10^{-12} ***
X7	-0.087	-0.124	0.090	1.319	0.187
X8	-0.166	-0.197	0.029	6.741	1.570×10^{-11} ***
X9	-0.074	-0.197	0.028	6.893	5.470×10^{-12} ***
X10	-0.223	0.197	0.034	5.718	1.080×10^{-8} ***
X11	-0.128	0.146	0.067	2.167	0.030*
X12	-0.062	-0.184	0.039	4.705	2.540×10^{-12} ***
X13	-0.120	-0.192	0.031	6.141	8.220×10^{-12} ***

[1] The asterisks given in the table are defined as the significance code and indicate how important the estimators are 0 '***' 0.001 '**' 0.01 '*' 0.05 '.' '1

All of the features expect (*X7* and *X11*) are significant predictors given with three asterisk according to their p values. Coefficients of predictors all possess negative relationship with target variable that is, when the predictors increase, *Y* value decreases. Similarly, scaled coefficients of predictors also have negative relationship with the *Y* value except *X10* and *X11*. Figure (5.2) shows change in coefficients vs lambda value and standard deviation.



a)



b)

Figure 5.2 Change in coefficients vs a) lambda value and b) standard deviation

$$Y = 9.957 - 0.120X1 - 0.125X2 - 0.084X3 - 0.017X4 - 0.083X5 - 0.071X6 - 0.087X7 - 0.166X8 - 0.074X9 - 0.223X10 - 0.128X11 - 0.062X12 - 0.120X13 \quad (5.1)$$

Where, ***Y***: Electricity generation contributed to GDP, ***X1***: Human population, ***X2***: Cow milk consumption, ***X3***: Total amount of AW for different cattle barns, ***X4***: Solar installed capacity of Turkey, ***X5***: Biogas installed capacity of Turkey, ***X6***: Electricity generation from renewable energy in Turkey, ***X7***: Total amount of fertilizer consumption, ***X8***: World biogas energy production, ***X9***: World solar energy production, ***X10***: World total installed cost of solar energy, ***X11***: World total installed cost of biogas energy, ***X12***: Dairy cattle fodder price, ***X13***: Number

of dairy cattle. Figure (5.3) illustrates mean squared error (MSE) vs log λ graph for the train data set of RR. In train data the highest value of log λ with -8 gives higher MSE. However, when the log λ approaches between 0 and 2, MSE value also decreases. The optimum lambda value for the train data is 2.512 gives the lowest MSE with 0.425. Unlike the train data, while the MSE value is in a constant trend between -8 and 1.5, the log λ reaches the highest MSE value around 5. The optimum lambda and MSE value for the test data are 0.511 and 0.464, respectively.

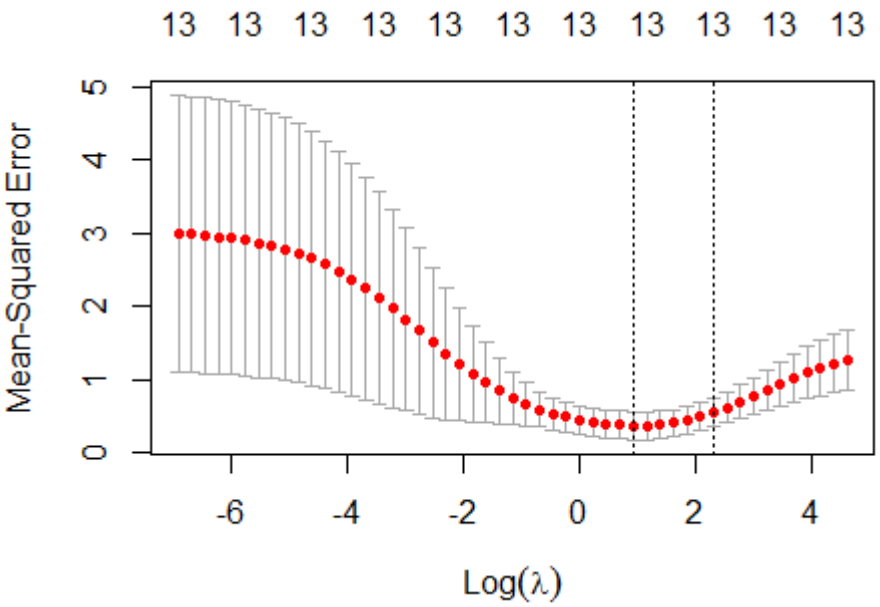


Figure 5.3 Mean squared error (MSE) vs log λ graph for the train data set of RR

As seen the Figure (5.4), the MSE value between the train and test data does not have much difference since cross validation method tries to produce minimum test MSE approaching the train data.

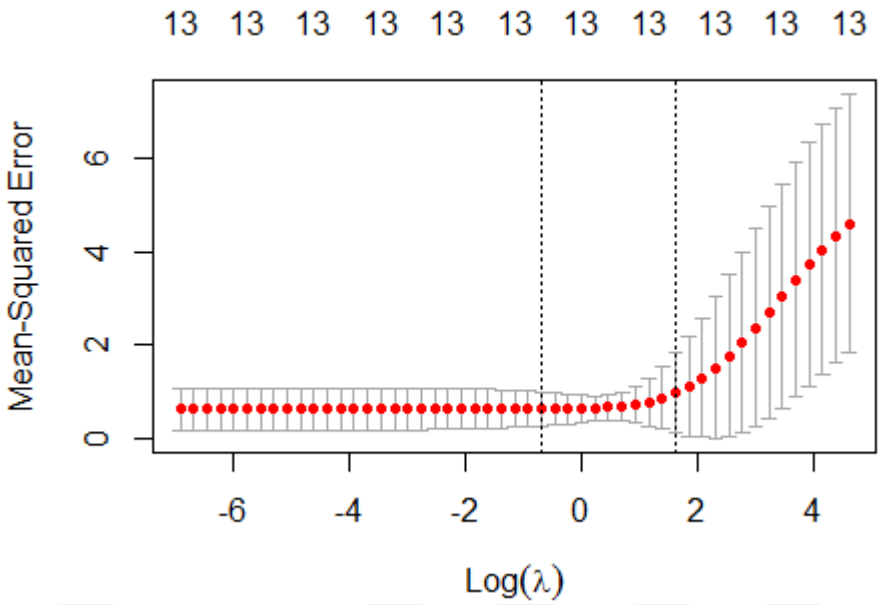


Figure 5.4 Mean squared error (MSE) vs log λ graph for the test data set of RR

R programming also plots importance of variables based on the dependent variable *Y* shown in Figure (5.5) is obtained from plots of R programming. World total installed cost of solar energy (*X10*) has strong effect on the share of electricity generation in GDP with percentage of 97. Energy production from biogas in the world (*X8*) and milk consumption (*X2*) have importance after installed cost of solar energy. Total AW of different solar and biomass HRES (*X3*), biogas installed capacity of Turkey (*X5*) and total amount of fertilizer consumption (*X7*) possess nearly same importance with value of about 35%. However, solar installed capacity of Turkey (*X4*) does not more impact on the share of electricity generation in GDP.

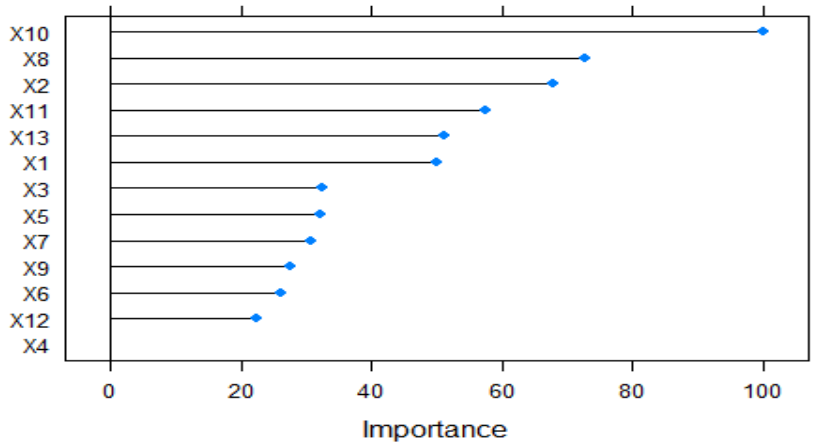


Figure 5.5 Importance of 13 dependent variables on the dependent variable Y

The LR model does not perform as well as RR in estimating RMSE and R^2 values. The RMSE and R^2 values obtained for train data are 0.590 (million $) and 0.66. Likewise, these values for test data are 1.007 million and 0.61, respectively. The lambda values for train and test data are found to be 0.501 and 0.100. In RR, all of the estimator coefficients are found in the model equation, whereas in LR it performs better when few estimators have significant coefficients and the remainder are either very small or equal to 0. It can be seen that all predictive coefficients have a certain effect on the dependent variable, since the RMSE value is higher in LR than in the RR model and the R2 value is considerably lower in LR than in RR. Therefore, it can be said that the RR model is more suitable for this study when compared with the LR model.

The ENR model estimates RMSE and R^2 values similar to RR value. Train data for RMSE and R^2 are 0.446 (million $) and 0.80 whereas these value for test data is calculated to be 0.347 (million $) and 0.95. The alpha and the lambda values for ENR are 0.171 and 1.123 respectively. Although ENR has higher R^2 and lower RMSE values in the test values, some coefficients could not be calculated in this regression. The reason for the missing coefficients may be caused by the ENR considering some independent variables unnecessary. Therefore, the RR model equation is the only model that provides all coefficients.

5.2 Results and Discussion of HRES Design with Co-firing

5.2.1 Comparison of Option A and B Based on Feed in Tariff

PV and biomass co-fired with NG are used in the design of the grid-connected HRES considering the availability of hazelnut shell resource. HOMER is used to select optimum system configuration, which fulfilled load demand of the HCP. Feed in tariffs before and after 2021 are the main factors that affect the profit and feasibility of the study since government incentives for biomass and solar energy dropped nearly 50-70% in 2021.

According to the simulation results, Option A is feasible in terms of life cycle cost and COE. Annual electricity production of Option A is estimated as 2,694,018 kW/yr. Most of the electricity generation are supplied from NG and biomass (NG-Biogas) co-fired generator with nearly 85.70% while electricity supply from PV panel and grid purchase are 6.10% and 8.19%, respectively. The amount of NG and hazelnut shell consumed are 196,023 m^3 and 6,991 ton/yr, respectively. Monthly electricity production of NG-Biogas, PV and grid purchase are given Figure (5.6). In the calculations, unmet load and capacity shortage are neglected, and excess electricity, which is denoted as surplus electrical energy, is negligible at around with 0.033% when compared to total electrical production. The share of renewable energy to meet the load demand of the HCP is 73.60%.

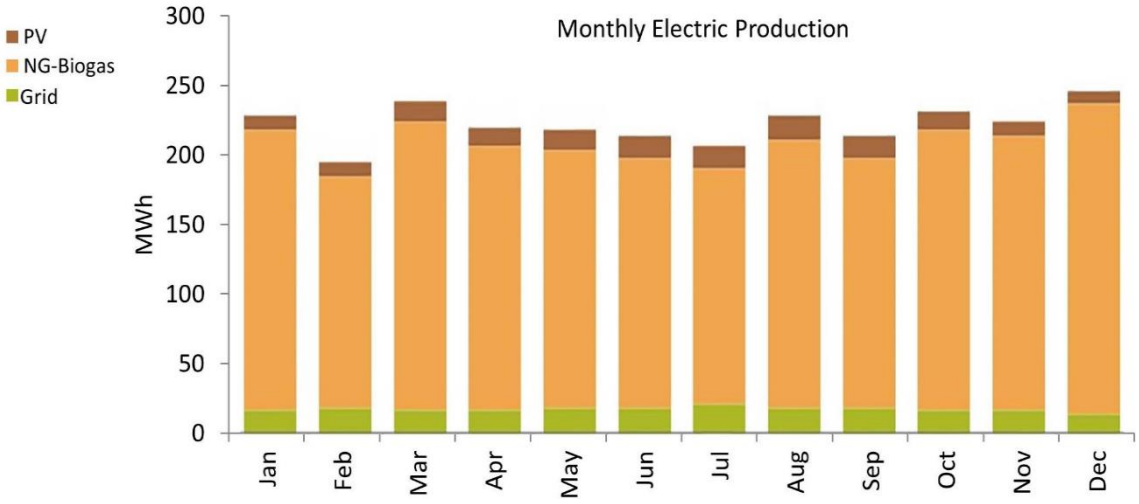


Figure 5.6 Monthly electric production from PV and biomass co-fired with NG of HRES

The optimum life cycle cost or NPC, initial capital cost, and operation cost of Option A are estimated as nearly $3.00 million (M), $2.97 M, and $2,836 per annum, respectively. The majority of the cost comes from the capital and replacement costs of NG-Biogas, while the lowest cost is the converter cost. Distribution of costs related to components are shown in Figure (5.7) (in which the unit of x-axis is project lifetime in years). The energy cost per unit for Option A is approximately 24% lower. This is mainly due to the effect of government incentives for biomass and solar energy. One of the important factors affecting the feasibility of the HRES system is the rising inflation rate in 2020. Because the lowest NPC value is seen when the inflation rate is the lowest. If the cost of the hazelnut shell, which is a by-product, is accepted as zero, the NPC value of the proposed system gives the lowest value but if the hazelnut shell is included in the operation cost, the system is not feasible. This topic is discussed in detail in Section 5.2.2 based on results.

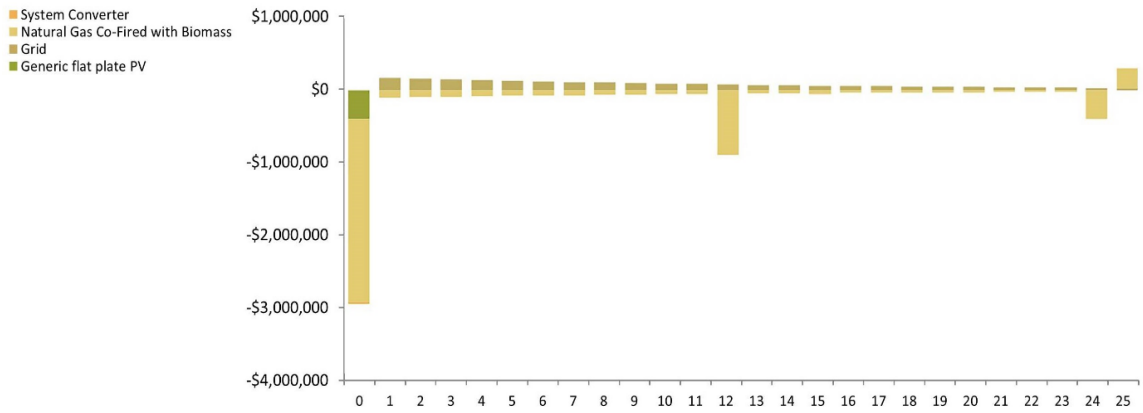


Figure 5.7 Distribution of costs related to the components of Option A

Option B has taken into account the feed-in tariff valid from 2021. NPC and COE of the Option B are found as nearly $3.100 M and $0.202, respectively. Unlike Option A, both NPC and COE are higher, and the share of renewable energy decreases from 74% to about 30%. Energy purchase from the grid (847,295 kWh) are more than twice of the energy sold (378,000 kWh) to the national grid. COE of the Option B ($0.202/kWh) is far from matching the industrial subscribers' electricity tariff ($0.129/kWh) since generator cost is also added to COE [71]. Thus, it is more feasible to use the cost obtained from the national grid instead of the cost obtained in Option B. Share of cost by component is mainly generated

from capital cost of the NG-Biogas system, which is about 82%. Only 4% of the cost is stemmed from the fuel cost since the load demand of the HCP provides energy from the grid. HOMER assumes the capital and replacement cost as zero, however the O&M cost of the grid accounts for approximately 18% of the total cost. Distribution of cost based on the component type is illustrated in Figure (5.8) (in which the unit of x-axis is project lifetime in years).

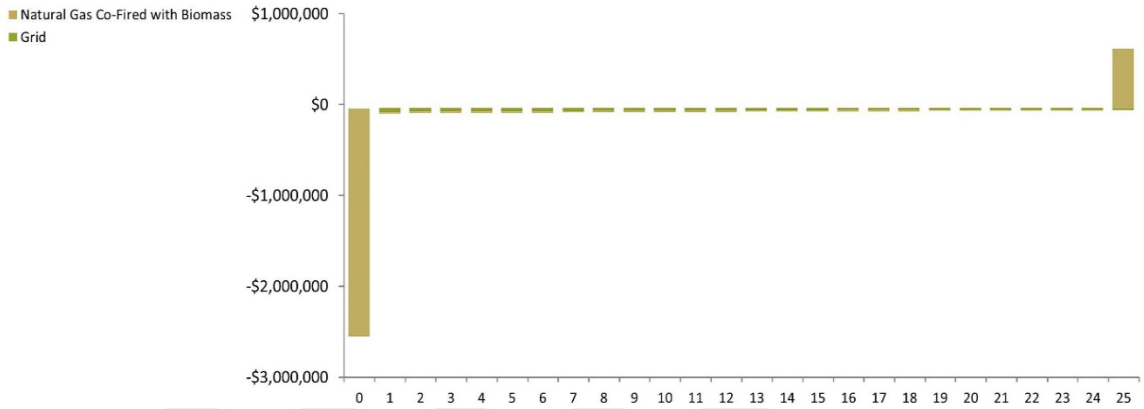


Figure 5.8 Distribution of costs related to the components of Option B

Electricity generation is mostly supplied from grid purchases with 62.60%, however the share of NG-Biogas is nearly half of the grid purchase with 37.10%, and negligible amount of energy generation comes from PV panel. Figure (5.9) illustrates monthly electricity production of Option B corresponding to system components. NG-Biogas generator is only operated 504 hours per year and consumption of hazelnut shell for generating biogas is 1,408 ton/yr. Simulation results of Option A and B are given in Table (5.9).

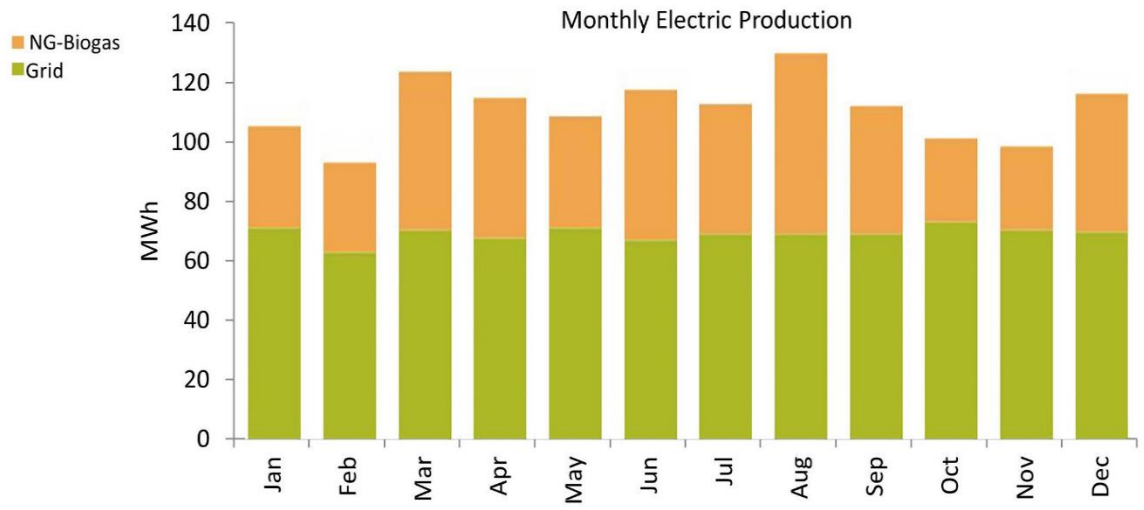


Figure 5.9 Monthly electricity production of Option B corresponding to the components

Table 5.9 Simulation results of Option A and B

Sellback Rate ($/kW)	PV (kW)	NG-Biogas (kW)	Grid (kW)	Converter (kW)	NPC ($)	COE ($)	Operating Cost ($/yr)	Initial Capital ($)	RF (%)
0.080	null	1,500	250	null	3.10 M	0.201	48,556	2.55 M	29.8
0.133	125	1,500	750	97.7	3.00 M	0.098	2,836	2.97 M	73.6

5.2.2 Sensitivity Analysis for HRES

Results of the sensitivity analysis based on the following sensitivity variables: Grid sale capacity, expected inflation rate, nominal discount rate, biomass price, and sellback rate are given in Table (5.10), respectively. The total NPC is the most important economic metric, which is taken as the basis for determining whether the HRES system is feasible or not. The other significant economic metric is COE, which is calculated based on the total NPC and CRF. The sensitivity variables are compared to these two basic economic metrics and results are discussed in the following sections.

Table 5.10 The value of sensitivity variables

Biomass Price ($/ton)	Sellback Rate ($/kWh)	Grid Sale Capacity (kW)	Expected Inflation Rate (%)	Nominal Discount Rate (%)
0	0.080	250	11.85	10
38	0.133	500	15.00	15
76		750	20.00	20

5.2.3 Sensitivity Variables Effect on TNPC and COE

Grid sale capacity is selected between 250 and 750 kW in order to assess both TNPC and COE changes. While the cost of COE tends to decrease continuously, the TNPC decreases slightly up to 500 kW but shows a steady upward trend after that point. The variation of grid sale capacity between 250 and 750 kW is shown in Figure (5.10).

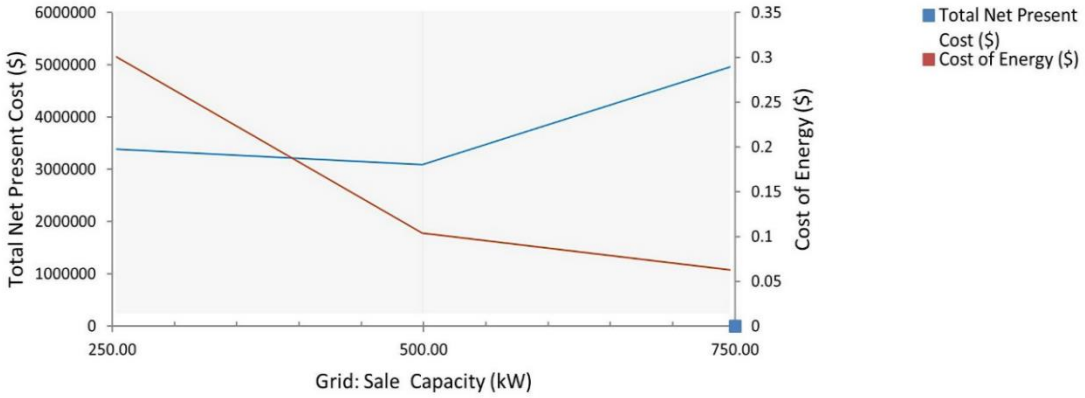


Figure 5.10 The variation of grid sale capacity between 250 and 750 kW

Change in expected inflation rate is varied between 11.85 and 20.00% and executed to the TNPC and COE. Continuously drop in COE is observed when expected inflation rate goes from 11.85% to 20.00% and the value of COE decreases nearly from $0.280/kWh to $0.135/kWh. However, TNPC first slight

increase till 15.00% and then sharply decrease up to 20.00%. Comparison of TNPC and COE values for expected inflation rate is illustrated in Figure (5.11).

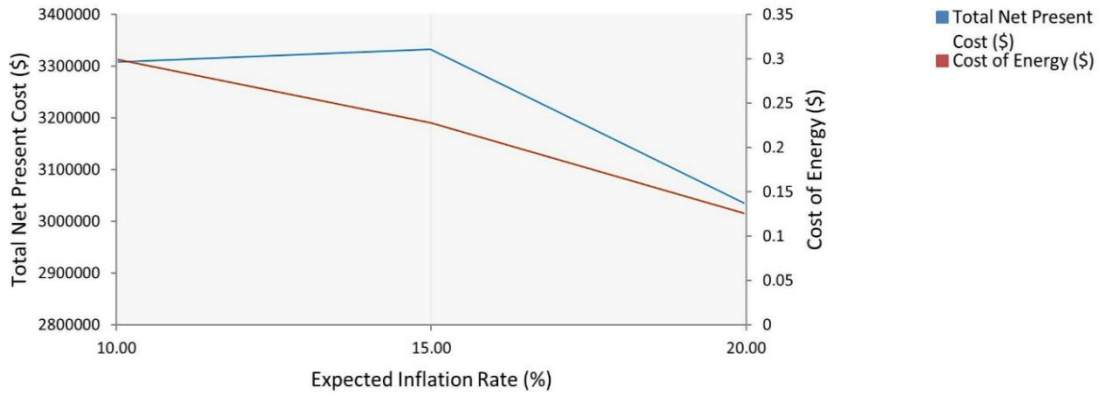


Figure 5.11 Comparison of TNPC and COE values for expected inflation rate

Both TNPC and COE have much lower values at about $2.80 M and $0.170/kW at 10.00% nominal discount rate, respectively; but when nominal discount rate reaches to 15.00% COE starts a relatively sharp decrease till to 20.00% while TNPC shows mostly slight increase. The impact of nominal discount rate on the TNPC and COE are shown in Figure (5.12).

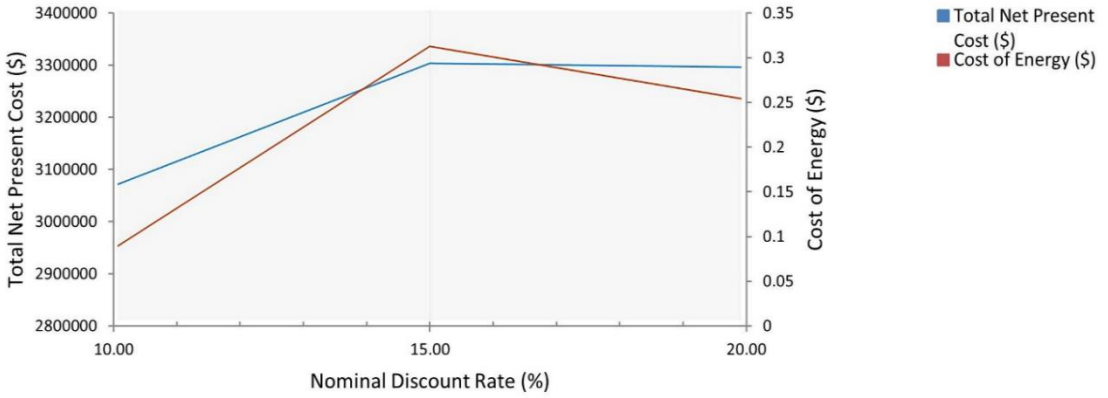


Figure 5.12 The impact of nominal discount rate on the TNPC and COE

Hazelnut shell (biomass) price is selected between zero and $76/ton in order to observe variation in TNPC and COE. When hazelnut shell price increases zero to $38/ton both TNPC and COE increase significantly. On the other hand, biomass price does not have significant effect on the TNPC and COE between $38/ton and $76/ton. The outcome of hazelnut shell price on TNPC and COE are given in Figure (5.13).

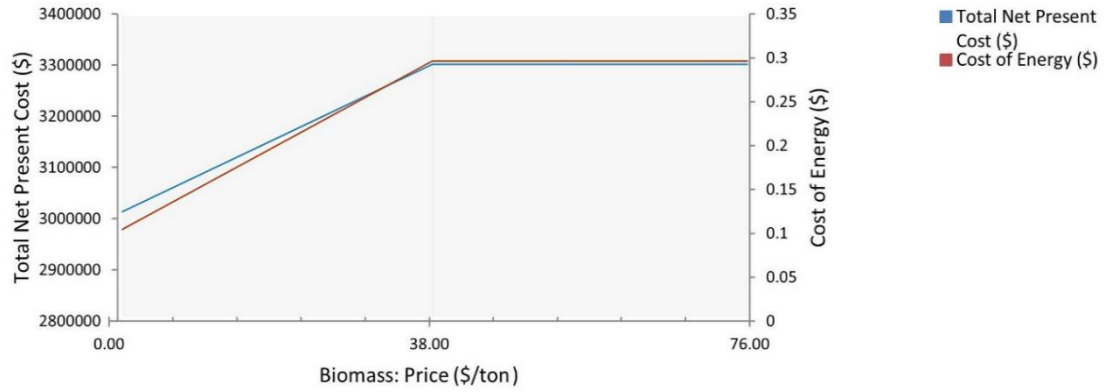


Figure 5.13 The outcome of hazelnut shell price on TNPC and COE

Significant amount of decrease in feed in tariff for biomass energy inversely affects TNPC and COE values. Both of them have strong downward trend compared to sellback rate from $3.22 M to $3.02 M and from $0.225/kWh to $0.100/kWh when price varies between $0.080/kWh and $0.133/kWh. The price change of sellback rate is shown in Figure (5.14).

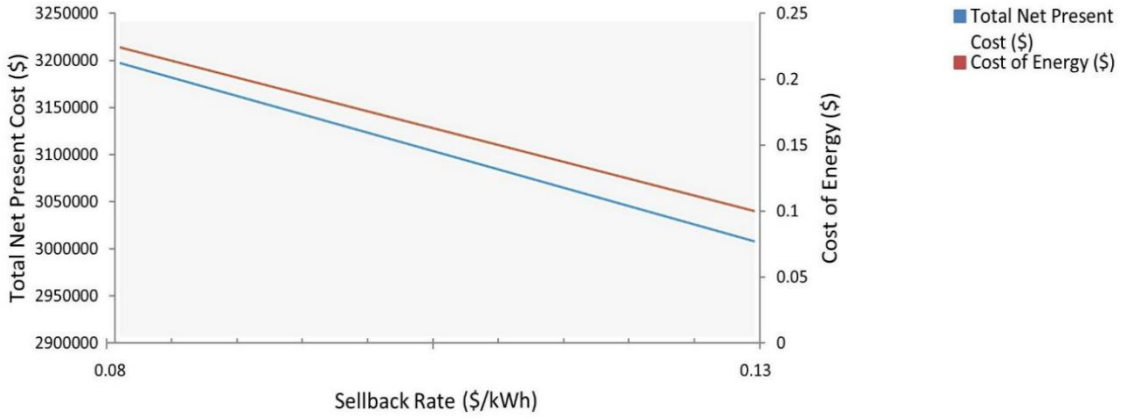


Figure 5.14 The price change of sellback rate

The feasibility of the proposed study is mainly based on the change in feed in tariff after 2021 in Turkey. This makes both standalone biomass and PV, and those hybrid systems not feasible. The increase in energy cost (approximately 56%) makes these options unfeasible investments for the energy investor because the cost of energy supplied from the national grid is cheaper. In addition, high discount and inflation rates and fluctuations in foreign currencies increase investment and operational costs. Although the hazelnut shell is the waste of the HCP, it is used as a fuel in the market for a relatively low cost. If the hazelnut shell

is accepted as a worthless waste of the HCP and the biomass raw material cost is neglected, then the HRES becomes a feasible option with the lowest NPC. However, if the hazelnut shell cost per ton is included in the operation cost, HRES is not feasible in terms of NPC and COE.

5.2.4 Comparison of Four Different Scenarios Based on NPC COE and Greenhouse Gas Emission Analysis

Four different configurations of the proposed study are analyzed in terms of NPC, COE and greenhouse gas emissions analysis. Among the scenarios, the lowest NPC is found in Scenario-4, and also the COE of Scenario-4 is lower than Scenario-2 and Scenario-3 and quite similar to that of Scenario-1. NPC and COE of Scenario-1 are $3.250 M and $0.094/kW, respectively while those values in Scenario-3 are $4.05 M and $0.133/kW, respectively. Co-firing of hazelnut shell with NG positively affects both NPC and COE of Scenario-1. Similarly, contribution of renewable energy fraction in Scenario-3 is zero, which is considered as the worst scenario in terms of environmental concerns, however 18.3% of RF is obtained in Scenario-1. Scenario-2 and 4 are based on HRES configuration including PV panel, converter, generator and grid-connected system. In scenario-2, NG generator is operated only natural gas, but in scenario-4, co-firing option is selected. The RF of Scenario-4 is 73.6% and more than twice when compared to Scenario-2 which has a RF value of 30.6%. The COE purchased from the national grid is $0.129/kW, which is higher than the values attained from Scenario-2 ($0.120/kW) and Scenario-4 ($0.098/kW), respectively. Total fuel consumption of Scenario-4 is four times greater than that of Scenario-2, however NPC and initial capital cost of Scenario-4 are lower than that of Scenario-2. Detailed analysis of four different scenarios based on the electricity production, fuel consumption and RF are shown in Table (5.11). As a result, the co-firing system in Scenario-4 is economically the most feasible amongst all scenarios.

Table 5.11 Detailed analysis of four different scenarios based on the electricity production, fuel consumption and RF

Number of Scenario	System Configuration	NG-with Bio co-firing (kW)	NG-without Bio co-firing (kW)	PV (kW)	Converter (kW)	NPC ($)	COE ($)	Initial Capital ($)	Total Fuel (m^3/yr)	RF (%)
1	NG with biogas co-firing-grid)	1,500	null	null	null	3.25M	0.09	2.55M	22.2	18
2	PV and NG Without biogas co-firing-grid	null	1,500	250	211	3.80M	0.12	3.40M	48.8	30
3	NG without biogas co-firing-grid)	null	1,500	null	null	4.05M	0.13	2.55M	74.3	0
4	PV and NG with biogas co-firing-grid	1,500	null	125	97.7	3.00M	0.09	2.97M	196	73

The annual electricity demand for Scenario-4 when purchased from national grid (220,698 kWh/yr) is about one-tenth of NG with biogas co-firing generator (2,308,989 kWh/yr). This is due to contribution of co-firing of hazelnut shell in the HRES system. Amount of average fuel consumption of NG-Biogas co-firing generator throughout the year is displayed in Figure (5.15). The peak consumption is mostly carried out in February, April and May, and consumption of other months stays stable. Although electricity generation from PV panel for Scenario-4 is around 6.10%, it makes some trade-off with NG with biogas co-firing generator. Amount of average hazelnut shell produced from HCP is 27.4 ton/day, and the amount of hazelnut shell used in gasification is 19.2 ton/day. As a result, approximately 70% of hazelnut shells are used in HRES system daily.

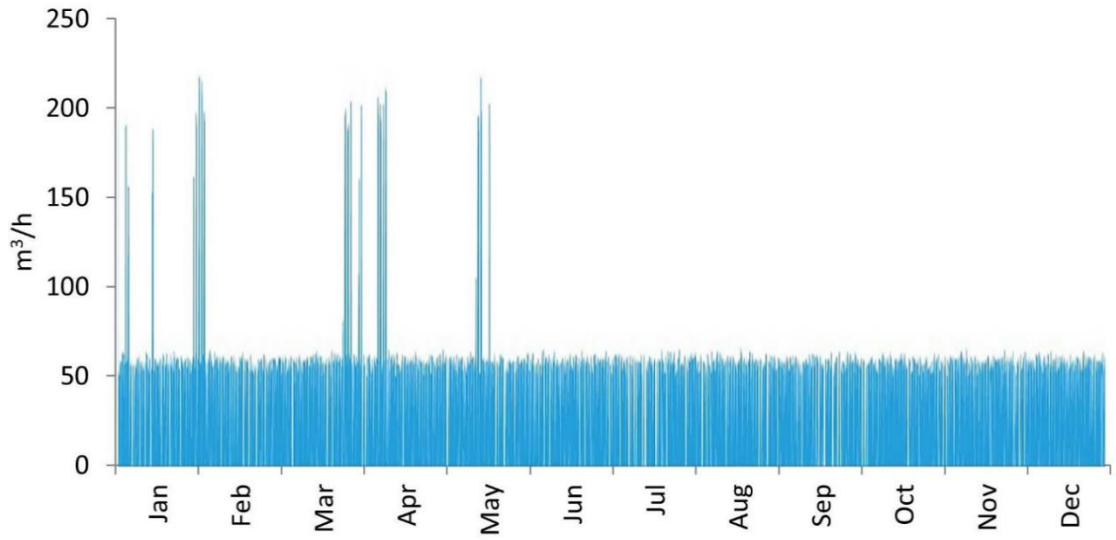


Figure 5.15 Amount of average fuel consumption of NG-Biogas co-firing generator throughout the year

The environmental impacts are also analyzed in this proposed system based on greenhouse gas emissions. Unlike the economic indicators, emission of harmful gases is lowest in Scenario-2. In the presence of PV panel analyzed in Scenario-2, there is considerable amount of decrease in CO_2 emissions which are estimated as 28% and 41% reduction compared to Scenario-1 and 3, respectively. This is because electricity generation from solar energy is considered as carbon neutral path in HOMER. In Scenario-1 and 3 greater amounts of CO and CO_2 emissions are observed due to the absence of PV panel. The amount of total fuel used in Scenario-4, which is much higher than the ones obtained from other scenarios,

increases emissions of all harmful gases from both NG consumption and biogas generation from hazelnut shell, and emissions originated from grid based electricity consumption lead to this situation. The share of energy contribution from PV panels in Scenario-4 has a small impact on minimizing emissions because just nearly 6% of solar energy is used. While the amount of emissions in Scenario-2 is 489,988 kg/yr, which is more than five times of that in Scenario-4 (2,609,875 kg/yr). Emission values of all scenarios including CO_2, CO, unburned hydrocarbons, particulate matters, sulfur dioxides (SO_x) and NO_x are given in Table (5.12).

Table 5.12 Emission values of all scenarios including carbon dioxide, carbon monoxide, unburned hydrocarbons, particulate matters, sulfur dioxides and nitrogen oxides

Emission Values of Four Scenarios	Carbon Dioxide (kg/yr)	Carbon Monoxide (kg/yr)	Unburned Hydrocarbon (kg/yr)	Particulate Matter (kg/yr)	Sulfur Dioxide (kg/yr)	Nitrogen Oxides (kg/yr)
Scenario-1	835,393	714	0	20.10	2,329	2,636
Scenario-2	489,988	314	0	8.85	1,715	1,497
Scenario-3	680,840	478	0	13.50	2,329	2,141
Scenario-4	2,609,875	5,937	0	167.00	605	12,752

5.3 Conclusions

In HRES design of modular cattle barns, CM and solar energy potential of dairy cattle barns with more than 50 dairy cattle are technically and economically examined. Three cities with the largest number of dairy cattle are chosen for the solar and biomass hybrid system in order to predict theoretical solar & biomass hybrid potential of Turkey. In this study, modular dairy cattle barn hybrid systems incorporating biogas and PV have been designed for Turkey, and related technical and economic analysis are carried out. Both standalone configuration and grid-connected HRES configurations are analyzed to find the most feasible solution. In all different capacity of dairy cattle farms, the lowest NPC values are obtained from grid-connected hybrid system with value of $36,942, $54,219, $270,119, $721,516 and $3,097,716, respectively. As a result, NPC values, which is one of the major feasibility indicator of hybrid systems, shows that all dairy cattle farms more 50 cattle would provide profit if the hybrid system is used in these farms. Among different regression models, RR gives highest R^2 value of 0.92 and lowest RMSE value of 0.463 (million $). World total installed cost of solar energy (X10) has strongest effect on the share of electricity generation in GDP with 97%.

A HRES consisting co-firing of hazelnut shell with NG and solar energy is examined. The results clearly showed that the systems design given in this study could further be used to analyze the feasibility of different HRES considering utilization of biomass resources other than hazelnut shells conditional that the amount of biomass generation and energy content are similar. As a suggestion, future work in this field should focus on finding these biomass resources at geographical locations with high renewable energy (wind, geothermal, hydro etc.) potentials. The following key conclusions are attained from this study:

- Change in feed in tariff (Options A and B) before and after 2021 are used to compare the economics of the HRES design. Four different scenarios are analyzed. It is estimated that Option A has NPC and COE values of $3.00 M and $0.098/kW, respectively, which are lower than that of Option B.
- In addition, the energy cost per unit for Option A is approximately 24% lower than that of Option B due to higher government incentives for solar

and biomass energy when compared to electricity price tariff of the national grid. Among the four scenarios, NPC and COE values of Scenario-4 are the lowest but emissions of CO_2 and NO_x are the highest, which are 2,609,875 kg/yr and 12,752 kg/yr, respectively due to high consumption of NG and hazelnut shells for power generation.

- The highest NPC and COE values are obtained in Scenario-3, which are $4.05 M and $0.133/kW, respectively due to requirement for NG as fuel for the generator and consumption of electricity from the national grid which increased both NPC and COE. In the sensitivity analysis, increase in nominal discount rate and biomass price resulted in a rise in both TNPC and COE, while increase in expected inflation and sellback rates decreased both TNPC and COE.

Consequently, it is deemed that the results of this study could guide energy investors using HRES utilizing benefits of CM and co-firing with solar energy. It also encourages academics and researchers to investigate installation of PV panel on the roof and co-firing capabilities of other biomass resources in HRES configurations.

REFERENCES

[1] A. Demirbaş, "Biofuels Sources, Biofuel Policy, Biofuel Economy and Global Biofuel Projections," *Energy Convers. Manag.*, vol. 49, pp. 2106–2116, Aug. 2008, doi: 10.1016/j.enconman.2008.02.020.

[2] C. Godard, J. Boissy, and B. Gabrielle, "Life-cycle assessment of local feedstock supply scenarios to compare candidate biomass sources," *GCB Bioenergy*, vol. 5, Jan. 2013, doi: 10.1111/j.1757-1707.2012.01187.x.

[3] K. Openshaw, "Biomass energy: Employment generation and its contribution to poverty alleviation," *Biomass and Bioenergy*, vol. 34, pp. 365–378, Mar. 2010, doi: 10.1016/j.biombioe.2009.11.008.

[4] M. Ozturk *et al.*, "Biomass and bioenergy: An overview of the development potential in Turkey and Malaysia," *Renew. Sustain. Energy Rev.*, May 2017.

[5] N. L. Panwar, S. C. Kaushik, and S. Kothari, "Role of renewable energy sources in environmental protection: A review," *Renew. Sustain. Energy Rev.*, vol. 15, no. 3, pp. 1513–1524, 2011, doi: https://doi.org/10.1016/j.rser.2010.11.037.

[6] G. Berndes, M. Hoogwijk, and R. van den Broek, "The contribution of biomass in the future global energy supply: a review of 17 studies," *Biomass and Bioenergy*, vol. 25, no. 1, pp. 1–28, 2003, doi: https://doi.org/10.1016/S0961-9534(02)00185-X.

[7] A. Karagiannidis, M. Wittmaier, S. Langer, B. Bilitewski, and A. Malamakis, "Thermal processing of waste organic substrates: Developing and applying an integrated framework for feasibility assessment in developing countries," *Renew. Sustain. Energy Rev.*, vol. 13, no. 8, pp. 2156–2162, 2009, doi: https://doi.org/10.1016/j.rser.2008.09.035.

[8] P. C. Hulteberg and H. T. Karlsson, "A study of combined biomass gasification and electrolysis for hydrogen production," *Int. J. Hydrogen Energy*, vol. 34, no. 2, pp. 772–782, 2009, doi: https://doi.org/10.1016/j.ijhydene.2008.10.073.

[9] C. Koroneos, G. Xydis, and A. Polyzakis, "The Optimal use of Renewable Energy Sources—The Case of Lemnos Island," *Int. J. Green Energy*, vol. 10, no. 8, pp. 860–875, Sep. 2013, doi: 10.1080/15435075.2012.727929.

[10] M. Fadaeenejad, M. A. M. Radzi, M. Z. A. AbKadir, and H. Hizam, "Assessment of hybrid renewable power sources for rural electrification in Malaysia," *Renew. Sustain. Energy Rev.*, vol. 30, pp. 299–305, 2014, doi: https://doi.org/10.1016/j.rser.2013.10.003.

[11] R. Sen and S. Bhattacharyya, "Off-grid electricity generation with renewable energy technologies in India: An application of HOMER," *Renew. Energy*, vol. 62, pp. 388–398, Feb. 2014, doi: 10.1016/j.renene.2013.07.028.

[12] S. Bhattacharjee and A. Dey, "Techno-economic performance evaluation of

grid integrated PV-biomass hybrid power generation for rice mill," *Sustain. Energy Technol. Assessments*, vol. 7, pp. 6–16, 2014, doi: https://doi.org/10.1016/j.seta.2014.02.005.

[13] S. ghaem sigarchian, R. Paleta, A. Pina, and A. Malmquist, "Feasibility study of using a biogas engine as backup in a decentralized hybrid (PV/wind/battery) power generation system – Case study Kenya," *Energy*, vol. 90, Jul. 2015, doi: 10.1016/j.energy.2015.07.008.

[14] A. Singh and P. Baredar, "Techno-economic assessment of a solar PV, fuel cell, and biomass gasifier hybrid energy system," *Energy Reports*, vol. 2, pp. 254–260, 2016, doi: https://doi.org/10.1016/j.egyr.2016.10.001.

[15] C. Ghenai and I. Janajreh, "Design of Solar-Biomass Hybrid Microgrid System in Sharjah," *Energy Procedia*, vol. 103, pp. 357–362, Dec. 2016, doi: 10.1016/j.egypro.2016.11.299.

[16] R. Rajbongshi, D. Borgohain, and S. Mahapatra, "Optimization of PV-biomass-diesel and grid base hybrid energy systems for rural electrification by using HOMER," *Energy*, vol. 126, pp. 461–474, 2017, doi: https://doi.org/10.1016/j.energy.2017.03.056.

[17] J. N. Zala and P. Jain, "Design and optimization of a biogas-solar-wind hybrid system for decentralized energy generation for rural India," *Int. Res. J. Eng. Technol*, vol. 4, pp. 649–656, 2017.

[18] M. B. Eteiba, S. Barakat, M. M. Samy, and W. I. Wahba, "Optimization of an off-grid PV/Biomass hybrid system with different battery technologies," *Sustain. Cities Soc.*, vol. 40, pp. 713–727, 2018, doi: https://doi.org/10.1016/j.scs.2018.01.012.

[19] L. Mellouk, M. Ghazi, A. Aaroud, M. Boulmalf, D. Benhaddou, and K. Zine-Dine, "Design and energy management optimization for hybrid renewable energy system-case study: Laayoune region," *Renew. Energy*, vol. 139, pp. 621–634, 2019.

[20] A. Pal and S. Bhattacharjee, "Effectuation of biogas based hybrid energy system for cost-effective decentralized application in small rural community," *Energy*, vol. 203, p. 117819, 2020.

[21] V. Suresh, M. Muralidhar, and R. Kiranmayi, "Modelling and optimization of an off-grid hybrid renewable energy system for electrification in a rural areas," *Energy Reports*, vol. 6, pp. 594–604, 2020.

[22] L. Ji, X. Liang, Y. Xie, G. Huang, and B. Wang, "Optimal design and sensitivity analysis of the stand-alone hybrid energy system with PV and biomass-CHP for remote villages," *Energy*, vol. 225, p. 120323, Mar. 2021, doi: 10.1016/j.energy.2021.120323.

[23] B. K. Das, M. S. H. K. Tushar, and R. Hassan, "Techno-economic optimisation of stand-alone hybrid renewable energy systems for concurrently meeting electric and heating demand," *Sustain. Cities Soc.*, vol. 68, p. 102763, 2021, doi: https://doi.org/10.1016/j.scs.2021.102763.

[24] A. Demiroren and U. Yilmaz, "Analysis of change in electric energy cost with

using renewable energy sources in Gökceada, Turkey: An island example," *Renew. Sustain. Energy Rev.*, vol. 14, no. 1, pp. 323–333, 2010, doi: https://doi.org/10.1016/j.rser.2009.06.030.

[25] B. E. Türkay and A. Y. Telli, "Economic analysis of standalone and grid connected hybrid energy systems," *Renew. Energy*, vol. 36, no. 7, pp. 1931–1943, 2011, doi: https://doi.org/10.1016/j.renene.2010.12.007.

[26] M. Gökçek and C. Kale, "Techno-economical evaluation of a hydrogen refuelling station powered by Wind-PV hybrid power system: A case study for İzmir-Çeşme," *Int. J. Hydrogen Energy*, vol. 43, no. 23, pp. 10615–10625, 2018.

[27] B. D. Mert, F. Ekinci, and T. Demirdelen, "Effect of partial shading conditions on off-grid solar PV/Hydrogen production in high solar energy index regions," *Int. J. Hydrogen Energy*, vol. 44, no. 51, pp. 27713–27725, 2019.

[28] E. Aykut and Ü. K. Terzi, "Techno-economic and environmental analysis of grid connected hybrid wind/photovoltaic/biomass system for Marmara University Goztepe campus," *Int. J. Green Energy*, vol. 17, no. 15, pp. 1036–1043, 2020.

[29] EMRA, "Regulation Amending the Electricity Market License Regulation," 2020. https://www.resmigazete.gov.tr/eskiler/2020/03/20200308-7.htm.

[30] M. S. Islam, R. Akhter, and M. A. Rahman, "A thorough investigation on hybrid application of biomass gasifier and PV resources to meet energy needs for a northern rural off-grid region of Bangladesh: A potential solution to replicate in rural off-grid areas or not?," *Energy*, vol. 145, pp. 338–355, 2018, doi: 10.1016/j.energy.2017.12.125.

[31] D. M. Alotaibi, M. Akrami, M. Dibaj, and A. A. Javadi, "Smart energy solution for an optimised sustainable hospital in the green city of NEOM," *Sustain. Energy Technol. Assessments*, vol. 35, pp. 32–40, 2019, doi: https://doi.org/10.1016/j.seta.2019.05.017.

[32] M. H. Jahangir and R. Cheraghi, "Economic and environmental assessment of solar-wind-biomass hybrid renewable energy system supplying rural settlement load," *Sustain. Energy Technol. Assessments*, vol. 42, p. 100895, 2020, doi: https://doi.org/10.1016/j.seta.2020.100895.

[33] P. Malik, M. Awasthi, and S. Sinha, "Techno-economic and environmental analysis of biomass-based hybrid energy systems: A case study of a Western Himalayan state in India," *Sustain. Energy Technol. Assessments*, vol. 45, p. 101189, 2021, doi: https://doi.org/10.1016/j.seta.2021.101189.

[34] M. M. Maghanaki, B. Ghobadian, G. Najafi, and R. J. Galogah, "Potential of biogas production in Iran," *Renew. Sustain. Energy Rev.*, vol. 28, pp. 702–714, 2013, doi: https://doi.org/10.1016/j.rser.2013.08.021.

[35] T. R. Sreekrishnan, S. Kohli, and V. Rana, "Enhancement of biogas production from solid substrates using different techniques—a review," *Bioresour. Technol.*, vol. 95, no. 1, pp. 1–10, 2004.

[36] R. J. Patinvoh, O. A. Osadolor, K. Chandolias, I. S. Horváth, and M. J. Taherzadeh, “Innovative pretreatment strategies for biogas production,” *Bioresour. Technol.*, vol. 224, pp. 13–24, 2017.

[37] Ministry of Energy and Natural Resources, “Biogas,” 2020. http://www.yegm.gov.tr/yenilenebilir/biyogaz.aspx. (accessed Feb. 03, 2020).

[38] B. Kara, Z. Emir, T. Seker, A. Bahadir, and K. Kaygusuz, “Current state and future prospects of biomass energy in Turkey,” *J. Eng. Res. Appl. Sci.*, vol. 6, no. 1, pp. 522–529, 2017.

[39] IRENA, “Bioenergy,” 2021. https://irena.org/bioenergy.

[40] T. Amon, B. Amon, V. Kryvoruchko, W. Zollitsch, K. Mayer, and L. Gruber, “Biogas production from maize and dairy cattle manure—influence of biomass composition on the methane yield,” *Agric. Ecosyst. Environ.*, vol. 118, no. 1–4, pp. 173–182, 2007.

[41] B. Stürmer, “Feedstock change at biogas plants–Impact on production costs,” *Biomass and bioenergy*, vol. 98, pp. 228–235, 2017.

[42] E. Monteiro, V. Mantha, and A. Rouboa, “Prospective application of farm cattle manure for bioenergy production in Portugal,” *Renew. Energy*, vol. 36, no. 2, pp. 627–631, 2011.

[43] J. L. Ramos-Suárez, A. Ritter, J. M. González, and A. C. Pérez, “Biogas from animal manure: A sustainable energy opportunity in the Canary Islands,” *Renew. Sustain. Energy Rev.*, vol. 104, pp. 137–150, 2019.

[44] M. S. Roni, S. Chowdhury, S. Mamun, M. Marufuzzaman, W. Lein, and S. Johnson, “Biomass co-firing technology with policies, challenges, and opportunities: A global review,” *Renew. Sustain. Energy Rev.*, vol. 78, pp. 1089–1101, 2017.

[45] EPA, “AgSTAR Data and Trends,” 2020. https://www.epa.gov/agstar/agstar-data-and-trends (accessed May 20, 2020).

[46] P. Aggarangsi, N. Tippayawong, J. C. Moran, and P. Rerkkriangkrai, “Overview of livestock biogas technology development and implementation in Thailand,” *Energy Sustain. Dev.*, vol. 17, no. 4, pp. 371–377, 2013.

[47] Ministry of Energy and Natural Resources, “Türkiye Biyokütle Enerjisi Potansiyeli Atlası,” 2019. https://bepa.enerji.gov.tr/ (accessed Jun. 25, 2021).

[48] C. Karaca and H. Ozturk, *Biogas Production Potential from Animal Manure in Osmaniye Province*. 2017.

[49] A. Demirbas, “Combustion characteristics of different biomass fuels,” *Prog. energy Combust. Sci.*, vol. 30, no. 2, pp. 219–230, 2004.

[50] J. L. Easterly and M. Burnham, “Overview of biomass and waste fuel resources for power production,” *Biomass and Bioenergy*, vol. 10, no. 2–3, pp. 79–92, 1996.

[51] B. A. Gold and D. A. Tillman, “Wood cofiring evaluation at TVA power plants,” *Biomass and Bioenergy*, vol. 10, no. 2–3, pp. 71–78, 1996.

[52] K. R. G. Hein and J. M. Bemtgen, “EU clean coal technology—co-combustion of coal and biomass,” *Fuel Process. Technol.*, vol. 54, no. 1–3, pp. 159–169, 1998.

[53] E. E. Hughes and D. A. Tillman, “Biomass cofiring: status and prospects 1996,” *Fuel Process. Technol.*, vol. 54, no. 1–3, pp. 127–142, 1998.

[54] M. Sami, K. Annamalai, and M. Wooldridge, “Co-firing of coal and biomass fuel blends,” *Prog. energy Combust. Sci.*, vol. 27, no. 2, pp. 171–214, 2001.

[55] D. A. Tillman, “Biomass cofiring: the technology, the experience, the combustion consequences,” *Biomass and bioenergy*, vol. 19, no. 6, pp. 365–384, 2000.

[56] J. Koppejan and S. Van Loo, *The handbook of biomass combustion and co-firing*. Routledge, 2012.

[57] IEA, “Good Practice Guidelines: Bioenergy Project Development and Biomass Supply,” 2009. https://www.ieabioenergy.com/blog/publications/good-practice-guidelines-bioenergy-project-development-and-biomass-supply/.

[58] C. Yin, L. Rosendahl, and S. Kær, “Grate-firing of biomass for heat and power production,” *Prog. Energy Combust. Sci.*, vol. 34, pp. 725–754, Dec. 2008, doi: 10.1016/j.pecs.2008.05.002.

[59] M. V Gil and F. Rubiera, “Coal and biomass cofiring: fundamentals and future trends,” in *New Trends in Coal Conversion*, Elsevier, 2019, pp. 117–140.

[60] E. Agbor, X. Zhang, and A. Kumar, “A review of biomass co-firing in North America,” *Renew. Sustain. Energy Rev.*, vol. 40, pp. 930–943, 2014.

[61] Danish Energy Agency, “Denmark’s Energy and Climate Outlook,” 2020. https://ens.dk/en/our-services/projections-and-models/denmarks-energy-and-climate-outlook.

[62] F. Cherubini, G. Jungmeier, and M. Mandl, “IEA Bioenergy Task 42-Countries report. IEA Bioenergy Task 42 on biorefineries: Co-production of fuels, chemicals, power and materials from biomass. Final report,” 2010.

[63] D. Tonini and T. Astrup, “LCA of biomass-based energy systems: a case study for Denmark,” *Appl. Energy*, vol. 99, pp. 234–246, 2012.

[64] IEA, “Energy Strategy 2050,” 2021. https://www.iea.org/policies/5122-energy-strategy-2050.

[65] K. A. Mullins, A. Venkatesh, A. L. Nagengast, and M. Kocoloski, “Regional allocation of biomass to US energy demands under a portfolio of policy scenarios,” *Environ. Sci. Technol.*, vol. 48, no. 5, pp. 2561–2568, 2014.

[66] T. O. Wilson, F. M. McNeal, S. Spatari, D. G. Abler, and P. R. Adler, “Densified biomass can cost-effectively mitigate greenhouse gas emissions and address energy security in thermal applications,” *Environ. Sci. Technol.*,

vol. 46, no. 2, pp. 1270–1277, 2012.

[67] E. Kapluhan, “ENERJİ COĞRAFYASI AÇISINDAN BİR İNCELEME: GÜNEŞ ENERJİSİNİN DÜNYA’DAKİ VE TÜRKİYE’DEKİ KULLANIM DURUMU,” *Coğrafya Derg.*, no. 29, pp. 70–98, 2014.

[68] IRENA, “Solar Energy Data,” 2020. https://www.irena.org/solar.

[69] G. Sistemleri, “Türkiye’nin Güneş Enerjisi Potansiyeli,” 2021. http://www.gunessistemleri.com/potansiyel.php.

[70] A. Naci and E. Ozgür, “Review of Turkey ’ s photovoltaic energy status : Legal structure , existing installed power and comparative analysis,” vol. 134, no. September, 2020, doi: 10.1016/j.rser.2020.110344.

[71] EMRA, “Electricity Market Tariffs List,” 2021. https://www.epdk.gov.tr/Detay/Icerik/3-0-1/tarifeler (accessed Mar. 08, 2021).

[72] S. Abdul-Wahab, K. Mujezinovic, and A. M. Al-Mahruqi, “Optimal design and evaluation of a hybrid energy system for off-grid remote area,” *Energy Sources, Part A Recover. Util. Environ. Eff.*, pp. 1–13, Aug. 2019, doi: 10.1080/15567036.2019.1656308.

[73] M. Bagheri, N. Shirzadi, E. Bazdar, and C. A. Kennedy, “Optimal planning of hybrid renewable energy infrastructure for urban sustainability: Green Vancouver,” *Renew. Sustain. Energy Rev.*, vol. 95, no. November 2017, pp. 254–264, 2018, doi: 10.1016/j.rser.2018.07.037.

[74] HOMER Pro User Manual, “HOMER pro 3.14,” 2020. https://www.homerenergy.com/products/pro/docs/latest/index.html (accessed Aug. 25, 2020).

[75] I. Yahyaoui, *Advances in Renewable Energies and Power Technologies: Volume 1: Solar and Wind Energies*. Elsevier, 2018.

[76] P. Stackhouse, A. J. Bernett, M. Bradley, T. Zhang, and C. Mikovitz, “Prediction Of Worldwide Energy Resources,” 2020. https://power.larc.nasa.gov/data-access-viewer/ (accessed May 10, 2020).

[77] Meat and Milk Board, “Domestic and Foreign Dairy Cattle Breeds,” 2020. https://www.esk.gov.tr/tr/10883/Yerli-ve-Yabanci-Sut-Sigir-Irklari (accessed May 12, 2020).

[78] N. T. Carlin, K. Annamalai, W. L. Harman, and J. M. Sweeten, “The economics of reburning with cattle manure-based biomass in existing coal-fired power plants for NOx and CO2 emissions control,” *Biomass and Bioenergy*, vol. 33, no. 9, pp. 1139–1157, 2009, doi: https://doi.org/10.1016/j.biombioe.2009.04.007.

[79] S. Türkdoğan, S. Dilber, and B. Çam, “Hibrit Enerji Sistemlerinin Şebekeden Bağımsız Bir Çiftlik Evinde Uygulanabilirliğinin Ekonomik ve Teknik Açıdan İncelenmesi,” *Sinop Üniversitesi Fen Bilim. Derg.*, vol. 3, no. 2, pp. 52–65, 2018, doi: 10.33484/sinopfbd.382391.

[80] J. M. Pereira, C. J. Álvarez, and M. Barrasa, “Prediction of Dairy Housing

Construction Costs," *J. Dairy Sci.*, vol. 86, no. 11, pp. 3536–3541, 2003, doi: https://doi.org/10.3168/jds.S0022-0302(03)73958-7.

[81] TNAU Agritech, "Housing for Dairy Cattle," 2009. http://agritech.tnau.ac.in/animal_husbandry/animhus_cattle_housing.html (accessed Apr. 03, 2020).

[82] Central Bank of Turkey, "Interest rate statistics," 2020. https://www.tcmb.gov.tr/wps/wcm/connect/EN/TCMB+EN/Main+Menu/Statistics/Interest+Rate+Statistics. (accessed Apr. 03, 2020).

[83] FRED, "Interest rates, discount rate for Turkey," 2019. https://fred.stlouisfed.org/series/INTDSRTRM193N (accessed Apr. 03, 2020).

[84] Mevlana Development Agency, "Karapınar İlçesi'nde Güneş Enerjisine Dayalı Elektrik Üretim Tesisi Yatırımları için Enerji İhtisas Endüstri Bölgesi Kurulmasına Yönelik Fizibilite Çalışması Raporu.," Konya, 2014. [Online]. Available: http://www.konyadayatirim.gov.tr/images/dosya/Karapınar Güneş Enerjisi Fizibilite Raporu.pdf.

[85] NREL, "US solar maintenance costs plummet as tech gains multiply," 2018. https://analysis.newenergyupdate.com/pv-insider/us-solar-maintenance-costs-plummet-tech-gains-multiply (accessed May 15, 2020).

[86] Ministry of Energy and Natural Resources, "Law on the Use of Renewable Energy Resources for Electric Energy Purposes," 2005. https://www.mevzuat.gov.tr/MevzuatMetin/1.5.5346.pdf (accessed Apr. 03, 2020).

[87] Global Petrol Prices, "Turkey electricity prices," 2019. https://www.globalpetrolprices.com/Turkey/electricity_prices/.

[88] D. Carty, "Training Data vs. Validation Data vs. Test Data for ML Algorithms," 2021. https://www.applause.com/blog/training-data-validation-data-vs-test-data.

[89] J. Brownlee, "Train-Test Split for Evaluating Machine Learning Algorithms," 2020. https://machinelearningmastery.com/train-test-split-for-evaluating-machine-learning-algorithms/.

[90] IBM Cloud Education, "Overfitting," 2021. https://www.ibm.com/cloud/learn/overfitting.

[91] IBM Cloud Education, "Underfitting," 2021. https://www.ibm.com/cloud/learn/underfitting.

[92] V. Gudivada, A. Apon, and J. Ding, "Data Quality Considerations for Big Data and Machine Learning: Going Beyond Data Cleaning and Transformations," *Int. J. Adv. Softw.*, vol. 10, pp. 1–20, Jul. 2017.

[93] S. Singh, "Understanding the Bias-Variance Tradeoff," 2018. https://towardsdatascience.com/understanding-the-bias-variance-tradeoff-165e6942b229.

[94] Anonymous, "Root Mean Square Error," 2020. https://c3.ai/glossary/data-

science/root-mean-square-error-rmse/.

[95] Pennstate Department of Statistic, “Coefficient of Determination,” 2021. https://online.stat.psu.edu/stat500/lesson/9/9.3.

[96] D. M. Lane, D. Scott, M. Hebl, R. Guerra, D. Osherson, and H. Zimmer, *Introduction to statistics*. Citeseer, 2017.

[97] P. Gupta, “Regularization in Machine Learning,” 2017. https://towardsdatascience.com/regularization-in-machine-learning-76441ddcf99a.

[98] C. Goyal, “Complete Guide to Regularization Techniques in Machine Learning,” 2021. https://www.analyticsvidhya.com/blog/2021/05/complete-guide-to-regularization-techniques-in-machine-learning/.

[99] H. Wang and H. Zheng, “Model Validation, Machine Learning BT - Encyclopedia of Systems Biology,” W. Dubitzky, O. Wolkenhauer, K.-H. Cho, and H. Yokota, Eds. New York, NY: Springer New York, 2013, pp. 1406–1407.

[100] J. Brownlee, “A Gentle Introduction to k-fold Cross-Validation,” 2018. https://machinelearningmastery.com/k-fold-cross-validation/.

[101] Data Camp, “Cross Validation,” 2021. https://campus.datacamp.com/courses/supervised-learning-with-scikit-learn/regression-2?ex=8.

[102] N. Shrestha, “Detecting Multicollinearity in Regression Analysis,” *Am. J. Appl. Math. Stat.*, vol. 8, pp. 39–42, Jun. 2020, doi: 10.12691/ajams-8-2-1.

[103] J. Daoud, “Multicollinearity and Regression Analysis,” *J. Phys. Conf. Ser.*, vol. 949, p. 12009, Dec. 2017, doi: 10.1088/1742-6596/949/1/012009.

[104] E. İmir Şıklar, “Çoklu bağıntılı doğrusal modellerde Ridge regresyon yöntemiyle parametre kestirimi: Türkiye’de (1963-1983) enflasyon analizi,” 1986.

[105] J. Neter, M. H. Kutner, C. J. Nachtsheim, and W. Wasserman, “Applied linear statistical models,” 1996.

[106] D. J. Olive, “Linear regression,” *Linear Regres.*, pp. 1–494, 2017, doi: 10.1007/978-3-319-55252-1.

[107] A. V. Dorugade and D. N. Kashid, “Alternative method for choosing ridge parameter for regression,” *Appl. Math. Sci.*, vol. 4, no. 9–12, pp. 447–456, 2010.

[108] M. Oleszak, “Regularization: Ridge, Lasso and Elastic Net,” 2019. https://www.datacamp.com/community/tutorials/tutorial-ridge-lasso-elastic-net (accessed Apr. 28, 2020).

[109] A. E. Hoerl and R. W. Kennard, “Ridge Regression: Biased Estimation for Nonorthogonal Problems,” *Technometrics*, vol. 12, no. 1, pp. 55–67, Feb. 1970, doi: 10.1080/00401706.1970.10488634.

[110] D.-H. Lee, “Econometric assessment of bioenergy development,” *Int. J. Hydrogen Energy*, vol. 42, no. 45, pp. 27701–27717, 2017, doi: https://doi.org/10.1016/j.ijhydene.2017.08.055.

[111] IRENA, “Renewable Energy Capacity Statistics,” Dubai, 2019. [Online]. Available: https://www.irena.org/publications/2019/Mar/Renewable-Capacity-Statistics-2019.

[112] TSI General Census, “General Census,” Ankara, 2019.

[113] TSI Husbandary Statistics, “Husbandary statistics,” Ankara, 2019.

[114] TSI Plant Production Statistics, “Plant Production Statistics,” Ankara, 2019.

[115] P. Angerer, T. Kluyver, and J. Schulz, “Serializable Representations,” 2020. https://cran.r-project.org/web/packages/repr/repr.pdf (accessed Apr. 20, 2020).

[116] M. Kuhn, “Classification and Regression Training,” 2020. https://cran.r-project.org/web/packages/caret/caret.pdf. (accessed Apr. 20, 2020).

[117] Tidyverse, “A Grammar of Data Manipulation,” 2020. https://dplyr.tidyverse.org/. (accessed Apr. 20, 2020).

[118] H. Wickham, J. Hester, and and R. Francois, “Read Rectangular Text Data,” 2018. .

[119] H. Wickham, “The split-apply-combine strategy for data analysis,” *J. Stat. Softw.*, vol. 40, no. 1, pp. 1–29, 2011, doi: 10.18637/jss.v040.i01.

[120] J. Freidman *et al.*, “Lasso and Elastic-Net Regularized Generalized Linear Models,” 2020. https://cran.r-project.org/web/packages/glmnet/glmnet.pdf (accessed Apr. 20, 2020).

[121] Energy Market Regulatory Board, *Law on the Use of Renewable Energy Sources for Electric Energy Generation*. Turkey, 2021, p. 5.

[122] EMRA, “Electricity Market Connection and System Usage Regulation,” 2017. https://www.epdk.gov.tr/Detay/Icerik/3-6726/elektrik-piyasasi-baglanti-ve-sistem-kullanim-yonetmeligi (accessed Feb. 10, 2021).

[123] EMRA, “TEİAŞ System Usage and System Operation Tariffs for 2020,” 2019. http://epdk.gov.tr/Detay/Icerik/3-23478/teias-2020-yili-sistem-kullanim-ve-sistem-isletim (accessed Jan. 18, 2021).

[124] S. Barakat, H. Ibrahim, and A. A. Elbaset, “Multi-objective optimization of grid-connected PV-wind hybrid system considering reliability, cost, and environmental aspects,” *Sustain. Cities Soc.*, vol. 60, p. 102178, 2020, doi: https://doi.org/10.1016/j.scs.2020.102178.

[125] Agricultural Engineers Chamber, “Dairy Industries and Statistics in World and Turkey,” Ankara, 2018. [Online]. Available: https://www.zmo.org.tr/genel/bizden_detay.php?kod=31590&tipi=38&sube=0.

[126] National Milk Council, “Turkish Dairy Sector Statistics Summary Report,” Ankara, 2018. [Online]. Available: https://ulusalsutkonseyi.org.tr/turkiye-

sut-sektor-istatistikleri-ozet-raporu-2450/.

[127] B. Afework, G. Layndon, J. Hanania, and J. Donev, “Levelized cost of energy,” 2018. https://energyeducation.ca/encyclopedia/Levelized_cost_of_energy (accessed May 25, 2020).

PUBLICATIONS FROM THE THESIS

Conference Paper

1. Y. Kırım, H. Sadıkoğlu and M. Melikoğlu, (2021). “Technical and Economic Investigation of a Barn with 200 Cattle Capacity Using Milk Cattle Waste and Photovoltaic Solar Panels in a Renewable Hybrid Energy System,” ISPEC 10th International Conference on Engineering & Natural Sciences, Siirt, Turkey.

Article

1. Y. Kırım, H. Sadıkoğlu, and M. Melikoğlu, “Development of a Hybrid Renewable Energy System with Co-Firing Option,” *Energy Sources, Part A Recover. Util. Environ. Eff.*, 2021, doi: 10.1080/15567036.2021.1967521.